**Distribution Agreement**

In presenting this thesis or dissertation as a partial fulfillment of the requirements for an advanced degree from Emory University, I hereby grant to Emory University and its agents the non-exclusive license to archive, make accessible, and display my thesis or dissertation in whole or in part in all forms of media, now or hereafter known, including display on the world wide web. I understand that I may select some access restrictions as part of the online submission of this thesis or dissertation. I retain all ownership rights to the copyright of the thesis or dissertation. I also retain the right to use in future works (such as articles or books) all or part of this thesis or dissertation.

Signature:

| _____ | _____ |
| --- | --- |
| Jung Hwa Kirschman | Date |

The Role of Host Factors in HIV-1 Entry and Assembly

By

Jung Hwa Kirschman
Doctor of Philosophy

Graduate Division of Biological and Biomedical Science
Immunology and Molecular Pathogenesis

| | |
|---|---|
| _____ | _____ |
| Gregory Melikian, Ph.D.<br>Advisor | Eric Hunter, Ph.D<br>Committee Member |
| _____ | _____ |
| Daniel Kalman, Ph.D.<br>Committee Member | Baek Kim, Ph.D<br>Committee Member |
| _____ | |
| Anice Lowen, Ph.D.<br>Committee Member | |

Accepted:

_____
Lisa A. Tedesco, Ph.D.
Dean of the James T. Laney School of Graduate Studies

_____
Date

# The Role of Host Factors in HIV-1 Entry and Assembly

By

Jung Hwa Kirschman
M.S., Seoul National University, 2010

Advisor
Gregory Melikian, Ph.D.

An abstract of
A dissertation submitted to the Faculty of the
James T. Laney School of Graduate Studies of Emory University
in partial fulfillment of the requirements for the degree of
Doctor of Philosophy
in the Graduate Division of Biological and Biomedical Sciences
in Immunology and Molecular Pathogenesis
2018

Abstract

The Role of Host Factors in HIV-1 Assembly and Entry

By Jung Hwa Kirschman

HIV-1 is a global health threat with no vaccine available. Current treatment regiments are generally effective, but life-long administration of antiretroviral drugs has side effects and is quite costly. Uncovering the molecular mechanisms underlying the HIV-1 life cycle is important for developing effective drugs. HIV-1 Env is the only viral surface protein and it functions by initiating fusion to the host cell membrane, thereby initiating infection. Env is a major target for neutralizing antibodies. However, due to a dense glycan shield covering the Env and complex conformational changes during the fusion process, access to Env neutralization epitopes is limited. We therefore examined how Env gets incorporated into virions and how it induces viral fusion with the host membrane. To incorporate into progeny virions, Env must be transported to the virus assembly sites on the plasma membrane and interact with the assembling structural Gag protein. Here we elucidated the role of Rab11 and FIP1C in Env trafficking during HIV-1 assembly (Chapter 2). We found that the C-terminal fragment of FIP1C, when expressed in cells, can sequester Env inside the endosomal recycling compartment and thereby block the Env incorporation into virions. This dominant negative effect is likely proceeded by endocytosis of Env from the plasma membrane and is dependent on tyrosine motifs in the Env cytoplasmic tail. We also examined the mechanism of restriction of HIV-1 fusion by the new restriction factor SERINC5 (Chapter 3). SERINC5 incorporates into virions in the absence of Nef and potently inhibits fusion of sensitive, but not resistant HIV-1 variants. Our results revealed that both sensitive and resistant Env glycoproteins are functionally inactivated over time and that the inactivation rate is increased upon SERINC5 incorporation into virions. Mutations that stabilize or destabilize specific regions on Env did not reveal a specific Env conformation that could be targeted by SERINC5. However, a CD4 mimetic compound accelerated SERINC5-mediated Env inactivation, while a conformational blocker that stabilizes a native Env structure delayed the functional inactivation of Env in the presence of SERINC5. Collectively, our studies provided new insights into the molecular mechanisms of HIV-1 interaction with the host proviral and restriction factors during virus assembly and entry into target cells.

# The Role of Host Factors in HIV-1 Entry and Assembly

By

Jung Hwa Kirschman
M.S., Seoul National University, 2010

Advisor
Gregory Melikian, Ph.D.

A dissertation submitted to the Faculty of the
James T. Laney School of Graduate Studies of Emory University
in partial fulfillment of the requirements for the degree of
Doctor of Philosophy
in the Graduate Division of Biological and Biomedical Sciences
in Immunology and Molecular Pathogenesis
2018

**Acknowledgements**

I would like to thank:

♦Gregory Melikian, for his ideas and brilliant approach toward the second part of this project and his great passion toward mentorship and Science and for granting the great opportunity to be his student. Without his consistent support, this thesis literally could not be done.

♦Paul Spearman, for his ideas and foundations of the first part of this work. His passion and insights has been infused into the first part of the work. I appreciate for giving me opportunities to learn about HIV virology and to attend my first two Cold Spring Harbor Laboratory Retrovirus meetings.

♦Spearman Lab members: Lingmei Ding, Jason Hammonds (Mentor), Mingli Qi (Mentor), Xuemin Chen and Lena for technical and material contributions critical for the first part of work

♦Melikian Lab members: Mariana Marin (Mentor), Chetan Sood, Ashwanth Francis, Caleb Mason, Kenyanna Taylor for technical and theoretical contributions to the second part of work

♦My Thesis committee members: Daniel Kalman, Baek Kim, Eric Hunter, and Anice Lowen for additional ideas critical for this work. Especially big thanks to Dan for infinite support to get through multiple challenges as graduate student

♦Jonathan Kirschman, for being supportive husband and my cats Kunyang and Magu for offering lots of emotional support since I started my PhD.

## Table of Contents

# Chapter I: Introduction

## Background

The HIV/AIDS epidemic is a global health problem of great significance. According to the World Health Organization (WHO), approximately 37 million people are currently living with the virus while 1.8 million people became infected in 2017. At least 940,000 deaths have occurred as a result of this virus. As of 2017, 59% of infected adults and 52% of kids were subject to lifelong antiretroviral therapy (ART). HIV prevalence in Africa is more severe than in any other continents, reaching 70 percent of the global population infected.

HIV is an enveloped RNA virus that targets specifically human immune cells, such as CD4 T cells and cells of monocyte lineage (macrophages). Following long term infection, CD4 T cell counts drops under 100 per ml of blood and this cause ineffective antibody response by B cells, leading to progression of AIDS and death within a few months to a few of years without treatment (1). Furthermore, HIV is exceedingly difficult to eradicate due to the presence of latently infected cells. These HIV-1 reservoirs are not cleared by immune cells.

HIV is commonly spread by sexual encounters or sharing contaminated needles or syringes. Examples of body fluids that carry HIV include blood, semen, vaginal fluids, and breast milk from HIV-infected individuals. For transmission to occur, these fluids should be transferred to a recipient's mucosal membranes, damaged tissues, or directly into the blood stream. Infection can occur from mother to child during delivery and breast

feeding, and the risk of infection is higher when the mother is not under anti-retroviral therapy.

*The origin of HIV*

The origin of HIV-1 among nonhuman primates has been traced back to SIVcpz, which affected chimpanzee colonies in the Southern Cameroon area in West Africa. It's still not clear how SIVcpz was transferred to humans for the first time, but bloodborne transmission during hunting is a possible route. Phylogenetic tree analysis of HIV-1 from nonhuman primates revealed three unique transmission events in early 1900s resulting in three distinct HIV-1 groups: major M group, N group and the outlier O group (2, 3). The virus may have transferred to humans at Kinshasa, Zaire where the first HIV-1 infection of M group was documented after tracing it from a 1959 blood sample (4). Group M is currently the predominantly circulating group and it has been divided into subtypes. Subtypes A, B, C, D, F, G, H, J, and K are currently recognized. HIV-1 subtypes, also called clades, are phylogenetically linked strains of HIV-1 that are similar in genetic distance from one another (5).

HIV-2 was originally found in West African nations where it infected >1% of the population in the late 1980s (6). Although the original zoonotic transmission route is not clear, HIV-2 is closely related to SIV from sooty mangabeys. HIV-2 infection is associated with an extensively long asymptomatic period compared to HIV-1 infection (7). In addition, HIV-2 infection is characterized by higher CD4 cell counts and lower viral RNA levels in blood than that seen in HIV-1 infection (8).

*HIV-1 transmission*

*Virus evolution during extreme selective pressure, the bottleneck for transmission*

According to a bottleneck theory (9, 10, 11, 12), during heterosexual transmission, a single HIV-1 variant can quickly (within a couple of weeks) establish a detectable viral load in the bloodstream. This HIV-1 variant is referred to as transmitted/founder virus (T/F virus). Accordingly, during acute infection, the recipient's blood is dominated by a homogenous virus population. However, during chronic infection, extremely diverse variants appear due to rapid mutations. HIV-1 T/F viruses are known to be majorly CCR5 tropic (13). Several studies revealed that T/F viruses do not effectively infect macrophages or other low-CD4 expressing cell types tropic (13, 14, 15, 16). One study has reported that infectious molecular T/F clones contain twice as many Env on virions than chronic HIV-1, perhaps due to mutation in the Env leader sequence, which increases Env density in the plasma membrane (17, 18). High Env density may enhance virus anchoring to mucosal cells in the genital tract mucosa, thereby aiding the virus entry and infection (19, 20).

*Antiretroviral therapy*

The current state-of-the-art treatment for HIV is a combination antiretroviral therapy (cART) which involves multiple drugs that have different modes of action. Early drugs approved by the FDA in the late 1980s included nucleoside reverse transcriptase inhibitors, followed shortly by protease inhibitors and non-nucleoside reverse transcriptase inhibitors. In the past decade, drugs that inhibit the integrase strand transfer activity have arrived on the market and are generally a preferred component of

antiretroviral regimens, alongside a protease inhibitor, due to high virologic efficacy and safety/tolerability profiles (21).

Overall, current antiretroviral treatments are able to reduce morbidity, increase survival times, and prevent transmission. Unfortunately, due to the presence of latently infected CD4 T cells produced during the initial acute infection, cART must be administered lifelong. Also, given that drugs can lose efficacy over time, develop adverse effects, or select for resistant viruses, alternative regimens may be required. Thus, a different class of drugs targeting other HIV pathways and functions, such as entry or maturation inhibitors, is urgently needed. Many of these types of inhibitors are not yet FDA approved, but are in advanced stages of clinical trials. A promising example is BMS-626529, which inhibits HIV-1 entry into cells by binding to the envelope protein (Env) and preventing a conformational change necessary to bind the HIV-1 coreceptor (22). Another promising strategy under intense study is the use of broadly neutralizing antibodies targeting conserved epitopes on the HIV-1 Env. Development of novel types of therapeutic approaches is necessary in order to better target multiple points of the HIV-1 replication cycle and curb infection.

Vaccine efforts have not yet led to an effective vaccine that can prevent infection. Efforts to develop HIV vaccines and novel therapies against the virus may benefit from new basic discoveries related to post-assembly Env structure and virus entry into cells. Currently, no inhibitors target the process of HIV-1 assembly. My project focuses on defining the host factors and cellular pathways through which HIV-1 assembles in an infected cell. Specifically, we elucidated the molecular and cellular processes underlying the incorporation of HIV-1 Env into a viral particle during assembly. Understanding the

mechanism of interaction between host factors and Env will provide important clues for developing new inhibitors to precisely block the HIV-1 assembly steps and to farther the fundamental understanding of the HIV-1 replication cycle.

*HIV replication cycle*

HIV-1 virus replication proceeds through several major steps including fusion with the host membrane, uncoating, reverse transcription, integration of the newly synthesized viral DNA into the host genome, transcription of viral RNA and synthesis of viral proteins resulting in assembly of progeny virions that infect nearby target cells. Multiple host proteins are engaged in the HIV-1 replication cycle. (23)

HIV-1 infection begins when its surface Env glycoprotein binds CD4 on the cell surface, which causes changes in Env conformation, which allow Env to engage co-receptors, CCR5 or CXCR4 (step 1) (24, 25, 26), (Figure 1). The formation of Env-CD4-co-receptor complex initiates further conformational changes in Env, leading to fusion between the viral and cell membranes and release of the viral core into the cytoplasm (step 2) (27, 28, 29). Subsequent uncoating of the viral core occurs through shedding of the capsid (CA) protein (step 3) (30). Uncoating appears to facilitate the reverse transcription step in which the two copies of viral RNA are converted into a double-stranded DNA by the HIV-1 reverse transcriptase (RT). This leads to the formation of a pre-integration complex (PIC) containing the viral genomic DNA and integrase (IN) (step 4) (31, 32). PICs are transported to the nucleus and enter the nucleus through the nuclear pore complexes (NPCs) (step 5) (31, 32). After PICs enter into the nucleus, the host chromatin-binding protein, lens epithelium-derived growth factor (LEDGF), facilitates

integration of viral DNA between the long terminal repeats (LTRs) catalyzed by the HIV-1 integrase (IN), leading to an integrated provirus (step 6) (31, 32, 33). Proviral DNA transcription mediated by the host RNA polymerase II (RNA pol II) and positive transcription elongation factor b (P-TEFb) generates unspliced mRNAs of various length with the help of viral protein Tat which promotes full-length transcription during the elongation phase of HIV-1 transcription (step 7) (34, 35, 36). Unspliced viral RNA is exported from the nucleus by the host CRM1 protein and viral Rev protein (step 8) (37, 38). Spliced viral RNA is translated producing viral proteins (step 9) (39). Two copies of unspliced single-stranded viral RNAs are incorporated into assembling virions at the plasma membrane (step 10). Viral particle budding and release from the host cell membrane (step 11) is mediated by the Endosomal Sorting Complex Required for Transport (ESCRT) (40, 41) and ALIX (42, 43). At the time of budding or shortly afterwards, virions undergo maturation whereby the HIV-1 protease cleaves the Gag and Pol polyproteins, thus generating infectious particles (step 12) (44). Current antiviral therapies are focused on targeting different steps of the virus life cycle and understanding the role of host restriction factors during HIV-1 replication will provide new opportunities for drug development.

*HIV-1 entry*

HIV-1 entry occurs through sequential interaction with host receptor CD4 and co-receptors, CCR5 or CXCR4 (24, 25). The coreceptor usage determines the cell types that are susceptible to infection. Engagement of CD4 and co-receptors triggers dramatic Env transformation. First, there are conformational changes in gp120 (V1/V2 and V3 loops,

bridging sheet) leading to formation of a co-receptor binding site (Figure 2B in Chapter 3 Intro). Second, CD4 and coreceptor binding leads to formation of gp41 pre-hairpin intermediates characterized by the formation/exposure of the N-terminal fusion peptide and N-terminal and C-terminal heptad repeat segments (HR1 and HR2, respectively) (45). Next, the fusion peptide is inserted into the target cell plasma membrane (46). Lastly, the folding of the gp41 heptad repeat regions HR1 and HR2 into the six-helix bundle structure promotes membrane fusion (27, 28, 29, 47).

*HIV-1 uncoating*

The HIV-1 core contains the viral genomic RNA, reverse transcriptase, integrase, and nucleocapsid proteins, encased within the cone-shaped shell made of the CA protein (48). Disassembly of the CA shell is indispensable for reverse transcription and virus infection (49, 50, 51, 52, 53). Numerous studies proved that HIV-1 uncoating is regulated by CA and cellular factors. The cellular proteins, such as cyclophilin A and CPSF6 (54, 55), bind the viral capsid and appear to influence infection by controlling uncoating (56, 57) In mature virions, CA, which consists of the N-terminal (NTD) and C-terminal (CTD) domains and forms hexamers and pentamers assembled into a cone-shaped shell (58, 59). A few pentamers provide the necessary curvature to the capsid shell and are positioned at the top and the bottom of a cone (59). The host restriction factor TRIM5-α is known to recognize the HIV-1 capsid lattice structure and accelerate virus uncoating/degradation (60, 61).

*Reverse transcription of HIV-1 genome*

HIV-1 RT has two p66 and p51 subunits. P66 contains two domains: RNA- and DNA-dependent DNA polymerase in the N-terminus, and RNase H at the C-terminus. Single-stranded viral RNA genome is reverse transcribed into double-stranded DNA. RT initially generates a minus-strand DNA, after which the RNase H degrades the RNA template. Minus-strand transfer occurs at the R sequence in the 3' ends of either of the two single-stranded RNAs (62, 63, 64, 65). Minus-stranded DNA synthesis is initiated after this strand-transfer and continues along the whole genome. The polypurine tract in the RNA genome, which is resistant to RNase H activity, serves as a primer for the plus-strand DNA synthesis. The reverse transcription process generates a dsDNA that is longer than the RNA genome from which it is derived: both ends of the DNA contain sequences from each end of the RNA (U3 from the 30 end and U5 from the 50 end). Thus, each end of the viral DNA has the same sequence, U3-R-U5; these are the long terminal repeats (LTRs) that will, after integration, flank the provirus.

Two types of RT inhibitors, nucleoside (NRTI) and non-nucleoside inhibitors (NNRTI), are used in clinic. NRTIs mimic natural dNTPs and become incorporated into the newly synthesizing viral DNA by RT. Lack of a 3'-hydroxyl group in NRTIs can block inclusion of subsequent nucleotides during the polymerase reaction, which can terminate further viral DNA synthesis. NNRTIs act as allosteric inhibitors with a highly flexible binding pocket against RT which causes the loss of primer grip (66). APOBEC3G is a host restriction factor targeting the reverse transcription step. It can incorporate into virions and deaminase the cystidine into uracil residues in the viral cDNA genome, which impairs the elongation of reverse transcripts (67, 68, 69). HIV-1

viral protein Vif counteracts APOBEC3G by direct binding and targeting to degradation by the proteasome (70, 71, 64(Ch3)).

*HIV-1 integration/transcription*

Integration results in covalent annealing of the viral dsDNA with the host cell DNA. HIV-1 IN interacts with the cellular factor LEDGF/p75, which promotes efficient infection and tethers IN to the preferred integration sites (33). Previous studies of the integration intermediates revealed the precise steps of cleavage and ligation between viral genome and host DNA (72, 73). In the first step (3′end processing), two nucleotides are removed from each 3′end of the linear blunt-ended viral DNA. In the second step (DNA-strand transfer), these 3′ends attack a pair of phosphodiester bonds on 5′ strands of the target DNA, across the major groove. In the resulting integration intermediate the 3′ends of the viral DNA are covalently joined to the target DNA. Integration is completed when the single-strand gaps and the two-nucleotide overhang at the 5′ends of the viral DNA are repaired by cellular enzymes.

After integration, transcription starts from the U3 promotor region located in the long terminal repeats (LTR), the transcription promoter site and the viral transactivator protein Tat is required for efficient transcript elongation. HIV-1 gene expression is driven by the LTR, which contains many binding sites for host and viral factors (74, 75, 76). During nuclear export, HIV-1 uses the cellular export machinery and its nuclear export

receptor Crm1 in addition to virus protein Rev to bypass pre-mRNA retention mechanisms (144).

*HIV-1 assembly*

HIV-1 assembles on the plasma membrane (PM) of T cells and of model epithelial cell lines, such as HeLa cells. In order to generate an infectious particle, the viral structural proteins and genome must converge in a coordinated fashion to two types of plasma membrane microdomains, such as lipid rafts and tetraspanin-enriched microdomains (TEMs), both of which have been proposed to be platforms for HIV-1 assembly (77). Lipid rafts are dynamic, submicroscopic domains enriched in sterols, sphingolipids, glycosylphosphatidylinositol-anchored (GPI-anchored) proteins, and proteins modified with saturated acyl chains (78, 79). TEMs are membrane microdomains organized by homo- and hetero-oligomerization of tetraspanins, a family of homologous proteins with four transmembrane domains (80). Tetraspanins, including CD9, CD63, and CD81, are incorporated into virus particles (81), co-immunoprecipitate with Gag (82), and strongly colocalize with Gag by immunofluorescence and electron microscopy assays (83, 84). Lipid rafts and TEMs can be biochemically distinguished as they have different detergent solubility, different sensitivities to cholesterol depletion, and distinct protein constituents (85). The mechanisms of transport of the major structural precursor protein (Pr55Gag or Gag) and Env to the PM are not well understood. Four models have been proposed to explain the incorporation of HIV Env into virions. (1) Passive incorporation: random diffusion of Gag and Env will end up coincidently incorporated into virions, (2) Direct Gag-Env interaction: Matrix domain of Gag is known to directly bind gp41 and this can

guide Env to assembly sites; (3) Gag-Env co-targeting; and (4) indirect Gag-Env interaction: certain host factors from producer cells can indirectly guide both Gag and Env to the PM (1, 2).

*Env synthesis and cleavage*

Originally synthesized as a trimeric gp160 precursor, a Type 1a transmembrane protein, Env is heavily glycosylated with N-linked and O-linked carbohydrates and is cleaved by a cellular furin or furin-like protease in the Golgi. Cleavage produces the two non-covalently associated subunits for each protomer of the Env trimer, the gp120 (surface) and gp41 (transmembrane) subunits (86, 24, 87). Mature Env trimer spikes are transported to the plasma membrane and assemble with Gag to form virion (88, 89).

*GP41 cytoplasmic tail (CT)*

The extraordinarily long cytoplasmic tail of Env is a unique feature of lentiviruses. Its functions are not fully understood. With some exceptions, such as feline immunodeficiency virus (FIV) and puma lentivirus (PLV), most members of this family have, on average, a 120 amino acid long CT, while the CTs of other retroviruses are less than 60-residues long. Equine infectious anemia virus (EIAV) has the longest Env tail (224aa) and the HIV Env cytoplasmic tail is 150aa-long. HIV-1 Env CT can be defined as possessing distinct domains based on biophysical properties. The membrane-spanning domain of Env CT is followed by a hydrophilic region (90), which comprises of a highly immunogenic region (HIR) that generates high levels of antibody production in HIV-infected individuals and SIV-infected rhesus macaques (91, 92, 93, 94). The gp41 CT

contains three amphipathic lentivirus lytic peptides (LLPs). Both LLP-1 and LLP-2 were confirmed to form α helices via amphipathic moieties, while LLP-3 resides between LLP-1 and LLP-2 (95, 96, 97). Based on in vitro studies, LLP-1, LLP-2 and LLP-3 are thought to guide gp41 tail to the plasma membrane by binding to lipid bilayers (94, 98, 99, 100). Env CT may stabilize the Env trimer spikes in their prefusion "spring-loaded" conformation which stores free energy for the process of virus-to-cell fusion (101, 102). Truncation of the gp41 CT has been shown to enhance the fusogenicity of the surface-expressed Env (103, 104, 105). LLP-1 and LLP2 have been suggested to contribute differently to Env incorporation into virions (106). A direct interaction of the LLP-1 amphipathic helix with the MA protein during the process of Env incorporation has been previously postulated (106). The mechanism by which Env CT stabilizes the metastable prefusion state of Env is unknown, but it has been proposed to occur through: (i) interaction with the matrix (MA) protein during maturation (107, 108, 109) and/or (ii) stabilization of the Env association of with the plasma membrane (110).

The interacting host partners of HIV-1 Env CT include AP-1, AP-2 adaptor proteins. AP-1 is responsible for intracellular trafficking between the trans-Golgi network (TGN) and endosomes via clathrin-mediated endocytosis, while AP-2 is involved in endocytosis and retrograde trafficking from the PM. (11, 21).

*MA and Env incorporation into virions.*

The matrix (MA) domain (p17) of the Gag protein plays important roles in Env incorporation into HIV and SIV virions (111,112, 113). MA anchors the Gag precursor protein to the inner leaflet of the plasma membrane through a myristoylated basic

membrane-binding domain (114, 115). Targeting of Gag to the budding site at the plasma membrane is also directed by MA (116, 117, 120). MA binds to phosphatidylinositol(4,5) bisphosphate on the inner leaflet while a large deletion in MA is known to redirect the HIV-1 virion assembly from PM to ER (118, 119, 120). Previous studies indicated a direct interaction of purified, bacterially expressed Env and MA that mapped to the C-terminal half of the Env CT (37) despite whether MA physically interact with gp41 CT is still not clear (118, 119). The Freed group has found that, in T-cell lines, small deletions in α-helix 2 (in the center of CT) disrupt the incorporation of Env glycoproteins into virions and significantly impair virus infectivity (122). Through the analysis of viral revertants, the Freed group has also demonstrated that a single amino acid change (34VI) in MA reverses the Env incorporation and infectivity defect imposed by a small deletion near the C terminus of the α-helix 2 (122). Conversely, single amino acid substitutions in MA (12LE, 30LE) can block incorporation of Env into virions. Thus, mutations in MA that block Env incorporation can be rescued by truncation of the N-terminus of LLP-2 segment of gp41 CT (123). The Gottlinger group showed that MA deleted viruses were unable to incorporate the wild-type HIV-1 Env protein complex, but that this defect could be corrected by a second-site mutation, which removed the large cytoplasmic domain of CT (122). Recent studies by Tedbury and Freed, showed that MA trimerization is required for HIV-1 Env incorporation into virus particles. Also, truncation of the long cytoplasmic tail of Env restores incorporation of Env into MA trimer-defective particles, thus rescuing infectivity. MA trimerization is required to form a Gag lattice capable of accommodating the long cytoplasmic tail of HIV-1 Env (124). Further studies are needed to fully elucidate the gp41 CT/MA interactions.

The long cytoplasmic tail of Env has been speculated to have specific domains involved in indirect or direct interactions with the Gag lattice. Eric Freed and Phillip Tedbury (125) suggested four models of Env incorporation in the plasma membrane: (1) Passive incorporation (2) Gag-Env co-targeting (3) Direct Gag-Env incorporation (4) Indirect Gag-Env incorporation (Figure 2. The passive incorporation model suggests no interaction between Gag and Env. Simple diffusion of Gag and Env will reach plasma membrane by chance for passive incorporation into virions. The direct Gag-Env interaction model is based on previous studies that identified interacting domains in MA and Env CT. The Gag–Env co-targeting model assumes that both proteins are enriched in virus assembly microdomains, such as lipid raft. The indirect Gag–Env interaction model provides an alternative explanation for Env incorporation that involves an unknown adaptor protein that interacts with both Env and Gag.

*Endocytic signals in the Env CT*

At least two domains proximal to the N-terminal and C-terminal regions of the gp41 CT are responsible for efficient Env endocytosis (Fig. 3). The first endocytosis domain resides next to the membrane-spanning domain and contains a highly conserved tyrosine motif (YXXϕ, where X is any amino acid and ϕ is a hydrophobic amino acid). HIV-1 NL4.3 has a $^{709}$GYSPL$^{713}$ sequence, while SIVmac239 has $^{720}$GYRPV$^{724}$. The µ2 subunit of AP-2 binds to these YXXϕ motifs and mediates Env endocytosis (126, 127, 128). Mutation of amino acids at positions 721 to 724 of the GYRPV motif caused reduced pathogenicity and significantly diminished the virion RNA in plasma of infected rhesus macaques. The first YXXϕ motif is highly conserved among HIV-1, HIV-2 and SIV. The

second YXXϕ motif is located near the C-terminus of CT. HIV-1 NL4-3 has another $^{766}$YHRL$^{769}$, which is responsible for NF-κB activation, but not endocytosis (129). SIVmac also has an additional YXXϕ motif that does not impact endocytosis. The last endocytosis motif of the CT is a dileucine motif at the C-terminus, which likely interacts with the σ2 subunit of AP-2 ($^{849}$LERILL$^{854}$ in HIV-1 NL4-3 while SIVcpz does not have this motif) (138, 142). When both YXXϕ and LL endocytic motifs within the CT are altered by mutations, Env endocytosis is significantly impaired and the surface level of Env increases dramatically (126, 127,135). There is also an additional dileucine motif in the very end of the C terminus that regulates Env endocytosis and it is highly conserved in among HIV-1, HIV-2 and SIV ($^{878}$LL$^{879}$ in SIVmac239) (138).

On average, only 7-14 Env trimers are present on an HIV-1/SIV particle compared to SIV tail deletion mutant which express 70-79 trimers, as determined by high performance liquid chromatography (HPLC), western blotting, and cryo EM studies (130, 131, 132, 133). The low number of virus-incorporated Env molecules is due to active Env internalization by clathrin-mediated endocytosis that greatly reduces the number of Env on the cell surface where the virus assembly occurs. After its arrival at the PM, Env is rapidly recycled via endocytosis/lysosome pathway (134, 147). Egan et al. (134) proposed that the MA domain of Gag can hold Env in the plasma membrane for incorporation into virions, preventing its endocytosis. The truncated SIV Env can be expressed on the surface 10 to 40 times higher than wild-type Env. Yuste et al. compared several SIV Env CT mutants containing premature stop codons and a mutation of the membrane-proximal YXXϕ motif and observed that the level of Env surface expression closely correlated with the level of Env incorporation into virions in CEMx174 cells and

rhesus immortalized T-cell line Rh221-89 (135). Numerous studies suggested the low number of Envs avoids avidity binding of Abs and reduces ADCC. (136, 137). Another possibility is that the relatively small number of Env might be advantageous to HIV-1, as this reduces the possibility of exposure of neutralizing epitopes to antibody recognition, leading to antibody-dependent cell-mediated cytotoxicity (ADCC) and complement-mediated cytotoxicity. Studies of SIV infection proved that increased surface Env levels after mutation in the first endocytic motif allowed a better control of virus pathogenesis by host immunity (138).

*Role of Env CT in virus incorporation*

Murakami and Freed (2000) showed that the Env CT is required for Env trafficking and incorporation into particles in peripheral blood mononuclear cells (PBMCs) and monocyte-derived macrophages (MDMs) (1). In his study, human CD4+ T-cell lines, such as CEM and Jurkat, showed significantly reduced incorporation of tail-truncated Env, while H9, MT-4 and HeLa cells showed slightly reduced incorporation compared to wild type Env. In contrast, the tail is not required for particle incorporation in some permissive cell types, such as 293T cells and M8166. CT truncation did not impair Env glycosylation, cleavage, trimerization, surface expression or the fusion activity. Also, a single-round infection assay showed that CT truncation did not affect specific infectivity both in permissive and non-permissive cells, which proves there is no structural impediment for virus entry. Interestingly, the SIV gp41 tail is progressively truncated when it is cultured in human cells (139-141, 145). Truncated gp41 can increase both infectivity and fusogenicity of SIV (44, 136, 146). HIV-1 infectivity and fusogenicity can

also be increased in certain cells types. Tail truncation only happens when SIV is cultured in human cells, but not in rhesus macaque cells, such as rhesus PBMCs. The SIV strains containing tail-truncated gp41 tail show reduced replication in rhesus PBMCs. After sequential passaging, the truncated gp41 tail tends to revert back to the original size of the gp41 tail, in contrast to the dominance of the truncated gp41 tail in human cell lines (139, 140, 141). In vivo studies also showed a similar phenomenon: truncated SIV Env mutants could rapidly revert back to the original size of the CT in rhesus macaques (141). When reversion of the truncated SIV Env was prevented, rhesus macaques had reduced viral loads and showed no clinical symptoms. The advantage of the truncated SIV gp41 tail in human cells may be originated from unknown host restriction factors acting differently between the two species. The mechanism underlying the selective advantage of the SIV gp41 CT truncations for replication in human cells, but not in rhesus macaque cells, is still unknown. As there are only very few rhesus cell lines, most tissue culture experiments examining the effects of the SIV gp41 CT truncation have been performed in human cell lines.

## Summary

In this study, I focused on two aspects of HIV-1 lifecycle: virus incorporation and stability of Env glycoprotein in the context of proviral and restriction factors Rab11-FIP1C and SERINC5, respectively. In the first chapter, we will show how Rab11-FIP1C guides HIV-1 Env trafficking *via* an endocytic pathway from the endosomal recycling compartment to the plasma membrane In the second chapter, I will focus on understanding the role of SERINC5 restriction on HIV-1 Env during virus entry in the

context of functional stability of Env. We believe our work will reveal new roles of host factors regulating and targeting HIV-1 Env which will suggest future strategies for therapeutic intervention.

Figure

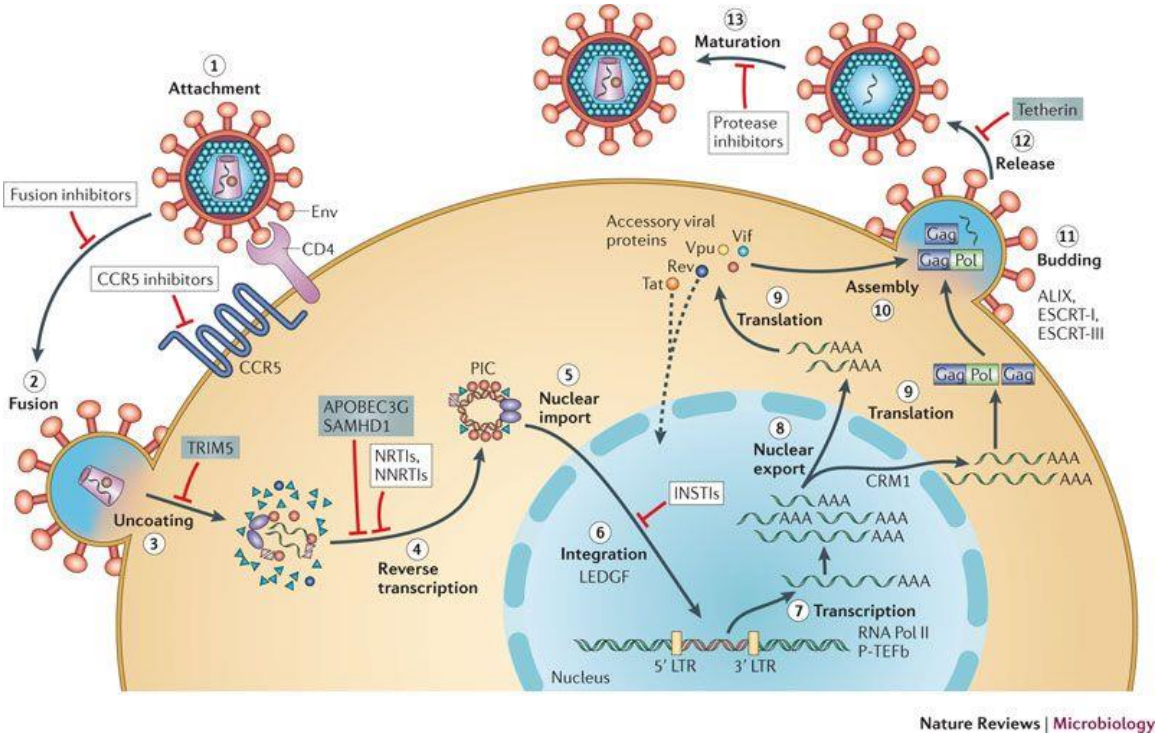


**Fig. 1. HIV-1 replication cycle**

Each steps in virus life cycle is stated as numbers and step-specific inhibitors are marked. After anchoring on the target CD4+ T helper cell, HIV-1 will proceed to fusion, viral genome replication and finally production of mature lentiviral particles on the assembly site and finally bud out virions for another transmission cycle. (Reproduced from Engelman 2012 Nature Rev Microbiol)

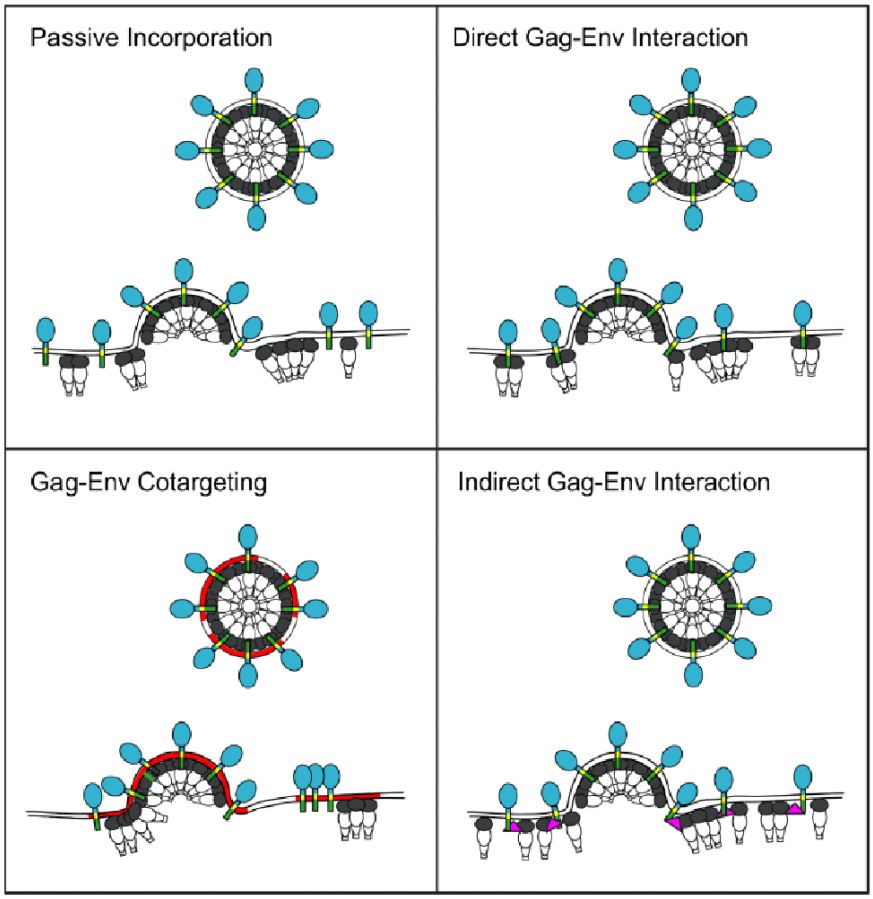


**Fig. 2. HIV-1 Env incorporation model**

Env is shown as gp120 (blue) and gp41 subunit (stalk anchored on the plasma membrane and viral membrane). Gag is attached to inner leaflet of plasma membrane as shown with four subunits (from the top: MA (matrix) P17; Capsid (CA) p24; Nucleocapsid (NC); p7, p6). A specific microdomain on the plasma membrane assembly site is indicated (red). Adaptor protein mediating the interaction between MA and Enc CT is marked (magenta). (Reproduced from Tedburry and Freed 2016 Trends Microbiol.)

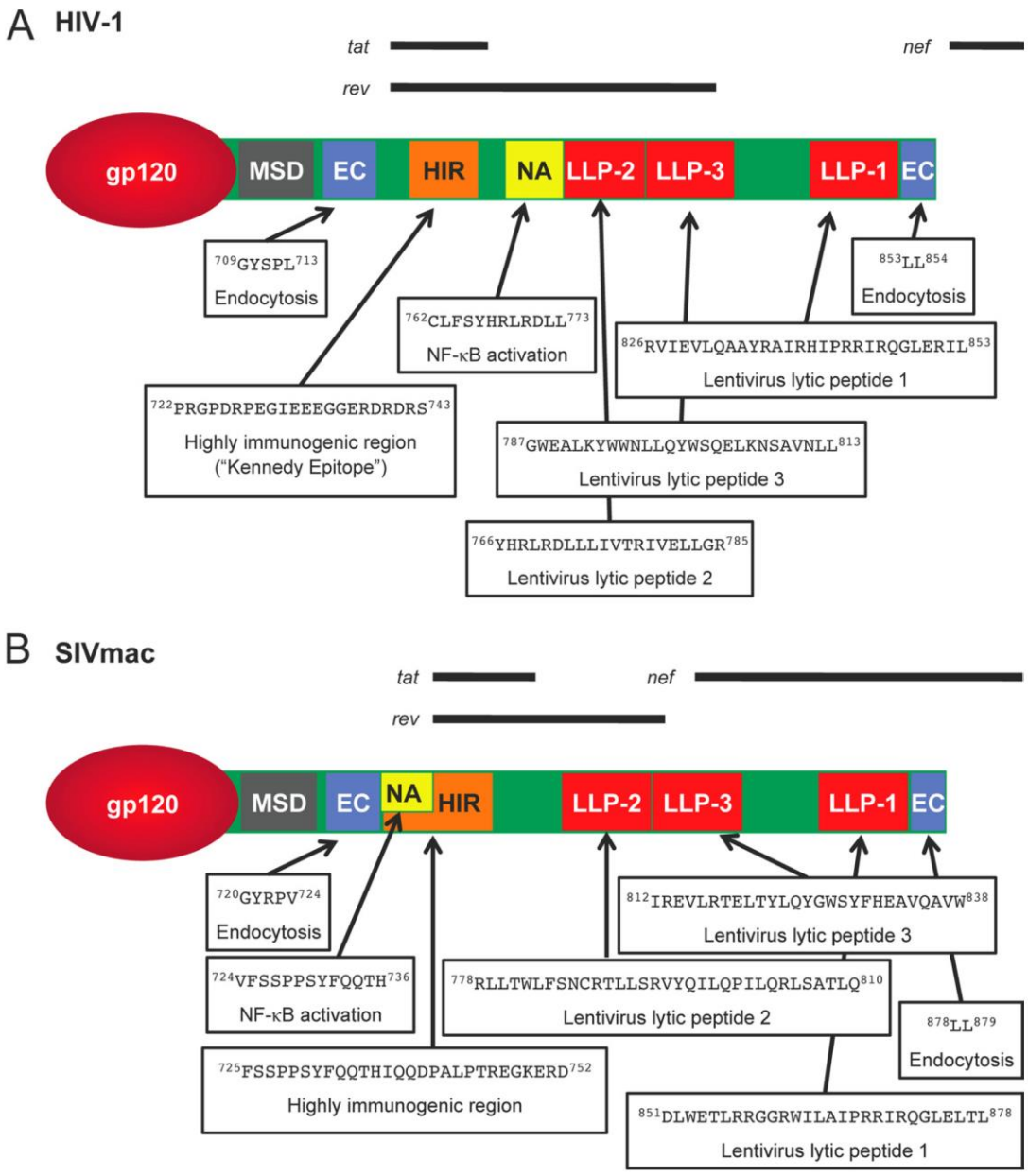


**Fig. 3. Env CT region of HIV-1 and SIVmac.**

(A) HIV-1. (B) SIVmac. Note that LLP-2 and LLP-3 sequences of SIVmac have not been precisely identified. MSD, membrane-spanning domain; EC, endocytosis motif;

(Reproduced from Postler and Desrosiers, 2013, JVI)

References

1. Mayr NM, Bin S. Moog C 2017. Non-Neutralizing Antibodies Directed against HIV and Their Functions. Front Immunol. 8:1590. https://doi.org/10.3389/fimmu.2017.01590

2. Korber B, Muldoon M, Theiler J, Gao F, Gupta R, Lapedes A, Hahn BH, Wolinsky S, Bhattacharya T. 2000. Timing the ancestor of the HIV-1 pandemic strains. Science 288(5472):1789-96. PMID: 10846155.

3. Keele BF et al. 2006. Chimpanzee Reservoirs of Pandemic and Nonpandemic HIV-1. Science 313(5786): 523–526. doi: 10.1126/science.1126531

4. Perelson AS, Neumann AU, Markowitz M, Leonard JM, Ho DD. 1996. HIV-1 dynamics in vivo: virion clearance rate, infected cell life-span, and viral generation time. Science 271(5255):1582-6. https://doi.org/10.1073/pnas.97.1.343.

5. Hemelaar J, Gouws E, Ghys PD, Osmanov S. 2006. Global and regional distribution of HIV-1 genetic subtypes and recombinants in 2004. AIDS 24;20(16):W13-23. DOI: 10.1097/01.aids.0000247564.73009.bc

6. O'Brien TR, George JR, Epstein JS, Holmberg, SD, Schochetman GS. (1992, July 17). Testing for Antibodies to Human Immunodeficiency Virus Type 2 in the United States. Centers for Disease Control and Prevention MMWR 41(RR12);1-9 Retrieved from https://wonder.cdc.gov/wonder/prevguid/m0038078/m0038078.asp

7. Popper SJ, Sarr AD, Travers KU, Guèye-Ndiaye A, Mboup S, Essex ME, Kanki PJ. 1999. Lower human immunodeficiency virus (HIV) type 2 viral load reflects the difference in pathogenicity of HIV-1 and HIV-2. J Infect Dis. 180(4):1116-21. DOI: 10.1086/315010

8. MacNeil A, Sarr AD, Sankalé JL, Meloni ST, Mboup S, Kanki P. 2007. Direct evidence of lower viral replication rates in vivo in human immunodeficiency virus type 2 (HIV-2) infection than in HIV-1 infection. J Virol 81(10):5325-30. DOI: 10.1128/JVI.02625-06

9. Zhu T, Mo H, Wang N, Nam DS, Cao Y, Koup RA, Ho DD. 1993. Genotypic and phenotypic characterization of HIV-1 patients with primary infection. Science 261(5125):1179-81. PMID: 8356453

10. Joseph SB, Swanstrom R, Kashuba AD, Cohen MS. 2015. Bottlenecks in HIV-1 transmission: insights from the study of founder viruses. Nat Rev Microbiol 13(7):414-25. doi: 10.1038/nrmicro3471.

11. Shaw GM, Hunter E. 2012. HIV transmission. Cold Spring Harb Perspect Med. 2(11) doi: 10.1101/cshperspect.a006965.

12. Wolinsky SM, Wike CM, Korber BT, Hutto C, Parks WP, Rosenblum LL, Kunstman KJ, Furtado MR, Muñoz JL. 1992. Selective transmission of human immunodeficiency virus type-1 variants from mothers to infants. Science 255(5048):1134-7. PMID: 1546316

13. Keele BF et al. 2008. Identification and characterization of transmitted and early founder virus envelopes in primary HIV-1 infection. Proc Natl Acad Sci U S A. 105(21):7552-7. doi: 10.1073/pnas.0802203105.

14. Ochsenbauer C et al. 2011. Generation of transmitted/founder HIV-1 infectious molecular clones and characterization of their replication capacity in CD4 T lymphocytes and monocyte-derived macrophages. Biochem Biophys J Virol. 86(5):2715-28. doi: 10.1128/JVI.06157-11

15. Salazar-Gonzalez JF et al. 2009 Genetic identity, biological phenotype, and evolutionary pathways of transmitted/founder viruses in acute and early HIV-1 infection. J Exp Med 206(6):1273-89. doi: 10.1084/jem.20090378.

16. Wilen CB et al. 2011. Phenotypic and immunologic comparison of clade B transmitted/founder and chronic HIV-1 envelope glycoproteins. J Virol 85(17):8514-27 doi: 10.1128/JVI.00736-11

17. Parrish NF et al. 2013. Phenotypic properties of transmitted founder HIV-1. Proc Natl Acad Sci U S A. 110(17):6626-33 doi: 10.1073/pnas.1304288110.

18. Asmal M et al. 2011. A signature in HIV-1 envelope leader peptide associated with transition from acute to chronic infection impacts envelope processing and infectivity. PLoS One. 6(8):e23673 doi: 10.1371/journal.pone.0023673

19. Centers for Disease Control and Prevention. (2018, August 13). HIV Transmission. Retrieved from https://www.cdc.gov/hiv/basics/transmission.html

20. Joseph SB, Swanstrom R, Kashuba ADM, Cohen MS. 2016. Rab coupling protein associates with phagosomes and regulates recycling from the phagosomal compartment. Nat Rev Microbiol. 13(7): 414–425. doi: 10.1038/nrmicro3471

21. Cihlar T, Fordyce M. 2016. Current status and prospects of HIV treatment. Curr Opin Virol. 18:50-6. doi: 10.1016/j.coviro.2016.03.004

22. Nowicka-Sans B et al. In vitro antiviral characteristics of HIV-1 attachment inhibitor BMS-626529, the active component of the prodrug BMS-663068. Antimicrob Agents Chemother. 56(7):3498-507. doi: 10.1128/AAC.00426-12.

23. Engelman A, Cherepanov P. 2012. The structural biology of HIV-1: mechanistic and therapeutic insights. Nat Rev Microbiol. 10(4):279-90. doi: 10.1038/nrmicro2747.

24. Kwong PD, Wyatt R, Robinson J, Sweet RW, Sodroski J, Hendrickson WA. 1998. Structure of an HIV gp120 envelope glycoprotein in complex with the CD4 receptor and a neutralizing human antibody. Nature 393(6686):648-59. DOI: 10.1038/31405

25. Rizzuto R, Pinton P, Carrington W, Fay FS, Fogarty KE, Lifshitz LM, Tuft RA, Pozzan T. 1998. Close contacts with the endoplasmic reticulum as determinants of mitochondrial Ca2+ responses. Science 280(5370):1763-6. PMID: 9624056

26. Chen Z et al. 2005. Crucial role of p53-dependent cellular senescence in suppression of Pten-deficient tumorigenesis. Nature 436(7051):725-30. DOI: 10.1038/nature03918

27. Chan DC, Fass D, Berger JM, Kim PS. 1997. Core structure of gp41 from the HIV envelope glycoprotein. Cell 89(2):263-73. PMID: 9108481

28. Weissenhorn W1, Dessen A, Harrison SC, Skehel JJ, Wiley DC. 1997. Atomic structure of the ectodomain from HIV-1 gp41. Nature 387(6631):426-30. DOI: 10.1038/387426a0

29. Buzon V, Natrajan G, Schibli D, Campelo F, Kozlov MM, Weissenhorn W. 2010. Crystal structure of HIV-1 gp41 including both fusion peptide and membrane proximal external regions. PLoS Pathog. 6(5):e1000880. doi: 10.1371/journal.ppat.1000880.

30. Pornillos O, Ganser-Pornillos BK, Yeager M. 2011. Atomic-level modelling of the HIV capsid. Nature. 469(7330):424-7. doi: 10.1038/nature09640.

31 Kohlstaedt LA1, Wang J, Friedman JM, Rice PA, Steitz TA. 1992. Crystal structure at 3.5 A resolution of HIV-1 reverse transcriptase complexed with an inhibitor. 256(5065):1783-90. PMID: 1377403

32. Jacobo-Molina A, Ding J, Nanni RG, Clark AD Jr, Lu X, Tantillo C, Williams RL, Kamer G, Ferris AL, Clark P. 21993. Crystal structure of human immunodeficiency virus type 1 reverse transcriptase complexed with double-stranded DNA at 3.0 A resolution shows bent DNA. Proc Natl Acad Sci U S A 90(13):6320-4. PMID: 7687065

33. Engelman A, Cherepanoz P. 2008. The Lentiviral Integrase Binding Protein LEDGF/p75 and HIV-1 Replication. PLoS Pathogen 4(3): e1000046. https://doi.org/10.1371/journal.ppat.1000046

34. Tahirov TH, Babayeva ND, Varzavand K, Cooper JJ, Sedore SC, Price DH. 2010. Crystal structure of HIV-1 Tat complexed with human P-TEFb. Nature 465(7299):747-51. doi: 10.1038/nature09131.

35. P D Bieniasz, T A Grdina, H P Bogerd, and B R Cullen. 1998. Recruitment of a protein complex containing Tat and cyclin T1 to TAR governs the species specificity of HIV-1 Tat. EMBO J 17(23): 7056–7065. doi:  10.1093/emboj/17.23.7056

36. Fujinaga K, Cujec TP, Peng J, Garriga J, Price DH, Graña X, Peterlin BM. 1998. The ability of positive transcription elongation factor B to transactivate human immunodeficiency virus transcription depends on a functional kinase domain, cyclin T1, and Tat. Trends J Virol 72(9):7154-9. PMID: 9696809

37. Daugherty MD, Liu B, Frankel AD.2010. Structural basis for cooperative RNA binding and export complex assembly by HIV Rev. Nat Struct Mol Biol 17(11):1337-42 doi: 10.1038/nsmb.1902.

38. DiMattia MA, Watts NR, Stahl SJ, Rader C, Wingfield PT, Stuart DI, Steven AC, Grimes JM. 2010. Implications of the HIV-1 Rev dimer structure at 3.2 A resolution for multimeric binding to the Rev response element. Proc Natl Acad Sci U S A. 107(13):5810-4. doi: 10.1073/pnas.0914946107.

39. Guerrero S, Batisse J, Libre C, Bernacchi S, Marquet R, Paillart JC. 2015. HIV-1 Replication and the Cellular Eukaryotic Translation Apparatus. Virology 7(1):199-218 doi: 10.3390/v7010199.

40. Carlton JM et al. 2007. Draft genome sequence of the sexually transmitted pathogen Trichomonas vaginalis. Science 315(5809):207-12. DOI: 10.1126/science.1132894

41. Morita E, Sandrin V, Chung HY, Morham SG, Gygi SP, Rodesch CK, Sundquist WI. 2007. Human ESCRT and ALIX proteins interact with proteins of the midbody and function in cytokinesis. EMBO 26(19):4215-27. DOI: 10.1038/sj.emboj.7601850

42. Göttlinger HG, Dorfman T, Sodroski JG, Haseltine WA. 1991. Effect of mutations affecting the p6 gag protein on human immunodeficiency virus particle release. Proc Natl Acad Sci U S A. 88(8):3195-9. PMID: 2014240

43. Strack B, Calistri A, Craig S, Popova E, Göttlinger HG. 2003. AIP1/ALIX is a binding partner for HIV-1 p6 and EIAV p9 functioning in virus budding. Cell 114(6):689-99. PMID: 14505569

44. Brik A, Wong CH. 2003. HIV-1 protease: mechanism and drug discovery. Org. Biomol. Chem. 5-14 DOI: 10.1039/B208248A

45. Melikyan GB. 1995. Common principles and intermediates of viral protein-mediated fusion: the HIV-1 paradigm. Retrovirology 5:111. doi: 10.1186/1742-4690-5-111.

46. Melikyan GB, Egelhofer M, von Laer D. 2006. Membrane-Anchored Inhibitory Peptides Capture Human Immunodeficiency Virus Type 1 gp41 Conformations That Engage the Target Membrane prior to Fusion. J Virol 80(7):3249-58. DOI: 10.1128/JVI.80.7.3249-3258.2006

47. Markosyan RM, Cohen FS, Melikyan GB. 2003. HIV-1 envelope proteins complete their folding into six-helix bundles immediately after fusion pore formation. Mol Biol Cell. 14(3):926-38. DOI: 10.1091/mbc.e02-09-0573

48. Briggs JA, Grünewald K, Glass B, Förster F, Kräusslich HG, Fuller SD. 2006. The mechanism of HIV-1 core assembly: insights from three-dimensional reconstructions of authentic virions. Structure. 14(1):15-20. DOI: 10.1016/j.str.2005.09.010

49. Mamede JI, Cianci GC1, Anderson MR1, Hope TJ2. 2017. Early cytoplasmic uncoating is associated with infectivity of HIV-1. Proc Natl Acad Sci U S A. 114(34):E7169-E7178. doi: 10.1073/pnas.1706245114.

50. Francis AC, Marin M, Shi J, Aiken C, Melikyan GB. 2016. Time-Resolved Imaging of Single HIV-1 Uncoating In Vitro and in Living Cells. PLoS Pathog. 12(6):e1005709. doi: 10.1371/journal.ppat.1005709.

51. Francis AC, Melikyan GB. 2018. Single HIV-1 Imaging Reveals Progression of Infection through CA-Dependent Steps of Docking at the Nuclear Pore, Uncoating, and Nuclear Transport. Cell Host Microbe. 23(4):536-548.e6. doi: 10.1016/j.chom.2018.03.009.

52. Forshey BM, von Schwedler U, Sundquist WI, Aiken C. 2002. Formation of a human immunodeficiency virus type 1 core of optimal stability is crucial for viral replication. J Virol. 76(11):5667-77. PMID: 11991995

53. Aiken C. 2006. Viral and cellular factors that regulate HIV-1 uncoating. Curr Opin HIV AIDS. 1(3):194-9. doi: 10.1097/01.COH.0000221591.11294.c1.

54. Lee K et al. 2010. Flexible use of nuclear import pathways by HIV-1. Cell Host Microbe. 7(3):221-33. doi: 10.1016/j.chom.2010.02.007.

55. Price AJ, Jacques DA, McEwan WA, Fletcher AJ, Essig S, Chin JW, Halambage UD, Aiken C, James LC. 2014. Host cofactors and pharmacologic ligands share an essential interface in HIV-1 capsid that is lost upon disassembly. PLoS Pathog. 10(10):e1004459. doi: 10.1371/journal.ppat.1004459.

56. De Iaco A, Santoni F, Vannier A, Guipponi M, Antonarakis S, Luban J. 2013. TNPO3 protects HIV-1 replication from CPSF6-mediated capsid stabilization in the host cell cytoplasm. Retrovirology. 10:20. doi: 10.1186/1742-4690-10-20.

57. Shah VB, Shi J, Hout DR, Oztop I, Krishnan L, Ahn J, Shotwell MS, Engelman A, Aiken C. The host proteins transportin SR2/TNPO3 and cyclophilin A exert opposing effects on HIV-1 uncoating. J Virol. 87(1):422-32. doi: 10.1128/JVI.07177-11.

58. Pornillos O, Ganser-Pornillos BK, Kelly BN, Hua Y, Whitby FG, Stout CD, Sundquist WI, Hill CP, Yeager M. 2009. X-ray structures of the hexameric building block of the HIV capsid. Cell. 137(7):1282-92. doi: 10.1016/j.cell.2009.04.063.

59. Pornillos O, Ganser-Pornillos BK, Yeager M. 2011. Atomic-level modelling of the HIV capsid. Nature. 469(7330):424-7. doi: 10.1038/nature09640.

60. Stremlau M, Perron M, Lee M, Li Y, Song B, Javanbakht H, Diaz-Griffero F, Anderson DJ, Sundquist WI, Sodroski J. 2006. Specific recognition and accelerated uncoating of retroviral capsids by the TRIM5alpha restriction factor. 103(14):5514-9. DOI: 10.1073/pnas.0509996103

61. Pertel T et al. 2011. TRIM5 is an innate immune sensor for the retrovirus capsid lattice. Nature. 472(7343):361-5. doi: 10.1038/nature09976.

62. Panganiban AT, Fiore D. 1988. Ordered interstrand and intrastrand DNA transfer during reverse transcription. Science 241(4869):1064-9. PMID: 2457948

63. Hu WS, Temin HM. 1990. Retroviral recombination and reverse transcription. Science. 250(4985):1227-33. PMID: 1700865

64. van Wamel JL, Berkhout B. 1998. The first strand transfer during HIV-1 reverse transcription can occur either intramolecularly or intermolecularly. Virology. 244(2):245-51. DOI: 10.1006/viro.1998.9096

65. Yu H, Jetzt AE, Ron Y, Preston BD, Dougherty JP. 1998. The nature of human immunodeficiency virus type 1 strand transfers. J Biol Chem 273(43):28384-91. PMID: 9774465

66. Das K et al. 1996. Crystal structures of 8-Cl and 9-Cl TIBO complexed with wild-type HIV-1 RT and 8-Cl TIBO complexed with the Tyr181Cys HIV-1 RT drug-resistant mutant. J Mol Biol 264(5):1085-100. PMID: 9000632

67. Guo Q et al. 2003. Biochemical and genetic characterizations of a novel human immunodeficiency virus type 1 inhibitor that blocks gp120-CD4 interactions. J Virol 77(19):10528-36. PMID: 12970437

68. Bishop KN, Verma M, Kim EY, Wolinsky SM, Malim MH. 2008. APOBEC3G inhibits elongation of HIV-1 reverse transcripts. PLoS Pathog. 4(12):e1000231. doi: 10.1371/journal.ppat.1000231.

69. Mangeat B, Turelli P, Caron G, Friedli M, Perrin L, Trono D. 2003. Broad antiretroviral defence by human APOBEC3G through lethal editing of nascent reverse transcripts. Nature. 424(6944):99-103. DOI: 10.1038/nature01709

70. Sheehy AM, Gaddis NC, Malim MH. 2003. The antiretroviral enzyme APOBEC3G is degraded by the proteasome in response to HIV-1 Vif. Nat Med. 9(11):1404-7. DOI: 10.1038/nm945

71. Yu X, Yu Y, Liu B, Luo K, Kong W, Mao P, Yu XF. 2003. Induction of APOBEC3G ubiquitination and degradation by an HIV-1 Vif-Cul5-SCF complex. 302(5647):1056-60. DOI: 10.1126/science.1089591

72. Fujiwara T, Mizuuchi K. 1998. Retroviral DNA integration: structure of an integration intermediate. Cell 54(4):497-504. PMID: 3401925

73. Brown PO, Bowerman B, Varmus HE, Bishop JM. 1989. Retroviral integration: structure of the initial covalent product and its precursor, and a role for the viral IN protein. Proc Natl Acad Sci U S A. 1989 Apr; 86(8):2525-9. PMID: 2539592

74. B Berkhout, K T Jeang. 1992. Functional roles for the TATA promoter and enhancers in basal and Tat-induced expression of the human immunodeficiency virus type 1 long terminal repeat. J Virol 66(1): 139–149. PMID: 1727476

75. Corboy JR, Buzy JM, Zink MC, Clements JE. 1992. Expression directed from HIV long terminal repeats in the central nervous system of transgenic mice. Science. 258(5089):1804-8. PMID: 1465618

76. Leonard J, Parrott C, Buckler-White AJ, Turner W, Ross EK, Martin MA, Rabson AB.1989. The NF-kappa B binding sites in the human immunodeficiency virus type 1 long terminal repeat are not required for virus infectivity. J Virol. 63(11):4919-24. PMID: 2795721

77. Hogue IB, Grover JR, Soheilian F, Nagashima K, Ono A. 2011. Gag induces the coalescence of clustered lipid rafts and tetraspanin-enriched microdomains at HIV-1

assembly sites on the plasma membrane. J Virol. 85(19):9749-66. doi: 10.1128/JVI.00743-11.

78. Lingwood D, Simons K.2010. Lipid rafts as a membrane-organizing principle. Science 327(5961):46-50. doi: 10.1126/science.1174621.

79. Coskun U, Simons K. 2010. Membrane rafting: from apical sorting to phase segregation. FEBS Lett. 584(9):1685-93. doi: 10.1016/j.febslet.2009.12.043.

80. Charrin S, le Naour F, Silvie O, Milhiet PE, Boucheix C, Rubinstein E. 2009. Lateral organization of membrane proteins: tetraspanins spin their web. 420(2):133-54. doi: 10.1042/BJ20082422.

81. Chertova E et al. 2006. Proteomic and biochemical analysis of purified human immunodeficiency virus type 1 produced from infected monocyte-derived macrophages. J Virol 80(18):9039-52. DOI: 10.1128/JVI.01013-06

82. Grigorov B, Attuil-Audenis V, Perugi F, Nedelec M, Watson S, Pique C, Darlix JL, Conjeaud H, Muriaux D. 2009. A role for CD81 on the late steps of HIV-1 replication in a chronically infected T cell line. Retrovirology. 6:28. doi: 10.1186/1742-4690-6-28.

83. Hogue IB, Hoppe A, Ono A. 2009. Quantitative fluorescence resonance energy transfer microscopy analysis of the human immunodeficiency virus type 1 Gag-Gag

interaction: relative contributions of the CA and NC domains and membrane binding. J Virol 83(14):7322-36. doi: 10.1128/JVI.02545-08.

84. Welsch S, Keppler OT, Habermann A, Allespach I, Krijnse-Locker J, Kräusslich HG. 2007. HIV-1 buds predominantly at the plasma membrane of primary human macrophages. PLoS Pathog 3(3):e36. DOI: 10.1371/journal.ppat.0030036

85. André M, Le Caer JP, Greco C, Planchon S, El Nemer W, Boucheix C, Rubinstein E, Chamot-Rooke J, Le Naour F. 2006. Proteomic analysis of the tetraspanin web using LC-ESI-MS/MS and MALDI-FTICR-MS. Proteomics. 6(5):1437-49.

86. Thomas DJ, Wall JS, Hainfeld JF, Kaczorek M, Booy FP, Trus BL, Eiserling FA, Steven AC. 1991. gp160, the envelope glycoprotein of human immunodeficiency virus type 1, is a dimer of 125-kilodalton subunits stabilized through interactions between their gp41 domains. J Virol. 65(7):3797-803. PMID: 2041094

87. Doores KJ, Bonomelli C, Harvey DJ, Vasiljevic S, Dwek RA, Burton DR, Crispin M, Scanlan CN. 2010. Envelope glycans of immunodeficiency virions are almost entirely oligomannose antigens. Proc Natl Acad Sci U S A. 107(31):13800-5. doi: 10.1073/pnas.1006498107.

88. Wyatt R, Sodroski J. 1998. The HIV-1 envelope glycoproteins: fusogens, antigens, and immunogens. Science. 280(5371):1884-8. PMID: 9632381

89. Allan, J. S., J. E. Coligan, T.-H. Lee, M. F. McLane, P. J. Kanki, J. E. Groopman, and M. Essex. 1985. A new HTLV-III/LAV encoded antigen detected by antibodies from AIDS patients. Science 230:810–813. PMID: 2997921

90. Muesing MA, Smith DH, Cabradilla CD, Benton CV, Lasky LA, Capon DJ. 1985. Nucleic acid structure and expression of the human AIDS/lymphadenopathy retrovirus. Nature 7-13;313(6002):450-8. PMID: 2982104

91. Broliden PA, von Gegerfelt A, Clapham P, Rosen J, Fenyö EM, Wahren B, Broliden K. 1992. Identification of human neutralization-inducing regions of the human immunodeficiency virus type 1 envelope glycoproteins. Proc Natl Acad Sci U S A. 89(2):461-5. PMID: 1370580

92. Kennedy RC, Henkel RD, Pauletti D, Allan JS, Lee TH, Essex M, Dreesman GR.1986. Antiserum to a synthetic peptide recognizes the HTLV-III envelope glycoprotein. Science. 231(4745):1556-9. PMID: 3006246

93. Postler TS , Martinez-Navio JM, Yuste E, Desrosiers RC. 2012. Evidence against extracellular exposure of a highly immunogenic region in the C-terminal domain of the simian immunodeficiency virus gp41 transmembrane protein. J Virol. 86(2):1145-57. doi: 10.1128/JVI.06463-11.

94. Vella C, Minor PD, Weller IV, Jenkins O, Evans D, Almond J. 1991. Recognition of poliovirus/HIV chimaeras by antisera from individuals with HIV infection. AIDS. 5(4):425-30. PMID: 1647790

95. Eisenberg D, Wesson M. 1990. The most highly amphiphilic alpha-helices include two amino acid segments in human immunodeficiency virus glycoprotein 41. Biopolymers. 29(1):171-7. DOI: 10.1002/bip.360290122

96. Kliger Y, Shai Y. 1997. A leucine zipper-like sequence from the cytoplasmic tail of the HIV-1 envelope glycoprotein binds and perturbs lipid bilayers. Biochemistry.36(17):5157-69. DOI: 10.1021/bi962935r

97. Murphy RE, Samal AB, Vlach J, Saad JS. 2017. Solution Structure and Membrane Interaction of the Cytoplasmic Tail of HIV-1 gp41 Protein. Structure. 25(11):1708-1718.e5. doi: 10.1016/j.str.2017.09.010.

98. Moreno MR, Pérez-Berná AJ, Guillén J, Villalaín J. 2008. Biophysical characterization and membrane interaction of the most membranotropic region of the HIV-1 gp41 endodomain. Biochim Biophys Acta. 1778(5):1298-307. doi: 10.1016/j.bbamem.2007.12.023.

99. Srinivas SK, Srinivas RV, Anantharamaiah GM, Segrest JP, Compans RW. 1992. Membrane interactions of synthetic peptides corresponding to amphipathic helical

segments of the human immunodeficiency virus type-1 envelope glycoprotein. J Biol Chem. 267(10):7121-7. PMID: 1551918

100. Haffar OK, Dowbenko DJ, Berman PW. 1991. The cytoplasmic tail of HIV-1 gp160 contains regions that associate with cellular membranes. Virology. 180(1):439-41. PMID: 1984664

101. Karlsson Hedestam GB, Guenaga J, Corcoran M, Wyatt RT. 2017. Evolution of B cell analysis and Env trimer redesign. Immunol Rev. 275(1):183-202. doi: 10.1111/imr.12515.

102. Carr CM, Kim PS. 1993. A spring-loaded mechanism for the conformational change of influenza hemagglutinin. Cell. 73(4):823-32. PMID: 8500173

103. Mulligan MJ, Yamshchikov GV, Ritter GD Jr, Gao F, Jin MJ, Nail CD, Spies CP, Hahn BH, Compans RW. 1992. Cytoplasmic domain truncation enhances fusion activity by the exterior glycoprotein complex of human immunodeficiency virus type 2 in selected cell types. J Virol. 66(6):3971-5. PMID: 1583738

104. Ritter GD Jr, Mulligan MJ, Lydy SL, Compans RW.1993. Cell fusion activity of the simian immunodeficiency virus envelope protein is modulated by the intracytoplasmic domain. Virology. 197(1):255-64. DOI: 10.1006/viro.1993.1586

105. Abrahamyan LG, Mkrtchyan SR, Binley J, Lu M, Melikyan GB, Cohen FS. 2005. The cytoplasmic tail slows the folding of human immunodeficiency virus type 1 Env from a late prebundle configuration into the six-helix bundle. J Virol. 79(1):106-15. DOI: 10.1128/JVI.79.1.106-115.2005

106. Kalia V, Sarkar S, Gupta P, Montelaro RC.2003. Rational site-directed mutations of the LLP-1 and LLP-2 lentivirus lytic peptide domains in the intracytoplasmic tail of human immunodeficiency virus type 1 gp41 indicate common functions in cell-cell fusion but distinct roles in virion envelope incorporation. J Virol. 77(6):3634-46. PMID: 12610139

107. Jiang J, Aiken C. 2007. Maturation-dependent human immunodeficiency virus type 1 particle fusion requires a carboxyl-terminal region of the gp41 cytoplasmic tail. J Virol. 81(18):9999-10008. DOI: 10.1128/JVI.00592-07

108. Murakami T, Ablan S, Freed EO, Tanaka Y.2004. Regulation of human immunodeficiency virus type 1 Env-mediated membrane fusion by viral protease activity. J Virol. 78(2):1026-31. PMID: 14694135

109. Wyma DJ, Jiang J, Shi J, Zhou J, Lineberger JE, Miller MD, Aiken C. 2004. Coupling of human immunodeficiency virus type 1 fusion to virion maturation: a novel role of the gp41 cytoplasmic tail. J. Virol. 78:3429–3435 PMID: 15016865

110. Wyss S, Dimitrov AS, Baribaud F, Edwards TG, Blumenthal R, Hoxie JA. 2005. Regulation of human immunodeficiency virus type 1 envelope glycoprotein fusion by a membrane-interactive domain in the gp41 cytoplasmic tail. J Virol. 79(19):12231-41. DOI: 10.1128/JVI.79.19.12231-12241.2005

111. Dorfman T, Mammano F, Haseltine WA, Göttlinger HG. 1994. Role of the matrix protein in the virion association of the human immunodeficiency virus type 1 envelope glycoprotein. J. Virol. 68:1689–1696 PMID: 8107229

112. González SA, Affranchino JL, Gelderblom HR, Burny A. 1993. Assembly of the matrix protein of simian immunodeficiency virus into virus-like particles. Virology 194:548–556 DOI: 10.1006/viro.1993.1293

113. Manrique JM, Celma CCP, Hunter E, Affranchino JL, González SA. 2003. Positive and negative modulation of virus infectivity and envelope glycoprotein incorporation into virions by amino acid substitutions at the N terminus of the simian immunodeficiency virus matrix protein. J. Virol. 77:10881–10888 PMID: 14512538

114. Göttlinger HG, Sodroski JG, Haseltine WA. 1989. Role of capsid precursor processing and myristoylation in morphogenesis and infectivity of human immunodeficiency virus type 1. Proc. Natl. Acad. Sci. U. S. A. 86:5781–5785 PMID: 2788277

115. Zhou W, Parent LJ, Wills JW, Resh MD. 1994. Identification of a membrane-binding domain within the amino-terminal region of human immunodeficiency virus type 1 Gag protein which interacts with acidic phospholipids. J. Virol. 68:2556–2569 PMID: 8139035

116. Gallina A, Mantoan G, Rindi G, Milanesi G. 1994. Influence of MA internal sequences, but not of the myristylated N-terminus sequence, on the budding site of HIV-1 Gag protein. Biochem. Biophys. Res. Commun. 204:1031–1038 DOI: 10.1006/bbrc.1994.2566

117. Ono A, Orenstein JM, Freed EO. 2000. Role of the Gag matrix domain in targeting human immunodeficiency virus type 1 assembly. J. Virol. 74:2855–2866 PMID: 10684302

118. Ono A, Ablan SD, Lockett SJ, Nagashima K, Freed EO. 2004. Phosphatidylinositol (4,5) bisphosphate regulates HIV-1 Gag targeting to the plasma membrane. Proc. Natl. Acad. Sci. U. S. A. 101:14889–14894 DOI: 10.1073/pnas.0405596101

119. Chukkapalli V, Hogue IB, Boyko V, Hu Ono W-SA. 2008. Interaction between the human immunodeficiency virus type 1 Gag matrix domain and phosphatidylinositol-(4,5)-bisphosphate is essential for efficient Gag membrane binding. J. Virol. 82:2405–2417 DOI: 10.1128/JVI.01614-07

120. Fäcke M, Janetzko A, Shoeman RL, Kräusslich HG. 1993. A large deletion in the matrix domain of the human immunodeficiency virus gag gene redirects virus particle assembly from the plasma membrane to the endoplasmic reticulum. J. Virol. 67:4972–4980 PMID: 8331736

121. H Reil, A A Bukovsky, H R Gelderblom, and H G Göttlinger. 1998. Efficient HIV-1 replication can occur in the absence of the viral matrix protein. EMBO J. 17(9): 2699–2708. doi: 10.1093/emboj/17.9.2699

122. Murakami T, Freed EO. 2000. Genetic evidence for an interaction between human immunodeficiency virus type 1 matrix and alpha-helix 2 of the gp41 cytoplasmic tail. J. Virol. 74:3548–3554 PMID: 10729129

123. Freed EO, Martin MA. 1995. Virion incorporation of envelope glycoproteins with long but not short cytoplasmic tails is blocked by specific, single amino acid substitutions in the human immunodeficiency virus type 1 matrix. J. Virol. 69:1984–1989 PMID: 7853546

124. Tedbury PR, Novikova M, Ablan SD, Freed EO. Biochemical evidence of a role for matrix trimerization in HIV-1 envelope glycoprotein incorporation. Proc Natl Acad Sci U S A. 113(2):E182-90. doi: 10.1073/pnas.1516618113.

125. Tedbury P, Freed O. 2014. The role of matrix in HIV-1 envelope glycoprotein incorporation. Trends in Microbiology VOLUME 22, ISSUE 7, P372-378

126. Berlioz-Torrent C, Shacklett BL, Erdtmann L, Delamarre L, Bouchaert I, Sonigo P, Dokhelar MC, Benarous R. 1999. Interactions of the cytoplasmic domains of human and simian retroviral transmembrane proteins with components of the clathrin adaptor complexes modulate intracellular and cell surface expression of envelope glycoproteins. J. Virol. 73:1350–1361 PMID: 9882340

127. Bowers K, Pelchen-Matthews A, Hoening S, Vance PJ, Creary L, Haggarty BS, Romano J, Ballensiefen W, Hoxie JA, Marsh M. 2000. The simian immunodeficiency virus envelope glycoprotein contains multiple signals that regulate its cell surface expression and endocytosis. Traffic 1:661–674 PMID: 11208154

128. Ohno H, Aguilar RC, Fournier Hennecke M-CS, Cosson P, Bonifacino JS. 1997. Interaction of endocytic signals from the HIV-1 envelope glycoprotein complex with members of the adaptor medium chain family. Virology 238:305–315 DOI: 10.1006/viro.1997.8839

129. Postler TS, Desrosiers RC. 2012. The cytoplasmic domain of the HIV-1 glycoprotein gp41 induces NF-κB activation through TGF-β-activated kinase 1. Cell Host Microbe 11:181–193 DOI: 10.1016/j.chom.2011.12.005

130. Chertova E, Bess JWJ, Crise BJ, Sowder IR, Schaden TM, Hilburn JM, Hoxie JA, Benveniste RE, Lifson JD, Henderson LE, Arthur LO. 2002. Envelope glycoprotein incorporation, not shedding of surface envelope glycoprotein (gp120/SU), is the primary determinant of SU content of purified human immunodeficiency virus type 1 and simian immunodeficiency virus. J. Virol. 76:5315–5325 PMID: 11991960

131. Zhu P, Chertova E, Bess JJ, Lifson JD, Arthur LO, Liu J, Taylor KA, Roux KH. 2003. Electron tomography analysis of envelope glycoprotein trimers on HIV and simian immunodeficiency virus virions. Proc. Natl. Acad. Sci. U. S. A. 100:15812–15817 DOI: 10.1073/pnas.2634931100

132. Brandenberg OF, Magnus C, Rusert P, Regoes RR, Trkola A. 2015. Different infectivity of HIV-1 strains is linked to number of envelope trimers required for entry. PLoS Pathog. 11(1):e1004595. doi: 10.1371/journal.ppat.1004595.

133. Zhu P, Liu J, Bess J Jr, Chertova E, Lifson JD, Grisé H, Ofek GA, Taylor KA, Roux KH. 2006. Distribution and three-dimensional structure of AIDS virus envelope spikes. Nature. 441(7095):847-52 DOI: 10.1038/nature04817

134. Egan MA, Carruth LM, Rowell JF, Yu X, Siliciano RF. 1996. Human immunodeficiency virus type 1 envelope protein endocytosis mediated by a highly conserved intrinsic internalization signal in the cytoplasmic domain of gp41 is suppressed in the presence of the Pr55gag precursor protein. J. Virol. 70:6547–6556 PMID: 8794289

135. Yuste E, Reeves JD, Doms RW, Desrosiers RC. 2004. Modulation of Env content in virions of simian immunodeficiency virus: correlation with cell surface expression and virion infectivity. J. Virol. 78:6775–6785 DOI: 10.1128/JVI.78.13.6775-6785.2004

136. Pegu et al. 2013. Antibodies with High Avidity to the gp120 Envelope Protein in Protection from Simian Immunodeficiency Virus SIVmac251 Acquisition in an Immunization Regimen That Mimics the RV-144 Thai Trial. J Virol. 87(3): 1708–1719. doi: 10.1128/JVI.02544-12

137. Klein JS, Bjorkman PJ. 2010. Few and Far Between: How HIV May Be Evading Antibody Avidity. PLoS Pathog. 6(5): e1000908. doi: 10.1371/journal.ppat.1000908

138. Kuiken. 2009. HIV Sequence Compendium 2009 Report LA-UR 09–03280

139. Hirsch VM, Olmsted RA, Murphey-Corb M, Purcell RH, Johnson PR. 1989. An African primate lentivirus (SIVsm) closely related to HIV-2. Nature. 339(6223):389-92. DOI: 10.1038/339389a0

140. Kodama T, Burns DP, Kestler HW 3rd, Daniel MD, Desrosiers RC.1990. Molecular changes associated with replication of simian immunodeficiency virus in human cells. J Med Primatol. 19(3-4):431-7. PMID: 2231694

141. Kodama T, Wooley DP, Naidu YM, Kestler HW 3rd, Daniel MD, Li Y, Desrosiers RC. 1989. Significance of premature stop codons in env of simian immunodeficiency virus. J Virol. 63(11):4709-14. PMID: 2795718

142. Traub LM. 2009. Tickets to ride: selecting cargo for clathrin-regulated internalization. Nat. Rev. Mol. Cell Biol. 10:583–596 DOI: 10.1038/nrm2751

143. González SA, Burny A, Affranchino JL. 1996. Identification of domains in the simian immunodeficiency virus matrix protein essential for assembly and envelope glycoprotein incorporation. J. Virol. 70:6384–6389.

144. Lei EP, Silver PA. Protein and RNA export from the nucleus. 2002. Dev Cell. Mar;2(3):261-72.

145. Chakrabarti L, Emerman M, Tiollais P, Sonigo P. 1989. The cytoplasmic domain of simian immunodeficiency virus transmembrane protein modulates infectivity. J. Virol. 63:4395– 4403.

146. Yuste E, Johnson W, Pavlakis GN, Desrosiers RC. 2005. Virion envelope content, infectivity, and neutralization sensitivity of simian immunodeficiency virus. J. Virol. 79:12455–12463.

147. Rowell JF, Ruff AL, Guarnieri FG, Staveley-O'Carroll K, Lin X, Tang J, August JT, Siliciano RF. 1995. Lysosome-associated membrane protein-1-mediated targeting of the HIV-1 envelope protein to an endosomal/lysosomal compartment enhances its presentation to MHC class II-restricted T cells. J Immunol. 155:1818–28.

# Chapter II: HIV-1 Envelope Glycoprotein Trafficking through the Endosomal Recycling Compartment Is Required for Particle Incorporation

Junghwa Kirschman[1], Mingli Qi[1], Lingmei Ding[2], Jason Hammonds[2], Krista Dienger-Stambaugh[2], Jaang-Jiun Wang[2], Lynne A. Lapierre[3], James R. Goldenring[3], Paul Spearman[2]

[1] Department of Pediatrics, Emory University, Atlanta, Georgia, USA

[2] Department of Pediatrics, Cincinnati Children's Hospital Medical Center, Cincinnati, Ohio, USA

[3] Departments of Surgery and Cell Biology, Epithelial Biology Center, Vanderbilt University Medical Center, and the Nashville VAMC, Nashville, Tennessee, USA

Published in *Journal of Virology*, 2018, 12;92(5), PMID: 29212940

Abstract

The human immunodeficiency virus type 1 (HIV-1) envelope glycoprotein (Env) encodes specific trafficking signals within its long cytoplasmic tail (CT) that regulate incorporation into HIV-1 particles. Rab11-family interacting protein 1C (FIP1C) and Rab14 are host trafficking factors required for Env particle incorporation, suggesting that Env undergoes sorting from the endosomal recycling compartment (ERC) to the site of particle assembly on the plasma membrane. We disrupted outward sorting from the ERC by expressing a C-terminal fragment of FIP1C ($FIP1C_{560-649}$) and examined the consequences on Env trafficking and incorporation into particles. $FIP1C_{560-649}$ reduced cell surface levels of Env and prevented its incorporation into HIV-1 particles. Remarkably, Env was trapped in an exaggerated perinuclear ERC in a CT-dependent manner. Mutation of either the YxxL endocytic motif or the $YW_{795}$ motif in the CT prevented Env trapping in the ERC and restored incorporation into particles. In contrast, simian immunodeficiency virus SIVmac239 Env was not retained in the ERC, while substitution of the HIV-1 CT for the SIV CT resulted in SIV Env retention in this compartment. These results provide the first direct evidence that Env traffics through the ERC and support a model whereby HIV-1 Env is specifically targeted to the ERC prior to FIP1C- and CT-dependent outward sorting to the particle assembly site on the plasma membrane.

## Introduction

The mechanism of human immunodeficiency virus type 1 (HIV-1) envelope (Env) incorporation into developing particles is incompletely understood. Four possible models of Env incorporation have been proposed, including passive incorporation, direct Gag-Env interaction, Gag-Env cotargeting, and indirect Gag-Env interaction models (1, 2). Lentiviral envelope glycoproteins bear unusually long cytoplasmic tails (CTs) compared to those of other retroviruses (1, 3). Truncation of the HIV-1 CT does not disrupt incorporation into the developing particle when Env is expressed in certain permissive cell types, such as 293T or HeLa cells. However, the long Env CT is required for particle incorporation, infectivity, and cell-cell spread of virus in most T cell lines, in primary T lymphocytes, and in monocyte-derived macrophages (MDMs) (4). Distinct cellular trafficking signals have been identified within the HIV-1 CT. A membrane proximal YxxL motif interacts with the AP-2 clathrin adaptor complex and mediates clathrin-dependent endocytosis of Env (5–7). This motif has been shown to be important for mediating particle incorporation, infectivity, and basolateral targeting of Env (8–10). A dileucine motif located at the C terminus of the CT mediates interactions with the AP-1 clathrin adaptor complex (5, 11). Additional conserved tyrosine-based motifs and dileucine motifs are present within the CT and have variable effects on cell surface expression and virion incorporation, as judged by mutagenesis studies (12).

We previously described a role for Rab11-family interacting protein 1C (FIP1C; also known as Rab coupling protein or RCP) and Rab14 in HIV-1 Env trafficking and

particle incorporation (13). FIP1C forms a parallel homodimer capable of binding to two Rab molecules through its C-terminal Rab binding domain (RBD) (14, 15). In HeLa cells, FIP1C is largely concentrated in a perinuclear structure representing the endosomal recycling compartment (ERC) (16, 17). However, upon expression of HIV-1 Env, FIP1C redistributes to the cellular periphery along with Env (13). The redistribution of FIP1C depends upon specific sequences within the Env CT, as either a CT truncation mutant or the YW795SL mutant within the CT failed to elicit FIP1C redistribution (18). The YW795SL mutant was deficient in Env incorporation and replicated poorly in T cell lines, while a second-site revertant near the carboxyl-terminal end of the tail (L850S) restored FIP1C redistribution, Env incorporation, and replication to wild-type (WT) levels. These findings suggested to us that specific structural elements or motifs within the CT interact with FIP1C and Rab14, and that this interaction mediates Env trafficking from the ERC to the site of particle assembly on the plasma membrane (PM). However, there has been no direct evidence thus far supporting the presence of Env in the ERC, where it would need to transiently reside prior to outward sorting in complex with FIP1C and Rab14.

Expression of the carboxyl-terminal domains of FIP1C or of Rab11-FIP2 has been shown to disrupt transferrin recycling and alters the morphology of the ERC (16, 19, 20). Here, we investigated the role of the ERC in Env trafficking by disrupting outward sorting through expression of a carboxyl-terminal fragment of FIP1C. This intervention arrested HIV-1 Env trafficking, resulting in trapping of Env on perinuclear endosomal membranes that were Rab11 and Rab14 positive. Intracellular Env trapping mediated by truncated FIP1C significantly diminished Env incorporation into particles and particle

infectivity. Env trapping in the aberrant ERC was specific to FIP1C, as a comparable carboxyl-terminal fragment from Rab11-FIP2 failed to trap Env. Furthermore, arrest in the ERC was specific to the CT of HIV-1, as simian immunodeficiency virus (SIV) Env was not sequestered in the ERC unless its CT was swapped with that of HIV-1.

## Summary

The HIV-1 envelope glycoprotein is an essential component of infectious viral particles. While many aspects of Env structure and function have been elucidated, its intracellular trafficking pathway prior to reaching the site of particle assembly at the plasma membrane is not well understood. The HIV-1 envelope protein has a very long cytoplasmic tail that interacts with the host cell trafficking machinery. Here we utilized a truncated form of the trafficking adaptor FIP1C protein to arrest the intracellular transportof Env and demonstrated that Env becomes trapped within the endosomal recycling compartment. Intracellular trapping blocked Env incorporation into the released particles and markedly diminished infectivity. Mutations of specific trafficking motifs in the Env cytoplasmic tail prevented itstrapping in the recycling compartment. These results establish that trafficking to the endosomal recycling compartment is an essential step in HIV-1 Env incorporation into particle.

## Results

### *A C-terminal fragment of FIP1C blocks HIV-1 Env localization at the cell surface and prevents virion incorporation.*

To define the role of the ERC in Env trafficking, we expressed a truncated form of FIP1C ($FIP1C_{560–649}$) tagged to green fluorescent protein (GFP) in HeLa cells. Incorporation of Env into released HIV-1 particles was inhibited by $FIP1C_{560–649}$ in a dose-dependent fashion (Fig. 1A, top, Appendix Fig. 1). This effect was not due to reduced synthesis or enhanced degradation of Env, as $FIP1C_{560–649}$ had little effect on cellular levels of gp160 (Fig. 1A, bottom). Titration of full-length GFP-FIP1C did not inhibit Env incorporation (Fig. 1A, right lanes). The infectivity of released particles was diminished by $FIP1C_{560–649}$ in a manner proportional to the removal of Env from particles (Fig. 1B, left) and was slightly increased (rather than diminished) by expression of the full-length FIP1C (Fig. 1B, right). We next asked if truncated FIP1C altered cell surface Env levels. $FIP1C_{560–649}$ expression resulted in a significant reduction of cell surface Env, as measured by flow cytometry of nonpermeabilized cells (Fig. 1C, left), while cell surface levels were not significantly altered by wild-type FIP1C expression (Fig. 1C, right). These results indicated to us that $FIP1C_{560–649}$ exerts a negative effect on Env incorporation into virions through a mechanism that reduces Env cell surface levels but does not significantly alter total cellular Env, suggesting that Env is trapped in an intracellular location.

### *HIV-1 Env is trapped in the ERC by overexpression of $FIP1C_{560–649}$.*

To define the mechanism underlying the disruption in Env particle incorporation, we examined the subcellular distribution of Env when coexpressed with either wild-type FIP1C or FIP1C$_{560–649}$. Wild-type FIP1C demonstrated a prominent perinuclear localization but also some more diffuse and punctate signals in HeLa cells (Fig. 2A). FIP1C$_{560–649}$ was also found in a pronounced perinuclear compartment with less prominent peripheral puncta (Fig. 2B). We have previously shown that WT FIP1C is redistributed from the perinuclear ERC to the cellular periphery upon expression of HIV-1 Env with a fulllength CT (13, 18). Characteristic redistribution of wild-type FIP1C upon Env expression is shown in Fig. 2C. In stark contrast, FIP1C$_{560–649}$ remained tightly concentrated in a perinuclear location in the presence of HIV-1 Env (Fig. 2D). Remarkably, Env was found to colocalize very strongly with FIP1C$_{560–649}$, indicating trapping of Env within the ERC (Fig. 2D). Trapping of Env correlated with a loss of Env from the cell surface upon FIP1C$_{560–649}$ expression (Fig. 1C and 3A). To determine if Env trapping in the ERC was dependent upon the presence of the Env CT, we examined the distribution of CT144 Env, which lacks all but the membrane-proximal six residues of the CT. CT144 Env was not trapped by FIP1C$_{560–649}$ but was found on cellular membranes and largely excluded from the ERC (Fig. 2E). The level of CT144 Env on the cell surface was unaffected by FIP1C$_{560–649}$ expression (Fig. 3B). We reasoned that the trapping of Env could have been due to a general disruption of recycling from the ERC by overexpression of FIP1C$_{560–649}$ or could represent a specific feature of the FIP1C carboxyl-terminal segment. To examine the specificity of this finding, we expressed a similar fragment of the C terminus of Rab11-FIP2, FIP2$_{452–512}$. This construct expresses the RBD of FIP2 and is similar to one (FIP2$_{446–511}$) previously shown to disrupt

transferrin recycling (19). The subcellular distribution of $FIP2_{452–512}$ remained largely perinuclear in the presence of HIV-1 Env but did not result in Env trapping (Fig. 2F) and failed to diminish cell surface Env (Fig. 3D, compare titration to that of $FIP1C_{560–649}$ in C). The colocalization of Env and $FIP1C_{560–649}$ was much higher than that of Env and $FIP2_{452–512}$, as represented in these images and quantified from multiple image stacks (colocalization measurements are presented in Fig. 3E, F, and G).

*Role of tyrosine-based motifs in Env retention in the ERC.*

We have previously identified athe CT mutant, YW795SL, that is deficient in Env particle incorporation in a cell type-specific manner, and proposed that this mutant has a defect in FIP1C-dependent transport to the PM (18). If this is the case, then we would predict that the $YW_{795}SL$ Env escapes retention in the ERC elicited by $FIP1C_{560–649}$. Indeed, this was the case (Fig. 4A; $YW_{795}SL$ is referred to here as S5). We note that the overlap of Env and $FIP1C_{560–649}$ signal was partial upon expression of $YW_{795}SL$ Env, but clearly Env was present more abundantly on cytoplasmic membranes and the PM than was seen for WT Env (compare Fig. 4A to 2D). Cell surface Env levels reflected a slight downregulation of $YW_{795}SL$ Env compared to wild-type Env (Fig. 4E, compare to D). We next examined a revertant virus derived from serial passage of $YW_{795}SL$ in which a second-site change ($L_{850}S$) near the C terminus of the CT restored Env particle incorporation and infectivity (18). The $YW_{795}SL/L_{850}S$ revertant Env was retained in the ERC by $FIP1C_{560–649}$ in a manner similar to that of the wild type (Fig. 4B; the revertant is referred to as S5R Env). ERC retention was associated with a significant decrease in cell surface levels (Fig. 4F). The membrane-proximal YXXL motif of the CT has been shown

to be involved in AP-2- dependent endocytosis and to play a role in particle incorporation (6, 7, 21). We reasoned that AP-2-dependent endocytosis may be required to deliver Env to the ERC. We therefore expressed provirus incorporating the $Y_{712}C$ mutant that abrogates AP-2 interaction together with $FIP1C_{560–649}$. In this case, we observed no trapping of Env in the ERC (Fig. 4C), and the cell surface levels of $Y_{712}C$ Env were unaffected (Fig. 4G). The extent of Env retention in the ERC was quantified using Pearson's correlation coefficient (Fig. 4H) and the M2 correlation coefficient (representing Env pixels colocalizing with FIP1C pixels) from 10 representative three-dimensional (3D) image stacks for each of the trafficking mutants shown in Fig. 4A to C. The extent of trapping was greatest for $YW_{795}SL/L_{850}S$ revertant Env (S5R) and least for $Y_{712}C$, as can be seen from either measure (Fig. 4H and I), while differences in the degree of colocalization/trapping between S5 and S5R were more apparent when Env/FIP1C signal is measured by the M2 coefficient representing the red (Env) pixels colocalized with green pixels (Fig. 4I). The absence of $Y_{712}C$ trapping suggested to us that endocytosis of Env from the plasma membrane mediated by AP-2 is required for Env to reach the ERC, where $FIP1C_{560–649}$ is available to sequester Env.

We next asked if $YW_{795}SL$ Env and $Y_{712}C$ Env incorporation into virion particles was also differentially altered upon $FIP1C_{560–649}$ expression. WT NL4-3 Env incorporation was inhibited by $FIP1C_{560–649}$ expression as described above (Fig. 5A, left), while $YW_{795}SL$ Env was resistant to this effect (Fig. 5A, middle blots). The second-site revertant $YW_{795}SL/L_{850}S$ regained sensitivity to inhibition by $FIP1C_{560–649}$ (Fig. 5A, right). Both CT144 and $Y_{712}C$ Env-bearing proviruses were resistant to the effects of $FIP1C_{560–649}$ (Fig. 5B). In summary of this series of experiments, mutations disrupting

FIP1C-dependent trafficking ($YW_{795}SL$) or AP-2-dependent endocytosis ($Y_{712}C$) allowed Env to escape trapping by $FIP1C_{560–649}$ in the ERC and allowed normal levels of Env incorporation into particles budding from HeLa cells. We note that HeLa cells are permissive for Env incorporation into particles by truncated Env, such as CT144, suggesting that an alternative pathway allowing Env incorporation exists in this epithelial line that is not present in many T cell lines or in primary T cells and macrophages (4, 18). This also is likely to explain the robust incorporation of $YW_{795}SL$ Env into particles (Fig. 5A, middle), whereas this Env is inefficiently incorporated in most T cell lines and in primary T cells and macrophages (18).

*SIV Env avoids capture in the ERC by $FIP1C_{560–649}$.*

We next asked if the retention of HIV-1 Env in the ERC by $FIP1C_{560–649}$ was also seen with SIVmac239 Env. Upon expression of full-length $SIV_{mac239}$ provirus, we found that there was no significant trapping of Env by $FIP1C_{560–649}$ (Fig. 6A), while in parallel HIV-1 Env was almost quantitatively trapped as before (Fig. 6B). Cell surface levels matched the phenotype observed by immunofluorescence, as there was no significant shift in surface fluorescence of SIVmac239 Env upon expression of $FIP1C_{560–649}$ (Fig. 6E). To determine if differences in the Env CT led to this dramatically different phenotype, we employed a codon-optimized SIVmac239 Env and created a chimera bearing the ectodomain and TM of SIVmac239 fused to the CT of HIV-1 Env. SIVmac239 codon-optimized Env was not trapped in the ERC, reproducing results with expression from proviral DNA (Fig. 6C). The SIV-HIV chimera, in sharp contrast, was retained in the ERC upon $FIP1C_{560–649}$ expression (Fig. 6D). Cell surface levels of SIVmac239 Env were

unaffected by expression of FIP1C$_{560–649}$, while the surface distribution of the SIV-HIV CT chimera was shifted significantly (compare Fig. 6G to H). Taking this further, we performed Western blots to examine SIV Env incorporation into particles (Fig. 7). FIP1C$_{560–649}$ expression had no effect on SIV Env incorporation into particles, while in parallel experiments NL4-3 Env was efficiently depleted (Fig. 7A). Expression of codon-optimized HIV Env and Gag together with FIP1C$_{560–649}$ led to depletion of Env from particles (Fig. 7B, left), while SIV Env incorporation onto SIV Gag particles was unaffected (Fig. 7B, middle). Strikingly, replacing the CT of SIV with that of HIV-1 resulted in inhibition of Env incorporation into particles that was FIP1C$_{560–649}$ dependent (Fig. 7B, right). Thus, the lack of trapping of SIVmac239 Env by FIP1C$_{560–649}$ is reflected in normal cell surface levels and particle incorporation, while the SIV-HIV chimeric Env was trapped in the ERC, unable to reach the particle assembly site on the PM and unavailable for efficient incorporation into particles.

*FIP1C$_{560–649}$ induces an aberrant ERC and traps Env on ERC membranes.*

We next focused on the structure of the intracellular compartment responsible for Env trapping using superresolution optical microscopy and electron microscopy (EM). While at lower resolution the ERC appeared as a roughly spherical compartment with a diffuse distribution of FIP1C$_{560–649}$, upon higher resolution it appeared to consist of intertwined and packed tubules. Rab11 and FIP1C were not uniformly distributed on all tubules but demonstrated significant colocalization (Fig. 8A). Env was similarly concentrated more strongly on a subset of tubules (Fig. 8B). The center of the ERC

appeared somewhat hollow compared to the periphery (Fig. 8C to E). We extended this morphological study to the use of transmission electron microscopy (TEM). TEM images revealed compact clusters of tubules with an average diameter (or radius for those visualized on end) of 60 ± 10 nm (Fig. 8F). Control HeLa cells examined in parallel failed to reveal similar structures (not shown), indicating to us that this was an aberrant ERC similar to that described by Damiani and colleagues (20). Using immuno-EM, we found that Env was distributed along the ERC membranes (Fig. 8G). We conclude that FIP1C$_{560–649}$ elicits a condensation of ERC tubules, and that Env becomes trapped on tubular membranes by this intervention and is subsequently unable to reach the particle assembly site on the plasma membrane. The identity of this structure as the ERC was further validated by colocalization of FIP1C$_{560–649}$ with Rab14 and transferrin receptor and by the lack of colocalization of FIP1C$_{560–649}$ with late endosomal markers (Fig. 9, Appendix Fig. 2-4).

*Env CT-dependent internalization and capture within the aberrant ERC.*

Having shown that Env is trapped in the ERC in a CT-dependent manner, we next asked if Env present on the cell surface can reach this compartment (Suppl. Fig. 1, Appendix Fig. 5). To facilitate pulse labeling of cell surface Env, we created an artificial envelope construct composed of an N-terminal fluorogen-activating protein (FAP) domain fused to the TM and CT regions of HIV-1 Env (FAP-TMCT). This allowed fluorescent pulse labeling of FAP-TMCT on the cell surface in the absence of internal labeling by using the membrane-impermeant fluorogen MG-11p (22, 23). FAP-TMCT demonstrated PM labeling when cells were exposed to fluorogen on ice (Fig. 10A, z section in center of

cell, and B, at coverslip level). Expression of FIP1C$_{560–649}$ did not alter the cell surface labeling pattern of FAP-TMCT (Fig. 10C). At 37°C, however, FAP-TMCT was rapidly internalized from the cell surface. Internalized signal was apparent at the end of a 5-min pulse (Fig. 10D). FAP-TMCT signal was further internalized for 20 min and colocalized significantly with FIP1C$_{560–649}$ (Fig. 10E, with quantitation in M). By 60 min, colocalization of pulsed FAP-TMCT with FIP1C$_{560–649}$ was further enhanced (Fig. 10F, with quantitation in M). As controls, we employed a well-characterized membrane-anchored FAP construct that includes the platelet-derived growth factor (PDGF) receptor transmembrane domain and lacks any HIV sequence (23) and a modified version of FAP-TMCT in which the C-terminal 144 amino acids of the CT are absent (FAP-CT144). The FAP membrane control remained largely, but not entirely, on the cell surface over this time course (Fig. 10G to I). A portion of the surface-labeled FAP-CT144 was rapidly internalized (Fig. 10J) but did not appear to become significantly concentrated in the ERC over time (Fig. 10J to L). Signal from the internalized fraction of both control FAP proteins at 60 min colocalized only weakly with FIP1C$_{560–649}$ compared to that with FAP-TMCT (Fig. 10M). These results support a model in which the Env CT mediates internalization from the PM to the ERC, leading to CT-dependent sequestration in the aberrant ERC formed by FIP1C$_{560–649}$ expression.

# Discussion

HIV-1 Env and Gag must coordinately reach the plasma membrane during the process of particle assembly. How they do so remains unclear. Env is translated as the precursor gp160 protein on ER-bound ribosomes and subsequently forms trimers in the endoplasmic reticulum (ER) (24–28). During transit through the trans-Golgi network (TGN), a furin-like protease cleaves gp160 into SU and TM subunits (29, 30). The form of Env that reaches the surface of the cell is therefore a trimer of SU/TM heterodimers, presumably completely modified and competent for incorporation into virions. Gag is synthesized on cytosolic ribosomes and reaches the inner face of the plasma membrane by an alternate and poorly understood route, where it interacts with phosphatitdylinositol-4,5-bisphosphate (PIP2) and cholesterol-enriched membranes (31–33). The matrix (MA) region of Gag is essential for Env incorporation, as point mutations in MA have been identified that eliminate Env incorporation without disrupting particle assembly and budding (34–36). A direct interaction between Gag and the Env CT has been reported for HIV (37) and for SIV (38), but there has been little additional evidence supporting this. Env exclusion by MA mutants may instead be regulated by a steric clash between the MA lattice and the Env CT created by MA mutants that disrupt the MA trimer interface (39). In support of this model, it was recently shown that MA trimers exist in virions, and that mutations that eliminate trimerization correlated with a loss of Env incorporation (40). This work suggests that the long Env CT must fit within a central aperture within a hexamer of trimers formed by MA at the particle budding site.

We previously reported that the Rab-related adaptor protein FIP1C directs Env incorporation in a CT-dependent manner (13). The Rab protein recruited by FIP1C relevant for Env incorporation was shown to be Rab14. This suggested to us that Env must be delivered to and sorted from the ERC prior to reaching the site of particle assembly. This model is further supported by the finding that a $YW_{795}SL$ mutation in the CT disrupted Env incorporation in a cell type-specific manner identical to that of the CT144 Env lacking most of the cytoplasmic tail (18). A second-site mutant near the C terminus of the CT restored FIP1C-dependent incorporation of Env in Jurkat and H9 T cell lines and in macrophages. The FIP1C-dependent trafficking model of Env incorporation proposes that Env must traffic through the ERC prior to particle incorporation, and that interactions between the CT and the FIP1C/Rab14 complex direct outward sorting of Env to the particle assembly site. This model does not conflict with the steric model of Env exclusion by MA mutants discussed above, but rather helps to incorporate the role of specific trafficking signals in the CT in directing Env to the assembly site.

Here, we employed a dominant-negative approach to further define Env trafficking and the proposed requirement for ERC trafficking. A short C-terminal fragment of FIP1C ($FIP1C_{560–649}$) led to a dramatic trapping of Env in the modified ERC and inhibited incorporation of Env into particles. The YW795SL CT mutant largely escaped trapping in the ERC, while a second-site revertant in the distal CT restored the inhibitory effect of $FIP1C_{560–649}$. Thus, the dominant-negative ERC trapping effect was specific to residues within the Env CT. Furthermore, a similar fragment derived from Rab11-FIP2 failed to inhibit Env incorporation. These results support the ERC trafficking

model for Env incorporation and a specific requirement for FIP1C in outward sorting of Env.

The overexpression of a similar, slightly larger C-terminal fragment of FIP1C, termed H13, was reported previously to create an altered morphology of the ERC in RAW macrophages and to disrupt transferrin recycling to the PM in this cell type (20). A C2 domain deletion of FIP1C similarly caused an accumulation of phosphatidylserine containing membranes in the pericentriolar region of HeLa cells (41). The structures we observed by fluorescence microscopy and by EM in HeLa cells are likely analogous to the altered tubulovesicular endosomes seen in these two prior studies. Both H13 and $FIP1C_{560–649}$ express the FIP1C Rab binding domain, or RBD, which binds to Rab11 GTPase family members (Rab11a, Rab11b, and Rab25/Rab11c) and Rab14 (42). One potential mechanism for the dominant-negative inhibition seen upon RBD fragment overexpression is the sequestration of Rab GTPases required for outward sorting to the plasma membrane. In support of this, Rab11a and Rab14 were found in the current study to be sequestered in the aberrant ERC formed by $FIP1C_{560–649}$ (Fig. 8 and 9). Because Rab14 was previously shown to be required for Env incorporation (13), it seems likely that Rab14 sequestration is involved in Env trapping by $FIP1C_{560–649}$. Immuno-EM studies showed Env associated with tubular ERC membranes upon $FIP1C_{560–649}$ expression. A logical interpretation of these data is that the Env CT and the Rab14-FIP1C complex normally interact on these membranes prior to outward sorting to the particle assembly site on the PM, and that sequestration of the relevant Rab GTPase-FIP1C complex leads to cosequestration of Env in this compartment. It is also possible that the complex of Env with truncated FIP1C and Rab14 is unable to recruit the motor protein

required for transit out of the ERC to the plasma membrane site of assembly. Further experiments are under way to evaluate the model outlined here, including efforts to identify the relevant motor protein involved in Env transit out of the ERC and to define potential protein-protein interactions between FIP1C and the Env CT.

We have previously proposed that Env trimers on the PM must be endocytosed to the ERC in a step preceding outward sorting to the particle assembly site (depicted in Fig. 11). Env is known to be actively endocytosed by an AP-2/clathrin-dependent process that depends upon the $Y_{712}$XXL motif in the proximal portion of the CT (21), and this motif plays a key role in particle infectivity (8). Remarkably, we found that a $Y_{712}$C Env mutant was not trapped by FIP1C$_{560–649}$, consistent with a sequential trafficking model where AP-2-dependent endocytosis to the ERC is followed by FIP1C/Rab14-directed sorting to the particle assembly site on the PM. A second plausible model, however, would not require the appearance of Env first on the PM prior to directed sorting. Notably, the $Y_{712}$XXL motif on the Env CT also interacts with the TGN and endosome-associated AP-1 clathrin adaptor, and AP-1 may direct post-Golgi trafficking of Env through additional CT motifs, such as the C-terminal dileucine motif (11). In this scenario, AP-1-dependent trafficking could direct Env from the TGN to the sorting endosome/ERC, followed by FIP1C/Rab14-dependent outward sorting. Either scenario would be consistent with the fact that dominant-negative FIP1C$_{560–649}$ traps Env prior to outward sorting for particle incorporation. In support of the plausibility of the endocytosis model, we found that an FAP-tagged artificial Env incorporating the HIV-1 Env TM and CT domains was rapidly endocytosed and reached the aberrant ERC created by FIP1C$_{560–649}$ (Fig. 10). We do not suggest that this result rules out the

existence of the TGN-to-ERC pathway, but it does provide supportive evidence that Env on the PM can be endocytosed in a CT-dependent manner and subsequently reach the ERC.

We note the important limitation of performing these experiments in HeLa cells alone. As initially described by the Freed laboratory and also seen in our studies describing FIP1C's role, T cell lines such as Jurkat and H9, as well as primary T cells and macrophages, are nonpermissive for Env incorporation in the absence of the full-length CT (4, 13, 18). We expect that capture of Env with an intact CT would be retained in T cells and macrophages, while the permissive pathway allowing truncated Env to be incorporated would be absent, as in previous studies. While knockdown of FIP1C or Rab14 supports this conclusion (13, 18), unfortunately we have not been able to achieve sustained and efficient expression of $FIP1C_{560–649}$ in T cell lines and primary cells in order to directly reproduce the Env incorporation defects demonstrated here for $FIP1C_{560–649}$ in HeLa cells. We also recognize the potential for unintended effects upon overexpression of a protein that acts in a dominant-negative fashion. We employed overexpression of a similarly truncated FIP2 protein as a control for this but recognize that there may still be unintended effects from overexpression of truncated FIP1C. Confidence in the specificity of our findings was enhanced, however, by the lack of robust ERC trapping of the HIV-1 Env CT mutant $YW_{795}SL$ by $FIP1C_{560–649}$ and by the HIV CT-specific sequestration of HIV/SIV chimeric Env.

How does the regulation of Env incorporation by MA fit with the sequential trafficking model proposed here? In a convergent trafficking model, the delivery of Env by FIP1C/Rab14 to the site of a developing Gag lattice would be consistent with the

trimerization/steric interference model proposed by Tedbury and colleagues (40). Delivery to the common PM site would be followed in the case of MA mutants such as 29/31 KE by steric exclusion of the Env CT and lack of incorporation. Another exciting possibility is that the Gag-membrane interactions originate on tubular ERC membranes enriched in $PI(4,5)P_2$, where Env interacts with the FIP1C/Rab14 complex, and that cotrafficking of Gag and Env on vesicles to a common PM site contributes to incorporation of Env on particles. We note that cotrafficking cannot be obligatory for Gag, however, as disruption of Env trafficking by ERC sequestration does not alter the amount of Gag particles produced. The recognition that ERC trafficking is an essential step in the Env particle incorporation pathway will facilitate future studies to define how Gag and Env reach a common assembly site on the PM.

SIVmac239 Env in this study did not appear to utilize ERC transit for incorporation into virion particles, and this was shown to be dependent on the SIV Env CT. It is possible that FIP1C-dependent outward sorting from the ERC is unique to HIV-1, or that species-specific differences in host trafficking factors exist that do not allow interactions of the SIV CT with the human FIP1C/Rab14-mediated sorting pathway. It is interesting that SIV isolates propagated in human cells frequently truncate their cytoplasmic tails (43, 44), suggesting that host cell differences limit the ability of SIV with a full-length CT to propagate in human cells. Interactions with trafficking pathways, including AP-2/ clathrin-mediated endocytosis, have been implicated in determining SIV Env incorporation and infectivity (45–48). Still, the reasons that SIV CT truncations provide an advantage in human but a disadvantage in simian cells remain poorly defined. Comparisons of FIP1C-dependent trafficking pathways between human and simian cells

may prove informative in understanding these differences.

The inhibition of HIV-1 Env incorporation and particle infectivity using a dominant negative Env trapping strategy was specific to FIP1C and the HIV-1 Env CT. There are currently no antiretroviral drugs targeting Env incorporation. Future studies establishing how the Env CT interacts with components of the FIP1C/Rab14 trafficking complex thus are thus likely to prove provide insights intoinformative in understanding fundamental aspects of the HIV-1 assembly processes and should provide identify novel targets for antiretroviral drug development. Also, targeting the interaction between FIP1C and Env CT could be a good strategy for putative drug development. So far, we are missing information related to direct interaction between FIP1C and Env CT has not be demonstrated, but it would be an important direction for which needs to be confirmed in future studies.

*FIP1C as a dominant-negative inhibitor of Env trafficking*

We showed that a truncated FIP1C construct expressing the C-terminal Rab-binding domain acts as a dominant-negative inhibitor of Env trafficking and incorporation into virions. Also RBD-FIP1C sequesters Env in the ERC. Env trapping in the ERC is dependent upon an intact YW795, Y712 motif in the cytoplasmic tail. Also, we showed that the dominant negative effect of RBD-FIP1C is HIV-1 specific, and that SIV, HIV2 Env is not trapped.

*Rab14 and Rab11-FIP1C*

We previously showed that disruption in Rab-binding sites in FIP1C can impair trafficking of HIV-1 Env toward the plasma membrane (13, 15). The dual mutant FIP1C (S580N S582L) was used in parallel with dominant-negative C- terminal fragment of FIP ($FIP1C_{560-649}$) to see if Rab14 trafficking is affected. Fluorescent microscopy, flow cytometry analysis, and western blot data showed that $FIP1C_{560-649}$ failed to completely trap NL4-3 Env inside the ERC due to moderately impaired outward trafficking by Rab14 (Suppl. Fig. 2). Interestingly, the trapping phenomenon of Env in the presence of FIP1C $_{560-649}$ S580N S582L looked similar to the S5 tyrosine motif mutant (Suppl. Fig. 2C) which suggests (1) a motor protein which interacts with Rab14, such as Kinesin 16B (Kif16B), should colocalize with Env along with Rab 14 (54) (2) Live imaging of the ERC compartment with Rab14 and Env is necessary to understand the path of trafficking in and out of the ERC in the presence of $FIP1C_{560-649}$.

*FIP1C $_{560-649}$ and host restriction factor Tetherin*

We previously observed that the host restriction factor tetherin (BST-2 or CD317) is also trapped inside the ERC (data not shown). The dominant negative effect of FIP1C $_{560-649}$ was effective against Tetherin as well – endogenous Tetherin was sequestered in the ERC with $FIP1C_{560-649}$ (data not shown). We originally speculated ER-Golgi pathways were disturbed by $FIP1C_{560-649}$ but found that gag was not affected at all by this dominant negative effect and $FIP1C_{560-649}$ itself was not toxic to cells. It is most likely Tetherin became trapped in the ERC after endocytosis (55, 56, 57) since there is no evidence whether Tetherin binds to either HIV-1 Env or Rab 14. Further exploration into

other host restriction factors is necessary to determine if they are affected by the dominant negative effect of FIP1C$_{560-649}$ in different cell types.

*FIP1C $_{560-649}$ in human macrophages*

We transduced GFP-FIP1C$_{560-649}$ in monocyte-derived human macrophages based on a lentiviral system using vpx and VSVG packaging vectors. (58). We cultured the monocytes isolated from human blood samples and cultured with GM-CSF for 7-10 days before transduction of GFP-FIP1C$_{560-649}$ along with other packaging vectors. Next, we infected macrophages with AD8 provirus and fixed and stained with Env antibody. Trapping of Env was increased in later time points (Day 2: 58%, Day 4: 71% when fixed at 5 days of infection) (Suppl. Fig. 3 E F).The virus containing compartment marker, CD9, was mostly colocalized with Env and FIP1C$_{560-649}$ in the same compartment (if trapped). P24 Gag was also colocalized with Env at Day 5 and Day 9 (Suppl. Fig. 3 A-D). Overall, the combination of transduction and infection methods had limitations in (1) the expression levels of GFP-FIP1C$_{560-649}$ and (2) a low yield of macrophages infected after transduction. Also, the early infection stage is preferable in order the minimize the formation of abnormal syncytia formation in later stages; however, Env signal was weak and in each experiment there were populations showing heterogeneously trapped Env or even no trapping effect. For further analysis, optimizing the expression of viral proteins would allow better fidelity in measurements.

*FIP in other viruses*

The Rab 11 pathway is important to influenza A virus budding and filament formation (59) while Rab11 vesicles were found forming clusters in influenza A infected cells which contain viral ribonucleotides (60). It would be interesting if FIP1C acted as a proviral host factor in influenza- infected cells assuming that HA proteins of influenza may be a target for FIP1C. Other members of FIP including FIP3 and FIP2 which are rather known to have roles in regulating metastasis in breast cancer cells (61) and gastric cancer cells by modulating cell motility (62). Since Rab11 proteins can form complexes with motor proteins such as myosin, kinesin, and dynein, it would be interesting to see if other viral cargos also interact or hijack this Rab11 trafficking pathway. Even though direct interaction of FIP1C with HIV-1 Env was not shown, probing the interacting proteins in virus infected cells by proteomics may provide bigger windows for other possible proteins contributing to the FIP1C effect on Env.

## Materials and Methods

### *Cells and plasmids.*

HeLa cells were obtained from the American Type Culture Collection (ATCC; CRM-CCL-2). TZM-bl cells were obtained through the NIH AIDS Reagent Program, Division of AIDS, NIAID, NIH, from John C. Kappes, Xiaoyun Wu, and Tranzyme, Inc. HeLa and TZM-bl cells were maintained in DMEM (Dulbecco's modified Eagle medium) containing 10% fetal bovine serum (FBS) and 2 mM penicillin-streptomycin. pNL4-3 proviral plasmid was obtained through the NIH AIDS Reagent Program, Division of AIDS, NIAID, NIH, from Malcolm Martin. pNL4-3CTdel-144-2 Env was kindly provided by Eric Freed at NCI Frederick and is referred to as CT144 in the text. HIV-1 gp41 mutants $Y_{712}C$, S5, and S5R in the pNL4-3 backbone have been described previously (12, 18). GFP-FIP1C and GFP-FIP1$C_{560–649}$ have been described previously (18, 49). GFP-FIP2$_{452–512}$ was generated by PCR amplification using forward primer 5'-GCAGAATTCCACCTATGAAGAGGTTCTACAGGAGCTG-3' and reverse primer 5'-GCAGGATCCTTAACTGTTAGAGAATTTGC-3', followed by cloning into the EcoRI and BamHI sites of the pEGFP-C1 vector (Clontech). Codon-optimized JR-FL gp160 and SIVmac239 gp160 genes were synthesized by GenScript and cloned between EcoRI and EcoRV sites of pcDNA 5/TO (Thermo Fisher Scientific). SIV-HIV chimeric Env was created by overlap extension PCR using inner primers CCATTATACTTTCAGCAGACCTCTTTTCAGACTCTGCTGCCAGCACCTAGG (forward) and TGCTGGCAGCAGATGCTGAAAAGAGGTCTGCTGAAACTAGGA

TGGAGGGCT (reverse) and outer primers ACGAATTCGCCACCATGGGCTGCCTGGGAAATCGA (forward) and TGGATATCTTACAGCAGTGCCCGTTCCAGCCC (reverse) and cloned between EcoRI and EcoRV sites of pcDNA 5/TO. pVRC-3900 expressing codon-optimized HIV-1 Pr55Gag polyprotein (50) was kindly provided by Gary Nabel (VRC, NIH). Fluorogen-activated protein expression constructs were obtained from Spectragenetics (Pittsburgh, PA). Plasmid pMFAP-alpha2 (Spectragenetics) was used as a control and was employed to create pMFAP-TMCT, which placed the TM and CT domains from codon-optimized JR-FL Env (synthesized by GenScript) in frame with the N-terminal alpha2 FAP domain using Sal1 and Not1 sites of pMFAP-alpha2. Oligonucleotides for amplification of the HIV-1 Env TMCT were AGAGTCGACTTCATCATGATTGTGGGAG (Sal1 site, forward oligonucleotide) and CTTCGCGGCCGCTTACAGCAGTGCCCGTT (Not1 site, reverse oligonucleotide). The same plasmid backbone and PCR cloning strategy was used to create the CT truncation construct pMFAP-CT144, using the reverse oligonucleotide CTTCGCGGCCGCTTAATAGCCCTGCCGGACTCG.

*Virus release and infectivity assays*.

GFP-FIP1C$_{560–649}$ or GFP-FIP2$_{452–512}$ and pNL4-3 were cotransfected into HeLa cells using Lipofectamine 2000 (Thermo Fisher Scientific). Cells and supernatants were harvested 48 h posttransfection for analysis by Western blotting, p24 antigen quantitation, and flow cytometry. Infectivity of cell culture supernatants was measured using TZM-bl indicator cells following p24 normalization as previously

described (13). Viruses were pelleted from cell culture supernatants through a 20% sucrose cushion at 20,000 × g for 2 h at 4°C; cells were harvested and pelleted at 800 × g. Virus pellets and HeLa cell lysates were dissolved in radioimmunoprecipitation assay (RIPA) buffer containing protease inhibitors. Virus pellets and cell lysates were separated on 8 to 12% polyacrylamide gels and subjected to Western blotting using antibodies outlined below.

*Antibodies for Western blotting and immunostaining*.

Goat polyclonal antibody AHP2204, from AbD Serotec (D7324), was used for detecting HIV-1 gp120 and gp160 for Western blotting. Murine monoclonal 5009 from BTI Research Reagents was used for blotting HIV-1 gp41. Mouse anti-p24 monoclonal CA-183 (provided by Bruce Chesebro and Kathy Wehrly through the NIH AIDS Research and Reference Reagent Program) was used for enzyme-linked immunosorbent assay (ELISA) to measure HIV-1 Gag in virus-containing culture supernatant and virus pellets; the capture ELISA was performed as previously described (51). Rabbit antiserum to SIV gp120 was obtained from Advanced Biosciences Laboratories. Anti-SIVmac251 p17 monoclonal KK59, from Karen Kent and Caroline Powell, was obtained through the NIH AIDS Reagent Program and was used to detect SIV Gag in Western blotting. IRDye goat anti-mouse, IRDye rabbit anti-goat, and IRDye goat anti-rabbit secondary antibodies from LiCor Biosciences were used for Western blotting. All blots were acquired and analyzed using the LiCor Odyssey infrared detection system. The following antibodies were utilized in immunofluorescence assays: human anti-gp120 antibody IgG1 2G12 was kindly provided by James Crowe (Vanderbilt University), and

b12 and 447-52D were obtained from the NIH AIDS Reagent Program. Anti-Rab11a monoclonal antibody (clone 47) was from Millipore. Monoclonal antibodies detecting EEA1 (clone 14/EEA1), CD63 (clone H5C6), and Lamp1 (CD107a, clone H4A3) were obtained from BD Pharmingen. Anti-transferrin receptor monoclonal antibody (MEM-75) was from Abcam. Anti-TGN46 sheep polyclonal antiserum (AHP500) was purchased from Bio-Rad. Alexa Fluor secondary antibodies and 4',6-diamidino-2-phenylindole (DAPI) were obtained from Molecular Probes.

*Fluorescence microscopy*.

HeLa cells were plated in MatTek 35-mm poly–D-lysine-treated dishes (Brooke Knapp MatTek) overnight and then were cotransfected with HIV-1 provirus and GFP-FIP constructs using Lipofectamine (ThermoFisher Scientific), followed by incubation for 48 h. Before staining, cells were rinsed with phosphate-buffered saline (PBS) three times and fixed in 4% paraformaldehyde for 10 min at room temperature. Cells were washed with PBS three times with mild agitation after fixation and then permeabilized for 10 min with 0.2% Triton X-100, followed by washing with PBS. Dako blocking solution was applied to cells for 30 min under gentle shaking conditions. 2G12 antibody against HIV-1 gp120 was diluted in Dako antibody diluent to 1:300. Anti-goat secondary antibody was diluted in Dako antibody diluent to 1:1,000. All antibodies for immunostaining endocytosis markers were used between 1:1,000 and 1:5,000 dilutions in Dako antibody diluent solution. The coverslips were mounted in Prolong Gold (Thermo Fisher) overnight and imaged on the DeltaVision imaging system (GE Healthcare)

or the OMX imaging system (GE Healthcare) for structured illumination microscopy. The Volocity 6.3 software program (PerkinElmer) was employed for analysis and presentation of microscopic images obtained. Quantitation of colocalization between HIV-1 Env and GFP-FIP1C$_{560–649}$ was performed using Volocity software features, including derivation of Pearson's coefficient and M1 and M2 colocalization coefficients. Statistical differences between colocalization coefficients were calculated by Student's t test as recommended by Dunn et al. (52). For labeling experiments with FAP control, FAP-TMCT, or FAP-TMCT144, HeLa cells were transfected with GFP-FIP1C$_{560–649}$ and pulse labeled with the nonpermeable fluorogen MG-11p from Spectragenetics. Cells were examined the following day at 18 to 20 h after transfection. Cells were exposed to 200 nM MG-11P for 5 min, and then medium was removed and replaced with medium lacking fluorogen to prevent further labeling. Cells were incubated for the indicated times and fixed and imaged as described above, using the Cy5 channel for detection of FAP signal. Pearson's correlation coefficient was derived for 10 imaged fields of cells per construct/time point shown.

Figures

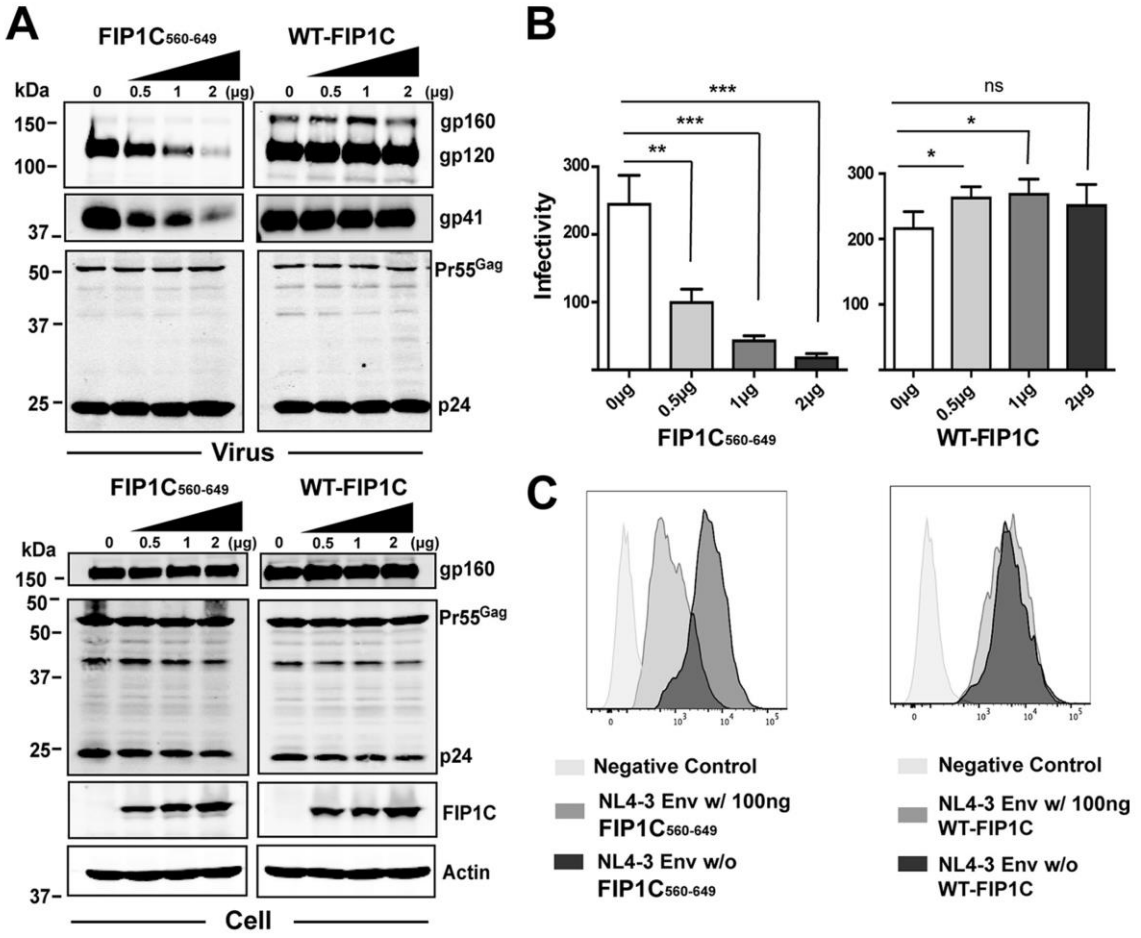


**Fig. 1. Truncated FIP1C inhibits Env incorporation and particle infectivity.**

(A) GFP-FIP1C and truncated mutant of FIP1C ($FIP1C_{560–649}$) plasmids were transfected in increasing concentrations together with a fixed amount of pNL4-3 proviral DNA into HeLa cells. Shown are results of this titration on viral protein content (upper blots) and cellular protein content (lower blots) 48 h posttransfection. (B) Infectivity of virus particles was quantified using TZM-bl cells following dose titration of $FIP1C_{560–649}$ (left) or wild-type FIP1C (right). Results are shown as blue cells/nanogram of p24 and are

presented as means ± standard deviations (SD). Statistical comparisons between groups were performed using the unpaired t test. Graphs shown are representative of major findings from three independent experiments. ns, $\rho > 0.05$; *, $\rho < 0.05$; **, $\rho < 0.001$; ***, $\rho < 0.0001$. (C) Cell surface staining for Env using anti-gp120 mouse monoclonal antibody BDI123 (Novus Biologicals) 48 h following transfection with the indicated constructs. Cells first were gated for GFP-FIP1C expression.

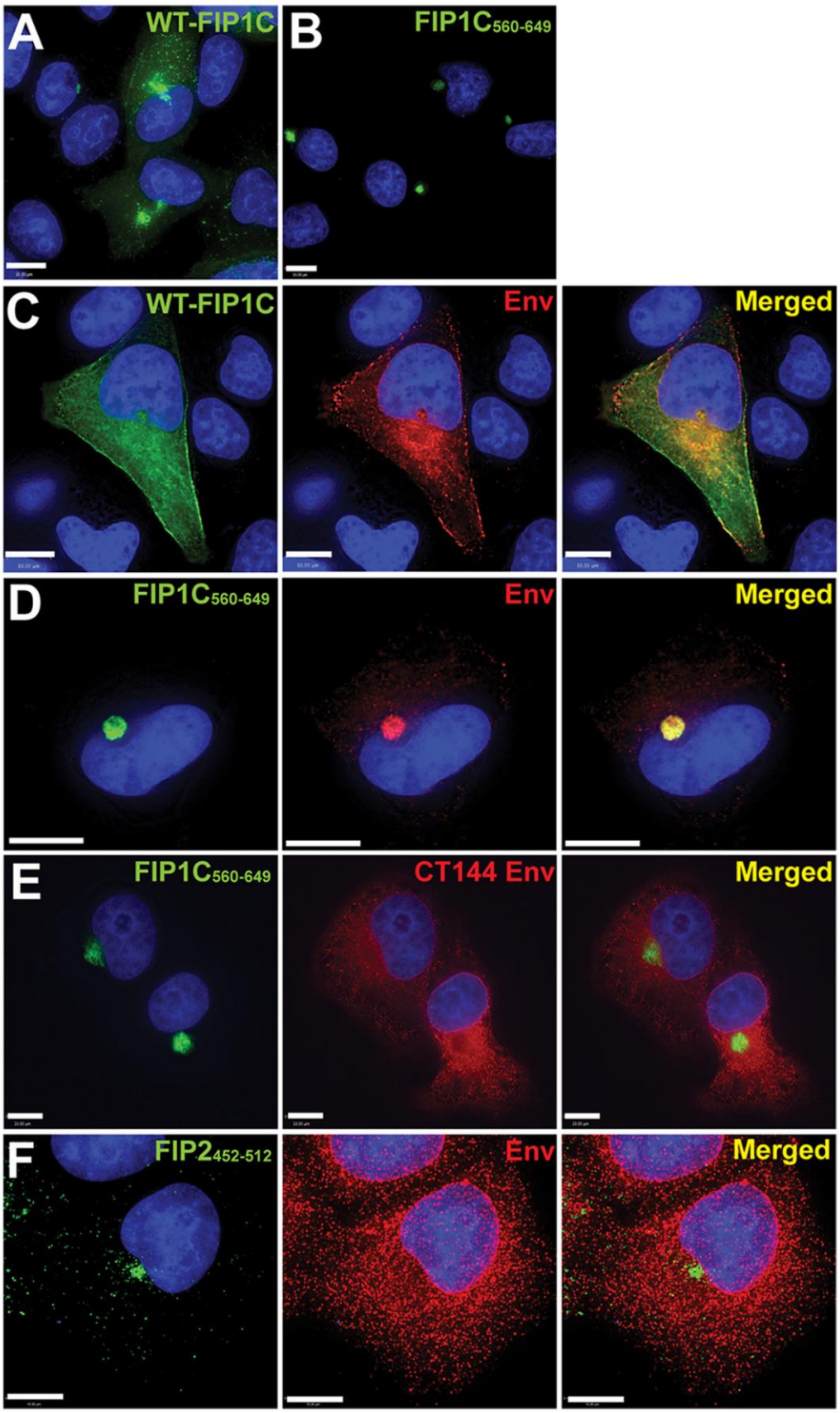
A
WT-FIP1C
B
FIP1C560-649
C
WT-FIP1C
Env
Merged
D
FIP1C560-649
Env
Merged
E
FIP1C560-649
CT144 Env
Merged
F
FIP2452-512
Env
Merged

**Fig. 2. FIP1C$_{560–649}$ sequesters Env in a perinuclear compartment in a CT-dependent manner.**

(A) Wild-type GFP-FIP1C subcellular distribution in HeLa cells when expressed alone. (B) Subcellular distribution of GFP-FIP1C$_{560–649}$. (C) Distribution of wild-type GFP-FIP1C when coexpressed with NL4-3 proviral DNA. Cells were fixed and immunolabeled with human neutralizing antibody 2G12 to stain HIV-1 gp120. Green, GFP-FIP1C; red, Env; rightmost image, overlay. (D) Distribution of FIP1C$_{560–649}$ when coexpressed with NL4-3 proviral DNA. Staining is as described for panel C. (E) Coexpression of FIP1C$_{560–649}$ and CT144 proviral plasmids stained and imaged as described for panel C. (F) GFPFIP2$_{452–512}$ and pNL4-3 proviral expression stained and imaged as described for panel C. All panels shown are from transfected HeLa cells. Images selected are representative of the major phenotypes found for more than 100 cells examined in repeated, independent experiments. Bars represent 10 um.

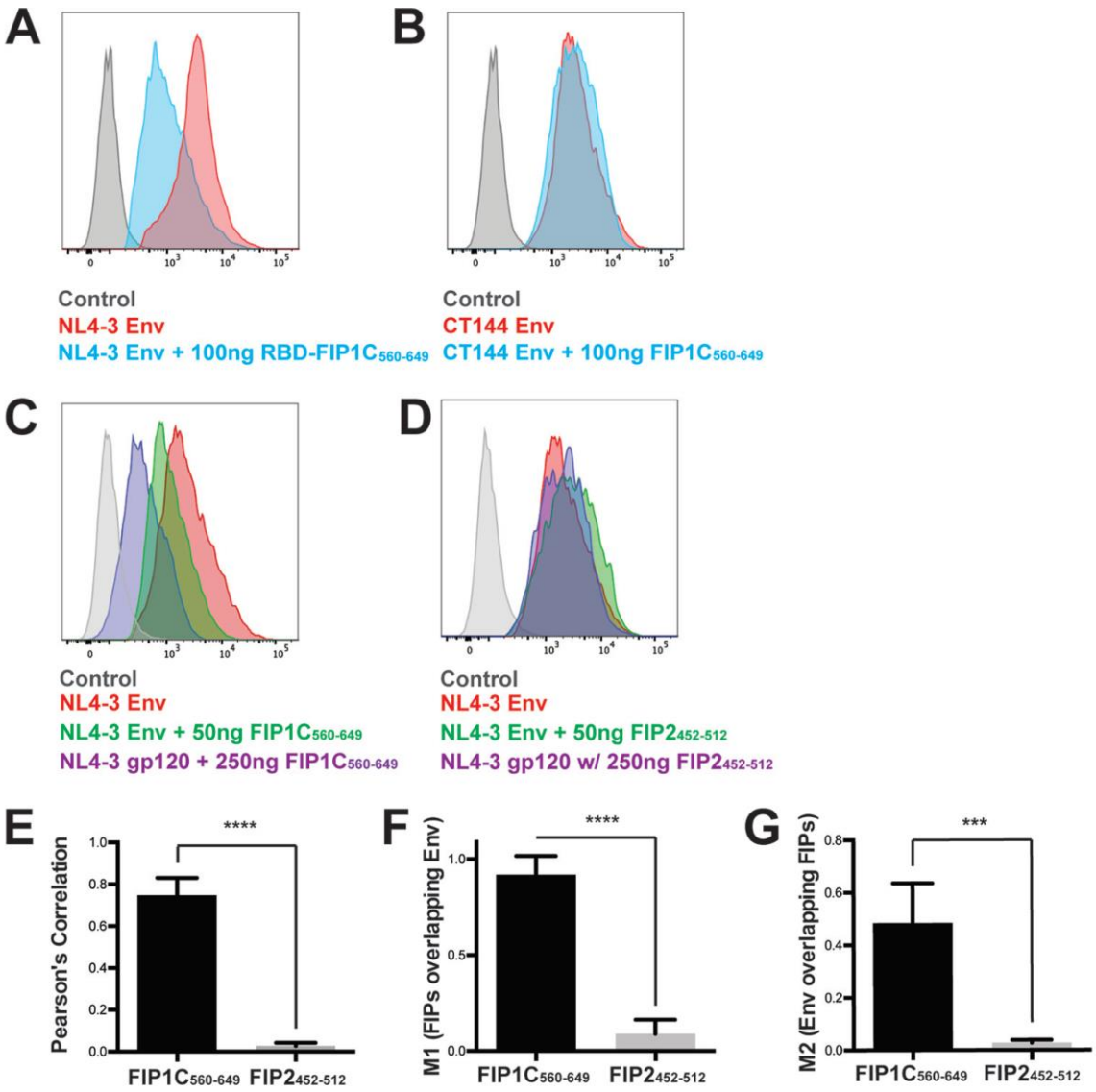


**Fig. 3. Cell surface levels of CT144 Env and effect of FIP1C$_{560–649}$ versus FIP2$_{452–512}$.** (A) HeLa cells were cotransfected with GFP-FIP1C$_{560–649}$ and pNL4-3 proviral plasmid and stained for Env using anti-gp120 mouse monoclonal antibody BDI123. Histograms of cell surface staining are shown in the absence (red) or presence (other colors as indicated) of FIP1C$_{560-649}$ expression. (B) CT144 proviral plasmid was substituted for wild-type Env and cell surface staining repeated with and without GFP-FIP1C$_{560–649}$. (C)

Dose titration of GFP-FIP1C$_{560–649}$ resulted in dose-dependent reduction in cell surface Env signal. (D) Dose titration of GFP-FIP2$_{452–512}$ had little effect on cell surface Env. (E) The degree of colocalization between GFP-FIPs and HIV-1 Env was measured by Pearson's correlation coefficient equation using Volocity 6.3 software after manual thresholding. Results are shown as means ± SD from a total of 10 representative images. ***, $\rho < 0.001$; ****, $\rho < 0.0001$. P values were calculated using the Student's unpaired t test using GraphPad Prism 6. (F and G) Correlation coefficients, FIP1C signal/Env (M1), or Env signal/FIP1C (M2) from the images examined for panel E.

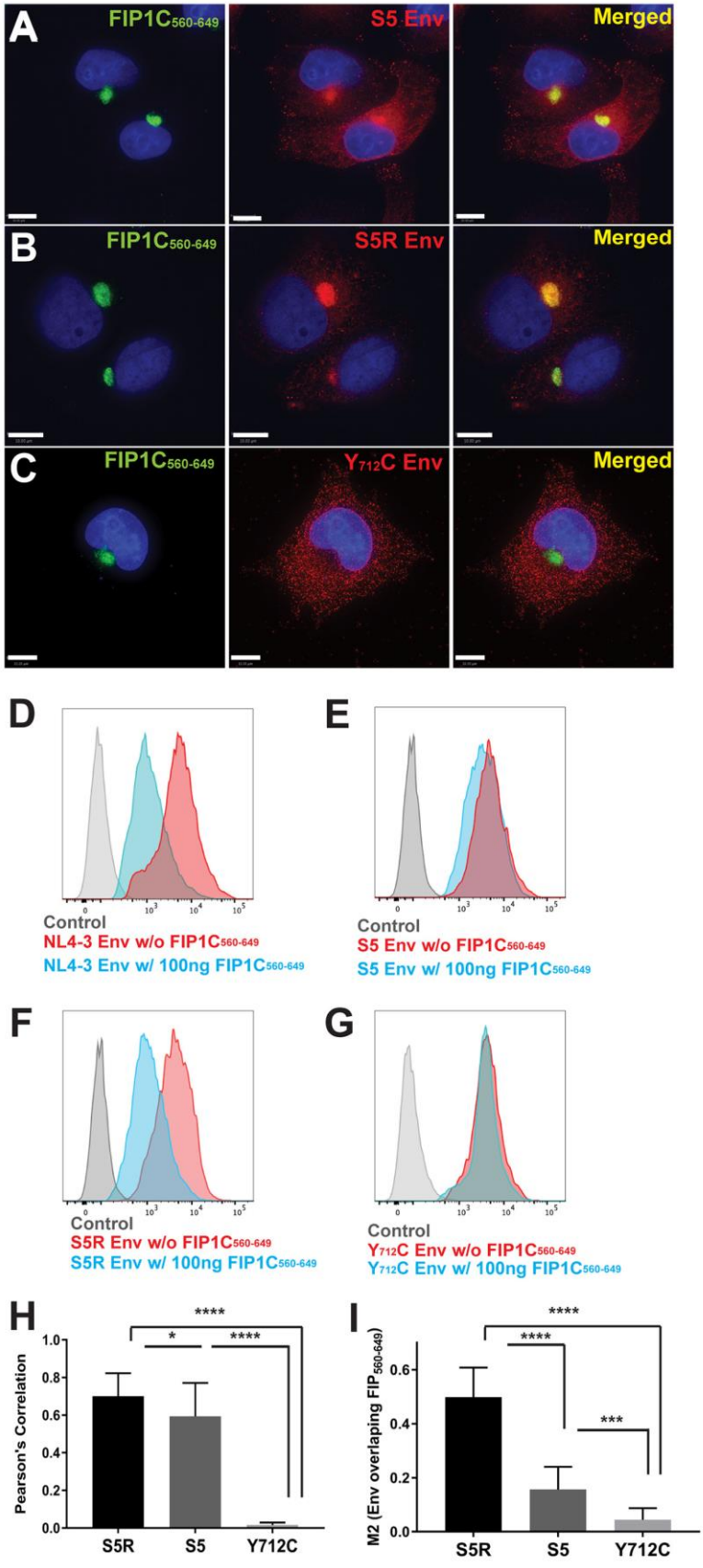
A
FIP1C560-649
S5 Env
Merged
B
FIP1C560-649
S5R Env
Merged
C
FIP1C560-649
Y712C Env
Merged
D
Control
NL4-3 Env w/o FIP1C560-649
NL4-3 Env w/ 100ng FIP1C560-649
E
Control
S5 Env w/o FIP1C560-649
S5 Env w/ 100ng FIP1C560-649
F
Control
S5R Env w/o FIP1C560-649
S5R Env w/ 100ng FIP1C560-649
G
Control
Y712C Env w/o FIP1C560-649
Y712C Env w/ 100ng FIP1C560-649
H
Pearson's Correlation
****
*
****
S5R
S5
Y712C
I
M2 (Env overlaping FIP560-649)
****
****
***
S5R
S5
Y712C

**Fig. 4. Trapping of Env by GFP-FIP1C$_{560–649}$ is dependent on specific trafficking motifs in the CT.**

(A) HeLa cells were cotransfected with GFP-FIP1C$_{560–649}$ and YW$_{795}$SL (S5) proviral plasmids. Forty-eight hours posttransfection, cells were fixed and stained with anti-HIV-1 gp120 antibody 2G12 (red). (B) HeLa cells cotransfected with GFP-FIP1C$_{560–649}$ and YW$_{795}$SL/L850S (S5R) proviral plasmids and stained for Env as described in panel A. (C) HeLa cells were cotransfected with GFP-FIP1C$_{560–649}$ and Y$_{712}$C proviral plasmids and stained for Env as outlined for panel A. All size bars represent 10 um. (D) Cell surface staining for NL4-3 Env with and without GFP-FIP1C$_{560–649}$ expression. Cells were fixed and stained for Env using anti-gp120 mouse monoclonal antibody BDI123. (E) S5 designates NL4-3 Env CT mutant YW$_{795}$SL. Cell surface staining performed for wild-type NL4-3 as described for panel D. (F) S5R is a second-site revertant virus in the Env CT, YW$_{795}$SL/L$_{850}$S. Cell surface staining was performed as described for panel D. (G) Cell surface staining of NL4-3 Y$_{712}$C mutant performed with and without FIP1C$_{560–649}$, as described for panel D. (H) Pearson's correlation coefficient. (I) M2 correlation coefficient, Env signal/FIP1C signal. Results are shown as means ± SD from a total of 10 representative 3D image stacks. *, $\rho < 0.04$; ***, $\rho < 0.001$; ****, $\rho < 0.0001$.

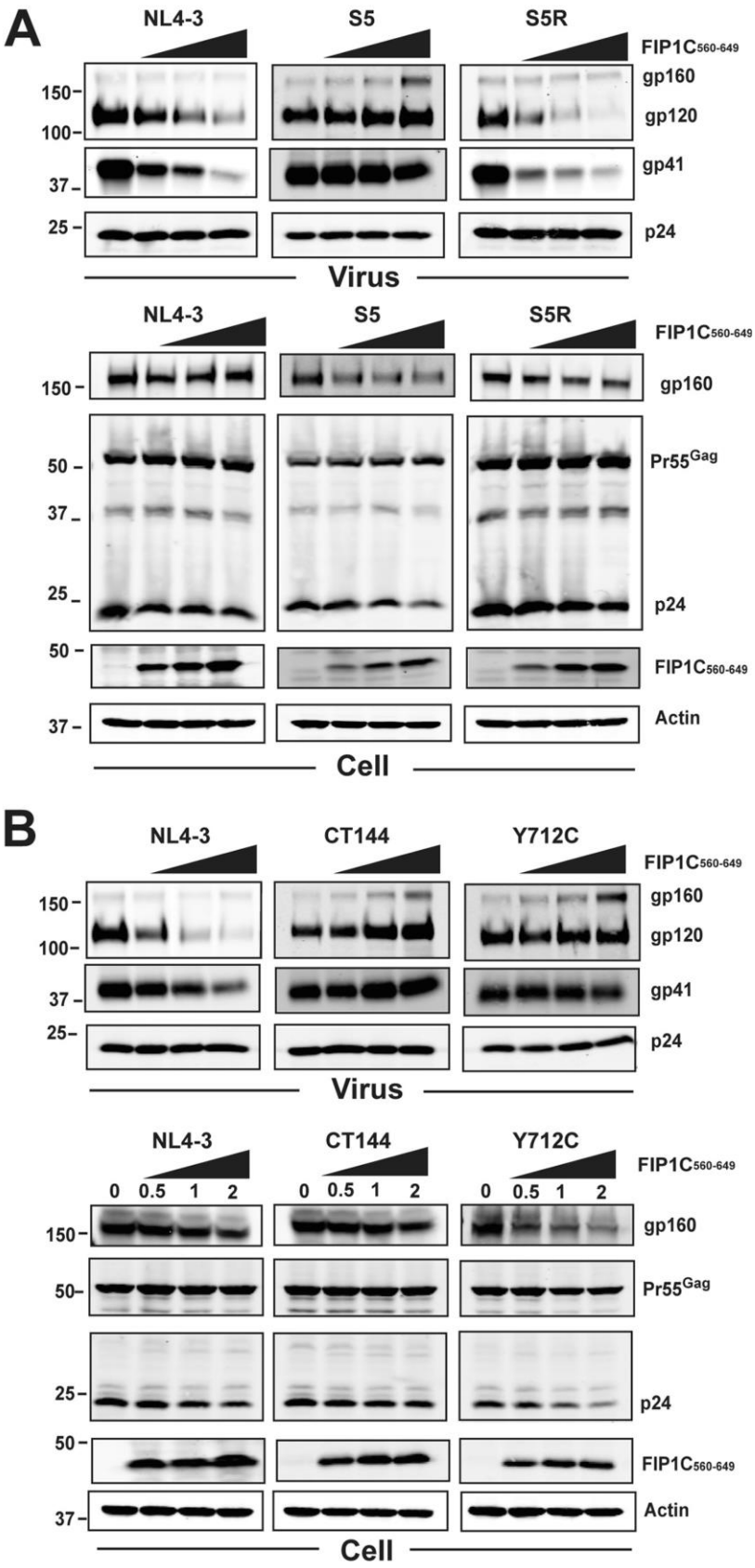
A
NL4-3
S5
S5R
FIP1C560-649
150
100
37
25
gp160
gp120
gp41
p24
Virus
NL4-3
S5
S5R
FIP1C560-649
150
gp160
50
37
25
Pr55Gag
p24
50
FIP1C560-649
37
Actin
Cell
B
NL4-3
CT144
Y712C
FIP1C560-649
150
100
37
25
gp160
gp120
gp41
p24
Virus
NL4-3
CT144
Y712C
FIP1C560-649
0 0.5 1 2
0 0.5 1 2
0 0.5 1 2
150
50
25
50
37
gp160
Pr55Gag
p24
FIP1C560-649
Actin
Cell

**Fig. 5. Effects of titration of FIP1C$_{560–649}$ on Env particle incorporation for Env CT trafficking mutants.**

(A) FIP1C$_{560–649}$ was cotransfected with the indicated proviral constructs at increasing amounts of DNA as indicated above the blots. Shown are Western blots for Env and Gag content in particles (top) and cell lysates (bottom). WT NL4-3 is shown as in Fig. 4 and serves as a control for inhibition of Env incorporation into particles. Note that S5 is the Env CT mutant YW$_{795}$SL, while S5R (revertant) is the second-site revertant in the CT, YW$_{795}$SL/L$_{850}$S. (B) Dose titration of FIP1C$_{560–649}$ as described for panel A, showing effects on CT144 and Y$_{712}$C Env compared to wild-type NL4-3. Particle blots are shown on the top, and cell lysates are below. Results are from HeLa cells.

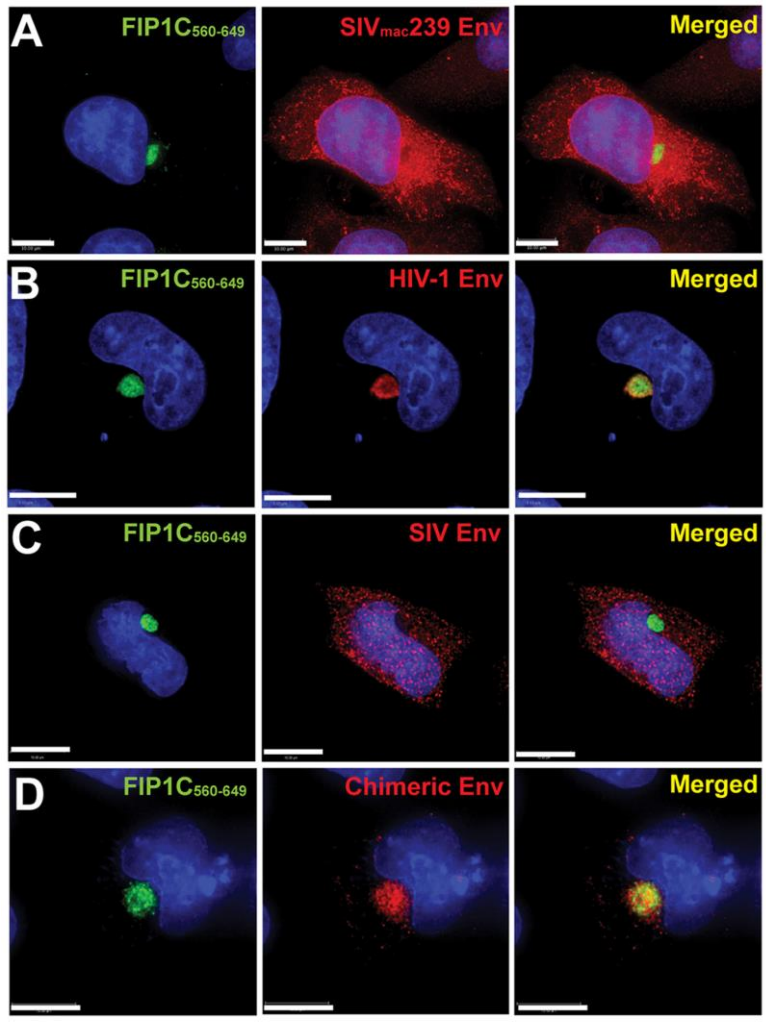
A
FIP1C560-649
SIVmac239 Env
Merged
B
FIP1C560-649
HIV-1 Env
Merged
C
FIP1C560-649
SIV Env
Merged
D
FIP1C560-649
Chimeric Env
Merged

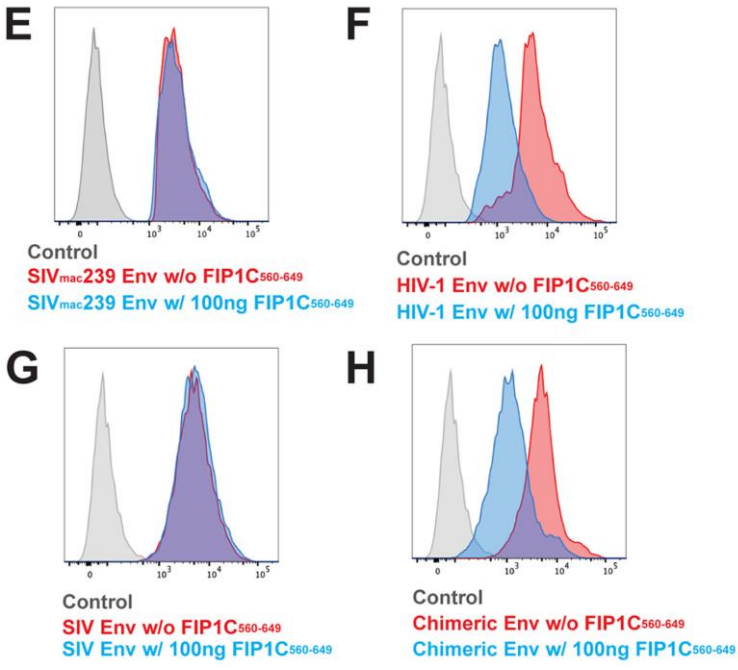
E
Control
SIVmac239 Env w/o FIP1C560-649
SIVmac239 Env w/ 100ng FIP1C560-649
F
Control
HIV-1 Env w/o FIP1C560-649
HIV-1 Env w/ 100ng FIP1C560-649
G
Control
SIV Env w/o FIP1C560-649
SIV Env w/ 100ng FIP1C560-649
H
Control
Chimeric Env w/o FIP1C560-649
Chimeric Env w/ 100ng FIP1C560-649

**Fig. 6. Dominant-negative FIP1C$_{560–649}$ fails to trap SIV Env in the ERC.**

(A) HeLa cells were cotransfected with GFP-FIP1C$_{560–649}$ and SIVmac239 proviral plasmids. After 48 h, cells were fixed and stained with anti-SIV gp120 rabbit serum (red). (B) Codon-optimized JR-FL Env was coexpressed with GFPFIP1C$_{560–649}$, followed by fixation and staining with 2G12 antibody (red). (C) Codon-optimized SIVmac239 Env coexpressed with GFP-FIP1C$_{560–649}$ and stained with anti-SIV gp120 rabbit serum (red). (D) SIV-HIV tail chimeric Env coexpressed with GFP-FIP1C$_{560–649}$ and stained with anti-SIV gp120 rabbit serum. Scale bars, 10 um (A, C, and D) and 5 um (B). (E) Cell surface staining of SIVmac239 Env with and without GFP-FIP1C$_{560–649}$ using anti-SIV gp120 rabbit sera. (F) Surface staining of JR-FL Env expressed from codon-optimized construct with and without coexpression of GFP-FIP1C$_{560–649}$. (G) Codon-optimized SIVmac239 Env cell surface staining with and without expression of GFP-FIP1C$_{560–649}$. (H) Cell surface Env signal of SIV-HIV chimeric Env, stained with anti-SIV gp120 rabbit sera with and without GFP-FIP1C$_{560–649}$ expression.

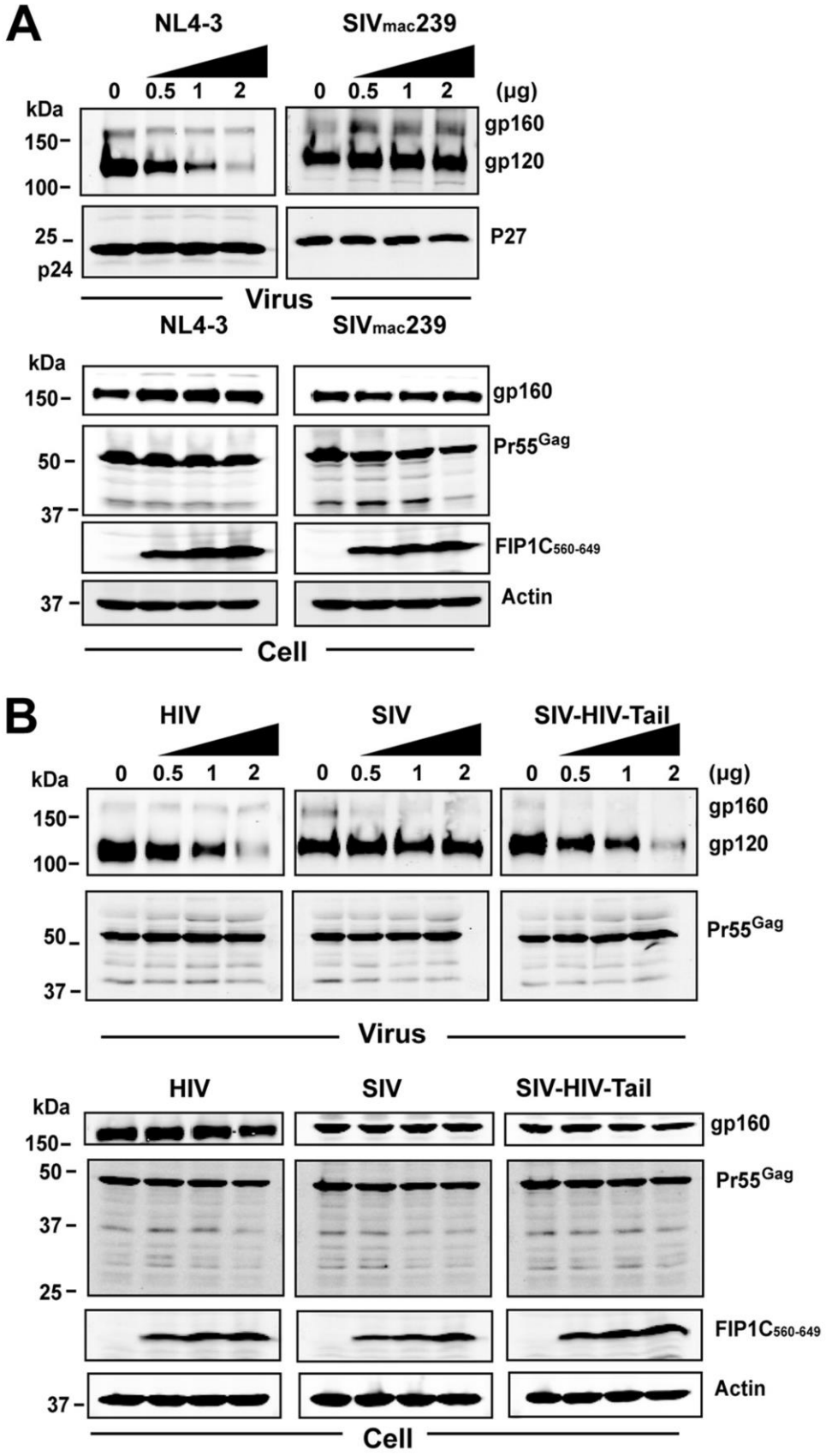
A
NL4-3
SIVmac239
0 0.5 1 2
0 0.5 1 2
(μg)
kDa
150
100
25
p24
gp160
gp120
P27
Virus
NL4-3
SIVmac239
kDa
150
50
37
37
gp160
Pr55Gag
FIP1C560-649
Actin
Cell
B
HIV
SIV
SIV-HIV-Tail
0 0.5 1 2
0 0.5 1 2
0 0.5 1 2
(μg)
kDa
150
100
50
37
gp160
gp120
Pr55Gag
Virus
HIV
SIV
SIV-HIV-Tail
kDa
150
50
37
25
37
gp160
Pr55Gag
FIP1C560-649
Actin
Cell

**Fig. 7. Dose titration of FIP1C$_{560–649}$ and effects on SIVmac239 Env incorporation.** (A) Comparison of effects of titration of FIP1C$_{560–649}$ on Env incorporation by NL4-3 versus SIVmac239 in HeLa cells. In this experiment, full-length SIVmac239 proviral DNA was cotransfected with increasing amounts of FIP1C$_{560–649.}$ (B) CT-dependent reduction in Env incorporation illustrated by SIV-HIV Env chimera. (Left) Codon-optimized HIV-1 (JR-FL) Env was coexpressed with codon-optimized HIV Gag and increasing amounts of FIP1C$_{560–649}$ DNA. (Middle) Codon-optimized SIVmac239 Env coexpressed with optimized SIVmac239 Gag and increasing amounts of FIP1C$_{560–649}$. (Right) Effects of FIP1C$_{560–649}$ expression on particle incorporation of a chimeric Env where the ectodomain and transmembrane domain of SIVmac239 Env was fused to the CT of HIV-1 Env. In this experiment, the Gag protein expressed was SIVmac239 Gag.

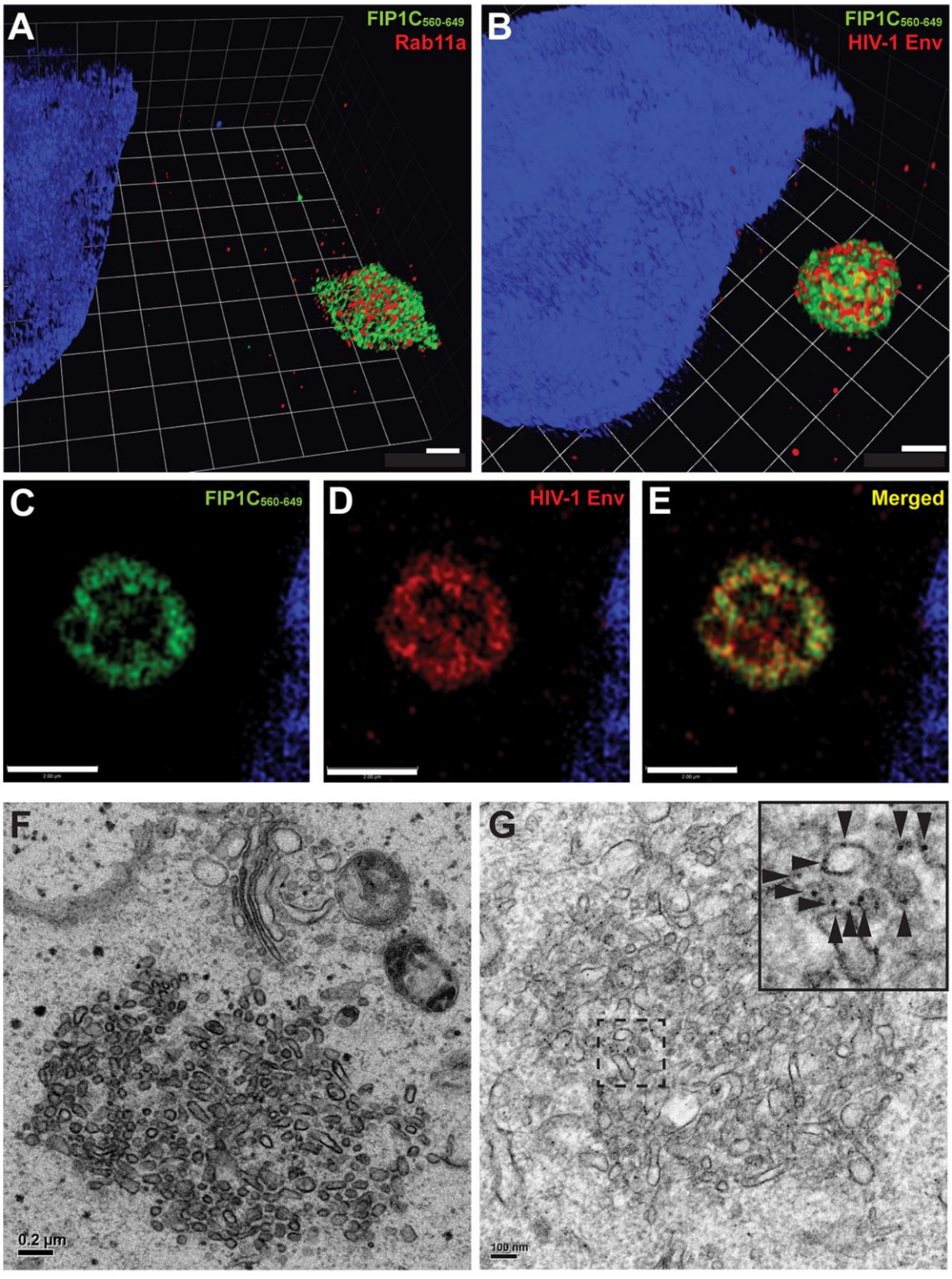
A
FIP1C560-649
Rab11a
B
FIP1C560-649
HIV-1 Env
C
FIP1C560-649
D
HIV-1 Env
E
Merged
F
0.2 µm
G
100 nm

**Fig. 8. GFP-FIP1C$_{560–649}$ creates an aberrant ERC that traps Env on endosomal membranes.**

(A) Structured illumination microscopy of aberrant ERC. HeLa cells transfected with GFP-FIP1C$_{560–649}$ and stained for Rab11a. Shown is a 3D projection of the aberrant ERC where both Rab11a and GFP-FIP1C concentrate. Blue color represents nuclear stain. Scale bar, 1 um. (B) Structured illumination microscopy for morphology of ERC with HIV-1 Env. HeLa cells were cotransfected with GFP-FIP1C$_{560–649}$ and pNL4-3 proviral DNA and stained for HIV-1 Env. Env is shown in red, with FIP1C in green. Scale bar, 1 um. (C to E) A section of ERC from the experiment depicted in panel B is shown to illustrate the less densely staining inner core. (F) Transmission electron microscopy image of the abnormal ERC induced by GFP-FIP1C$_{560–649}$. Scale bar, 200 nm. (G) Postembedding immunoelectron microscopy using a cocktail of anti-Env monoclonal antibodies 2G12, b12, and 447-52D, with detection using 10-nm protein A-gold beads. The hatched area in the image is shown in magnified form at the upper right corner, and arrowheads point out some of the individual gold beads. Scale bar, 100 nm.

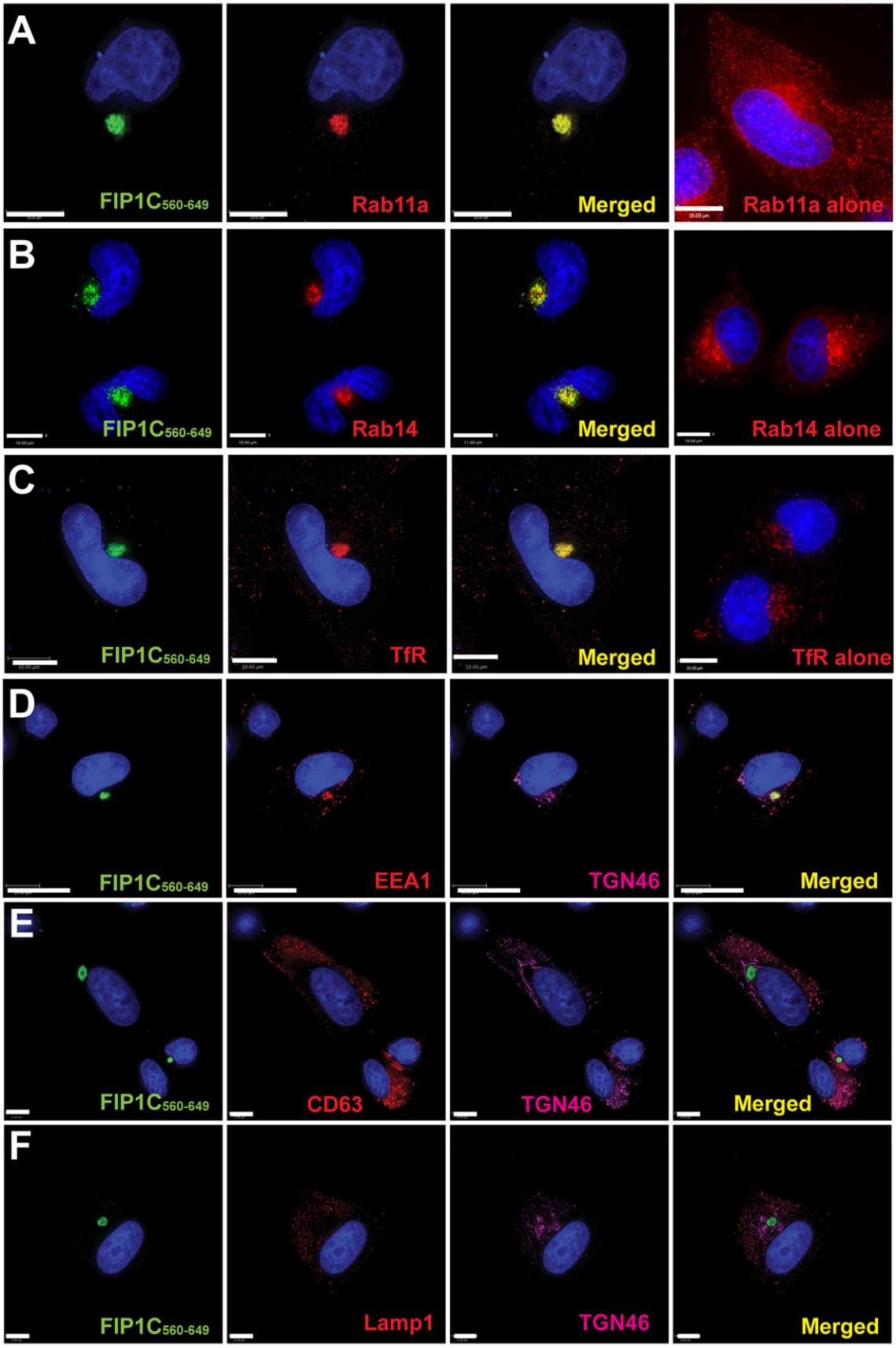
A
FIP1C560-649
Rab11a
Merged
Rab11a alone
B
FIP1C560-649
Rab14
Merged
Rab14 alone
C
FIP1C560-649
TfR
Merged
TfR alone
D
FIP1C560-649
EEA1
TGN46
Merged
E
FIP1C560-649
CD63
TGN46
Merged
F
FIP1C560-649
Lamp1
TGN46
Merged

**Fig. 9. Endosomal markers present in FIP1C$_{560–649}$-positive ERC.**

(A) To examine the enrichment of ERC markers in the FIP1C$_{560–649}$ compartment, we utilized immunofluorescence microscopy for a series of endosomal markers. All images shown here are from HeLa cells. Rab11a is shown concentrated in the FIP1C$_{560–649}$ compartment (left 3 images) compared with its normal distribution (rightmost image). (B) Rab14-mcherry (red) was coexpressed with GFP-FIP1C$_{560–649}$. The distribution of Rab14-mcherry alone is shown in the rightmost panel. (C) The distribution of endogenous transferrin receptor is shown together with the FIP1C$_{560–649}$-positive compartment compared to its normal distribution (rightmost image). (D) EEA1 distribution following expression of FIP1C$_{560–649}$, together with staining for TGN46. (E) CD63 distribution in the presence of FIP1C$_{560–649}$. TGN46 staining also is indicated. (F) LAMP1 and TGN46 distribution in the presence of FIP1C$_{560–649}$.

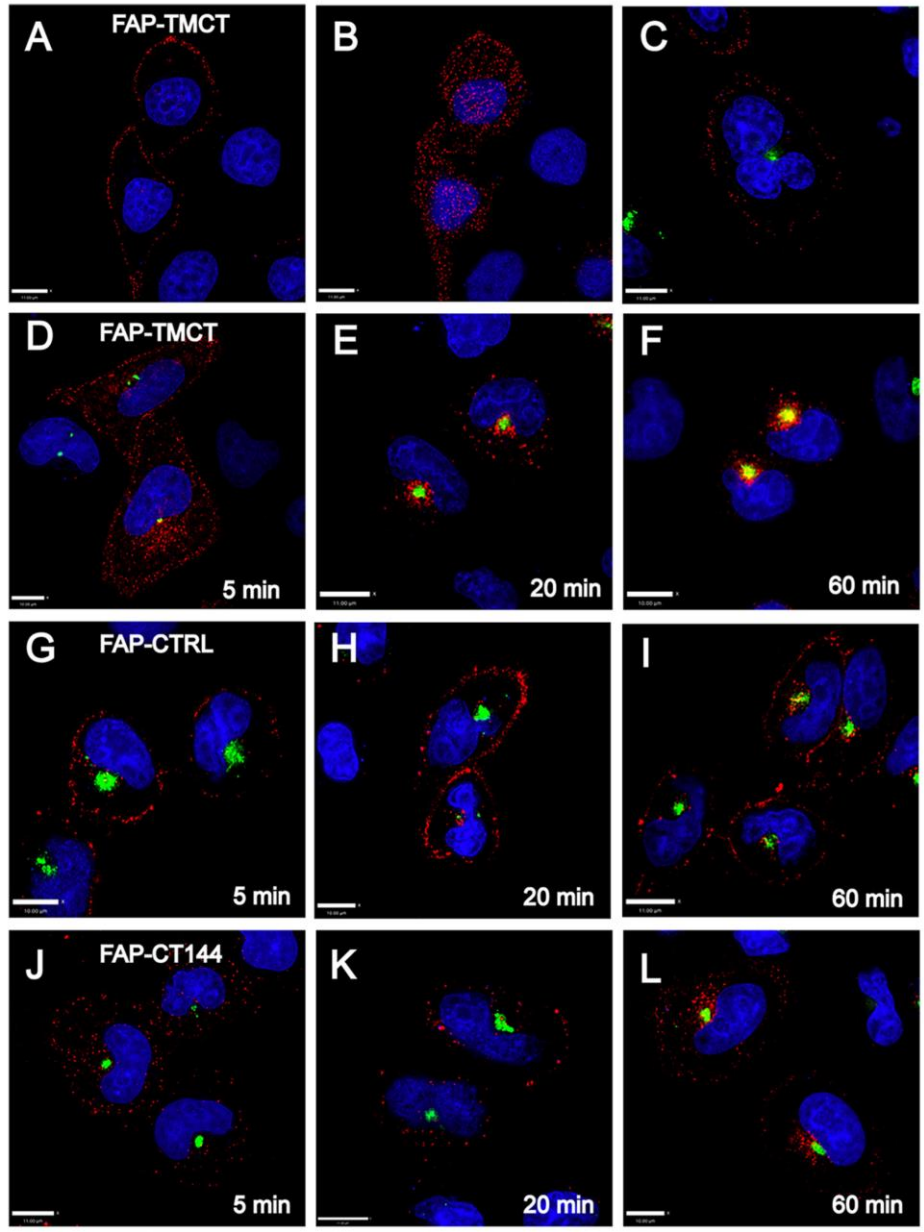
A
FAP-TMCT
B
C
D
FAP-TMCT
5 min
E
20 min
F
60 min
G
FAP-CTRL
5 min
H
20 min
I
60 min
J
FAP-CT144
5 min
K
20 min
L
60 min

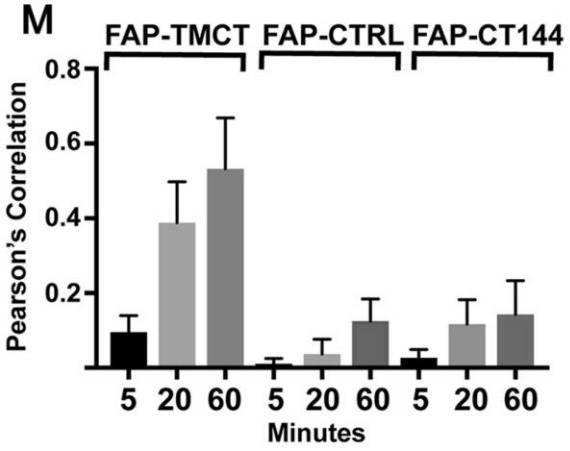
M
FAP-TMCT
FAP-CTRL
FAP-CT144
Pearson's Correlation
0.8
0.6
0.4
0.2
5 20 60 5 20 60 5 20 60
Minutes

**Fig. 10. Endocytosis and trapping of artificial Env in ERC.**

FAP-TMCT is an artificial envelope bearing the FAPalpha2 module at the N terminus fused to the TM and CT of HIV-1 Env. (A) FAP-TMCT labeled following a 10-min pulse with MG-11p on ice, showing a z section at approximately the midpoint of the cell. (B) Same cells as those described for panel A, showing labeling at the PM (coverslip level). Nuclei are superimposed for reference. (C) PM labeling on ice in HeLa cells expressing GFP-FIP1C$_{560–649}$. (D) HeLa cell expressing GFP-FIP1C$_{560–649}$ and pulse labeled with MG-11p for 5 min, shown immediately at the end of the pulse. (E) FAP-TMCT colocalization with GFP-FIP1C$_{560–649}$ after a 5-min pulse followed by a 20-min chase period. (F) FAP-TMCT colocalization with GFP-FIP1C$_{560–649}$ following a 5-min pulse and 60-min chase period. (G to I) Control membrane protein produced from pMFAP-alpha2 vector using methods described for panels D and E. (J to L) FAP-TMCT144 time course with time postlabeling indicated. Scale bars, 11 um. (M) Pearson's correlation was derived from image stacks representing 10 fields of cells from each time point. Error bars indicate standard deviations.

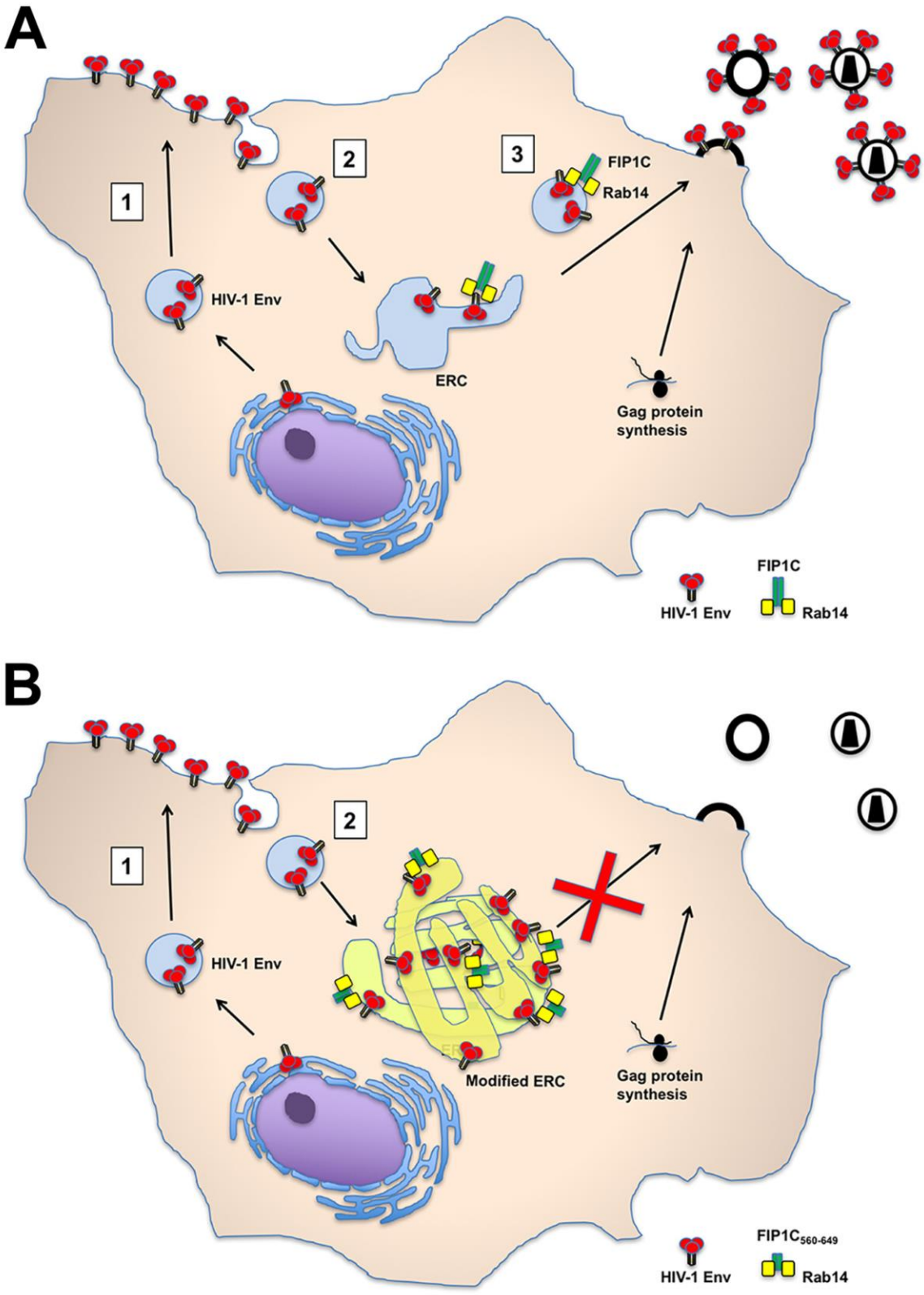
A
1
2
3
FIP1C
Rab14
HIV-1 Env
ERC
Gag protein synthesis
HIV-1 Env
FIP1C
Rab14
B
1
2
HIV-1 Env
Modified ERC
Gag protein synthesis
HIV-1 Env
FIP1C560-649
Rab14

**Fig. 11. Model for Env trafficking and retention in ERC by truncated FIP1C.**

A. Model of Env trafficking through the ERC. In this scheme, step 1 represents trafficking through the secretory pathway to the PM. Step 2 represents clathrin- and AP-2-dependent endocytosis to the ERC. Step 3 is dependent upon FIP1C and Rab14, in which Gag and Env come together at the PM assembly site. (B) Altered Env trafficking by $FIP1C_{560–649}$. In this model, steps 1 and 2 remain intact but Env is retained on ERC membranes, while step 3 is absent, resulting in particles lacking Env.

Supplemental figure

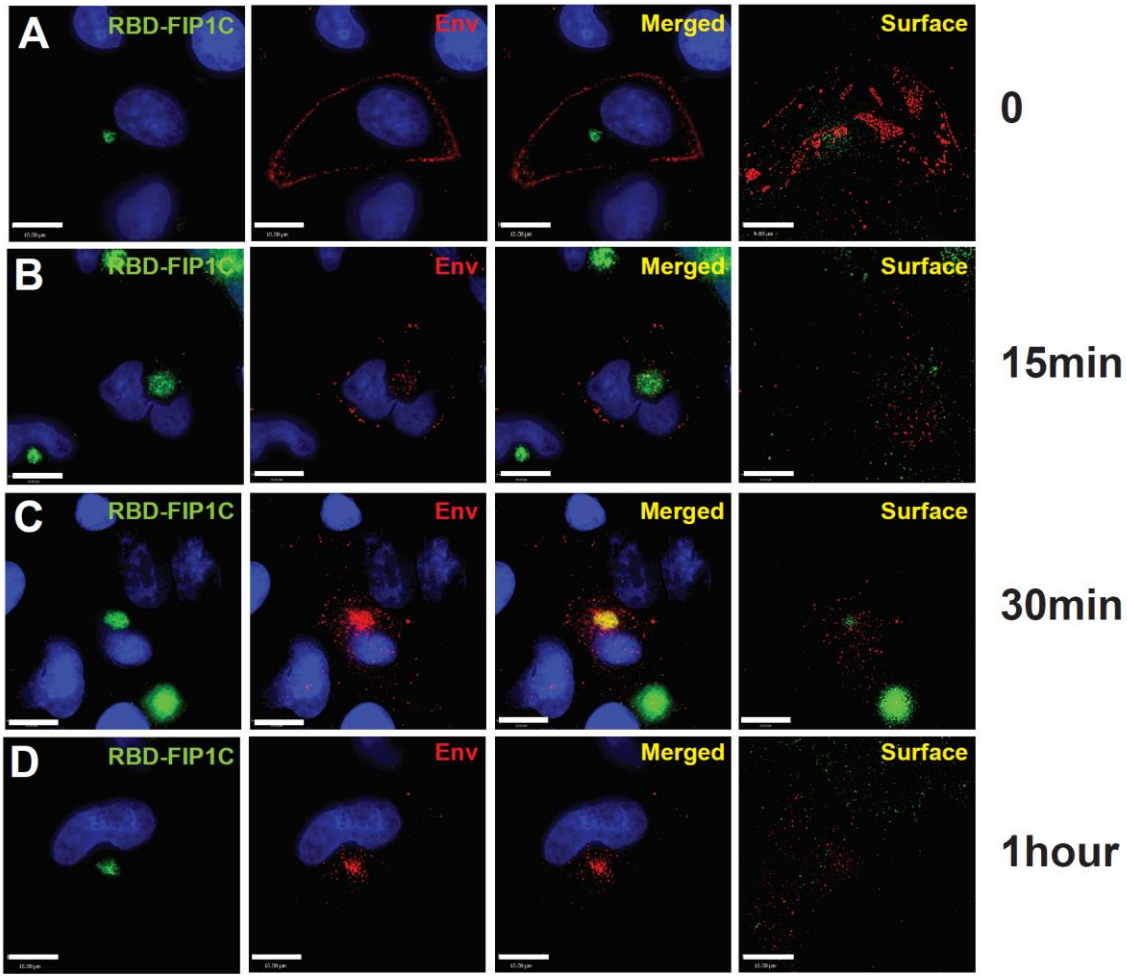


**Suppl. Fig. 1. Endocytosis and trapping of artificial Env in ERC.**

GFP-FIP1C$_{560–649}$ (GFP-RBD-FIP1C) and NL4-3 provirus were expressed in TZM-BL cells 48 hours before surface staining with 2G12 antibody. Mcherry secondary antibody was shown as red. Gp120 broadly neutralizing antibody was used to stain HIV-1 NL4-3 Env for 1 hour on the ice before starting chase to block the endocytosis of antibody/Env complex. At Each time point, the cells were fixed and permeabilized then stained with fluorophore-labeled secondary antibody and visualized under TIRF microscopy and Z-

stack imaging (Delta Vision). (A) Time 0: Env was stained with secondary antibody right after primary antibody staining. Env is located majorly on the cellular surface (B-D): At 15min pulse chase, already most of the envs are getting internalized into ERC. At 30 min, ERC is already enriched with Envs. Env trapping is still effective after 4 hours (data not shown).

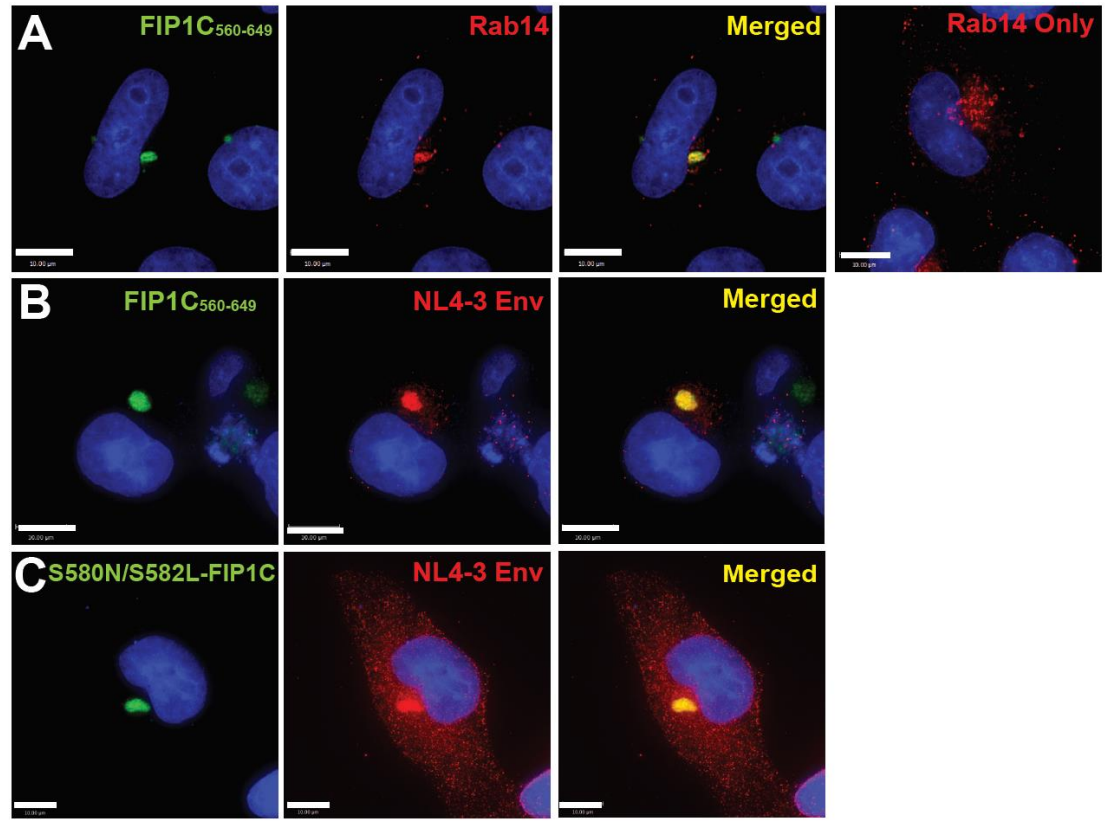
A
FIP1C560-649
Rab14
Merged
Rab14 Only
B
FIP1C560-649
NL4-3 Env
Merged
C
S580N/S582L-FIP1C
NL4-3 Env
Merged

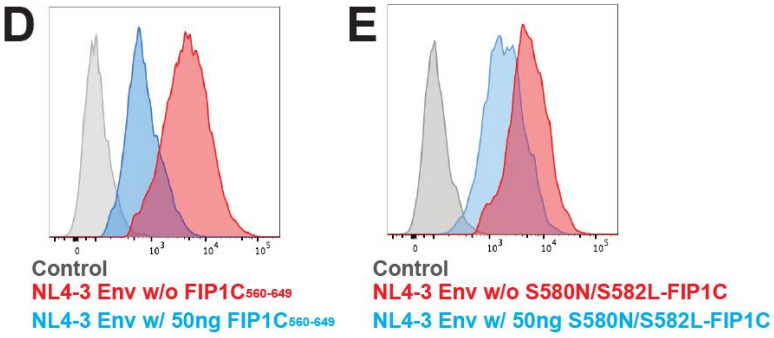
D
Control
NL4-3 Env w/o FIP1C560-649
NL4-3 Env w/ 50ng FIP1C560-649
E
Control
NL4-3 Env w/o S580N/S582L-FIP1C
NL4-3 Env w/ 50ng S580N/S582L-FIP1C

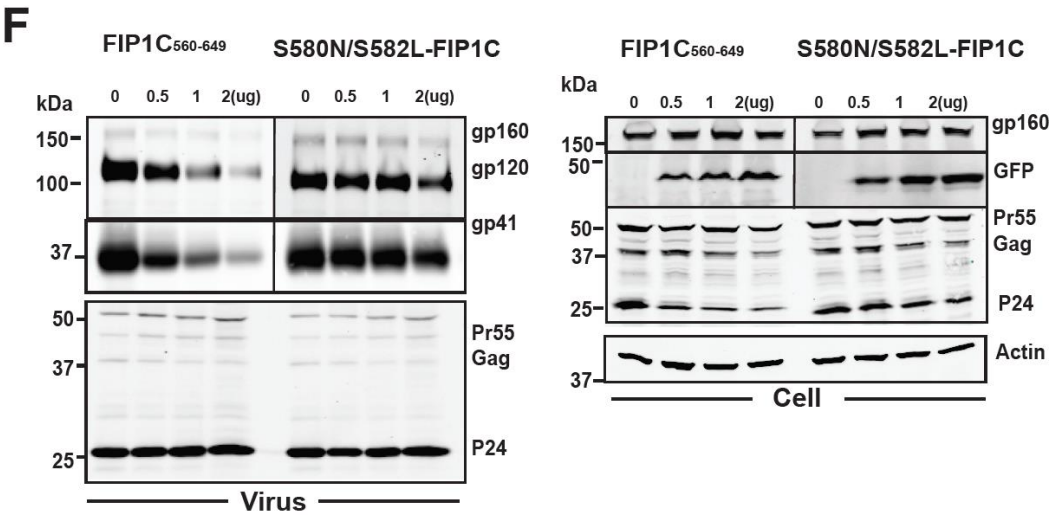
F
FIP1C560-649
S580N/S582L-FIP1C
kDa
0 0.5 1 2(ug) 0 0.5 1 2(ug)
150
100
37
50
37
25
gp160
gp120
gp41
Pr55
Gag
P24
Virus
FIP1C560-649
S580N/S582L-FIP1C
kDa
0 0.5 1 2(ug) 0 0.5 1 2(ug)
150
50
50
37
25
37
gp160
GFP
Pr55
Gag
P24
Actin
Cell

**Suppl. Fig. 2. Mutation in Rab14 binding sites in FIP1C$_{560–649}$ rescues Env from ERC.**

(A) Co-localization of Rab14 and FIP1C$_{560–649}$

(B) Co-localization of HIV-1 NL4-3 Env and FIP1C$_{560–649}$

(C) Partial co-localization of FIP1C$_{560–649}$ S580N/S582L and HIV-1 NL4-3 Env

(D-E) Flow cytometry analysis of FIP1C$_{560–649}$ S580N/S582L shows only mild decrease in surface Env expression.

(F) Western blot shows dominant negative effect of FIP1C$_{560–649}$ is reversed by Rab14-binding mutations in low-mid dose of FIP1C$_{560–649}$ S580N/S582L plasmid.

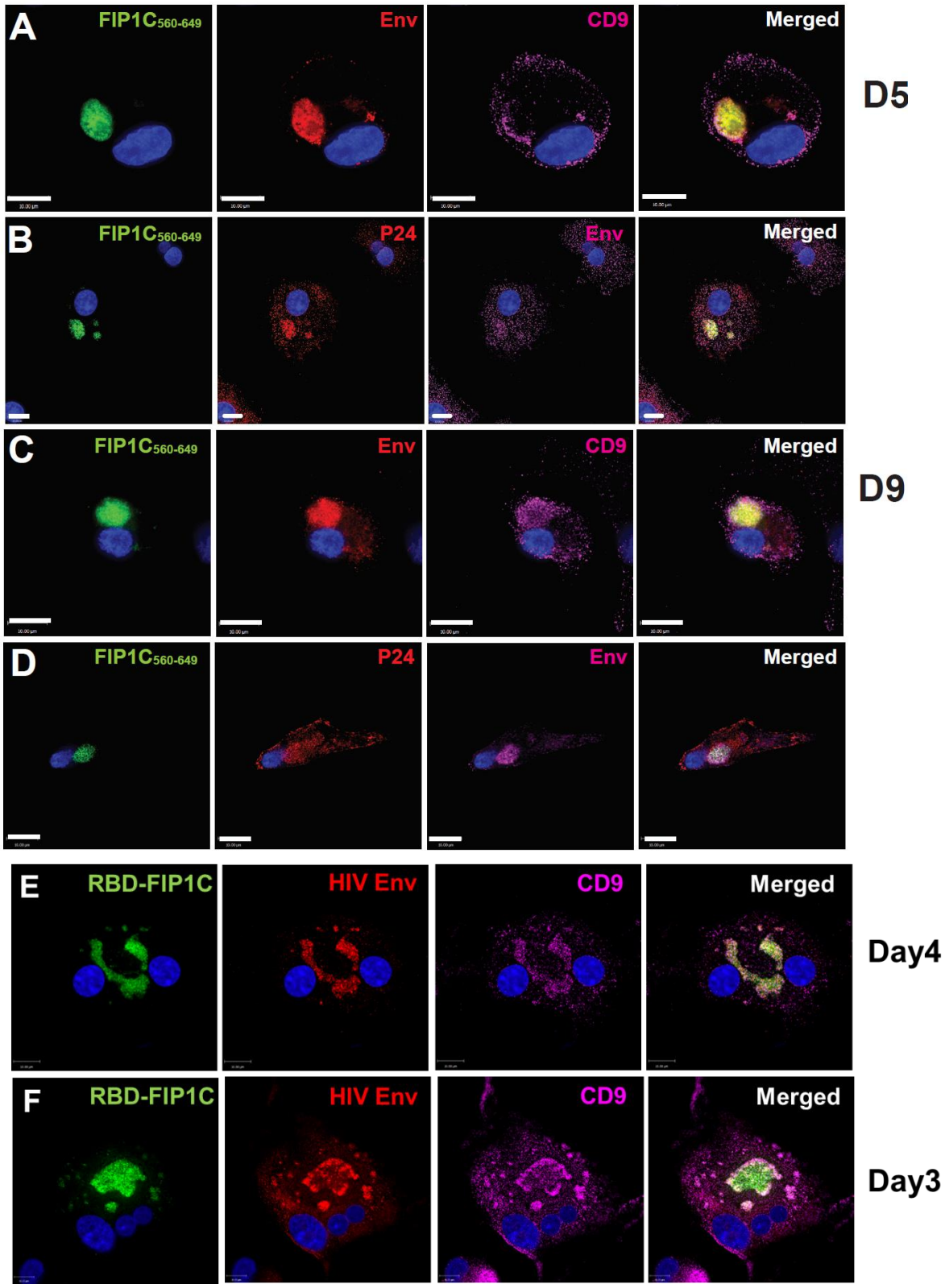
A
FIP1C560-649
Env
CD9
Merged
D5
B
FIP1C560-649
P24
Env
Merged
C
FIP1C560-649
Env
CD9
Merged
D9
D
FIP1C560-649
P24
Env
Merged
E
RBD-FIP1C
HIV Env
CD9
Merged
Day4
F
RBD-FIP1C
HIV Env
CD9
Merged
Day3

**Suppl. Fig. 3. FIP1C$_{560–649}$ can capture AD8 Env in some monocyte-derived human macrophages**

(A) Co-localization of AD8 Env and FIP1C$_{560–649}$ at Day 5 after transfection

(B) Co-localization of AD8 gag and FIP1C$_{560–649}$ at Day 5 after transfection

(C) Co-localization of AD8 Env and FIP1C$_{560–649}$ at Day 9 after transfection

(D) Co-localization of AD8 gag and FIP1C$_{560–649}$ at Day 9 after transfection

(E) Day 4: CD9 and AD8 Env

(F) Day 3: CD9 and AD8 Env. CD9 was used as a marker for virus-containing compartment (VCC) marker in virus-producing macrophages.

References

1. Checkley MA, Luttge BG, Freed EO. 2011. HIV-1 envelope glycoprotein biosynthesis, trafficking, and incorporation. J Mol Biol 410:582– 608. https://doi.org/10.1016/j.jmb.2011.04.042.

2. Johnson MC. 2011. Mechanisms for Env glycoprotein acquisition by retroviruses. AIDS Res Hum Retrovir 27:239 –247. https://doi.org/10.1089/aid.2010.0350.

3. Hunter E, Swanstrom R. 1990. Retrovirus envelope glycoproteins. Curr Top Microbiol Immunol 157:187–253.

4. Murakami T, Freed EO. 2000. The long cytoplasmic tail of gp41 is required in a cell type-dependent manner for HIV-1 envelope glycoprotein incorporation into virions. Proc Natl Acad Sci U S A 97:343–348. https://doi.org/10.1073/pnas.97.1.343.

5. Berlioz-Torrent C, Shacklett BL, Erdtmann L, Delamarre L, Bouchaert I, Sonigo P, Dokhelar MC, Benarous R. 1999. Interactions of the cytoplasmic domains of human and simian retroviral transmembrane proteins with components of the clathrin adaptor complexes modulate intracellular and cell surface expression of envelope glycoproteins. J Virol 73:1350 –1361.

6. Ohno H, Aguilar RC, Fournier MC, Hennecke S, Cosson P, Bonifacino JS. 1997. Interaction of endocytic signals from the HIV-1 envelope glycoprotein complex with members of the adaptor medium chain family. Virology 238:305–315. https://doi.org/10.1006/viro.1997.8839.

7. Rowell JF, Stanhope PE, Siliciano RF. 1995. Endocytosis of endogenously synthesized HIV-1 envelope protein. Mechanism and role in processing for association with class II MHC. J Immunol 155:473– 488.

8. Day JR, Munk C, Guatelli JC. 2004. The membrane-proximal tyrosinebased sorting signal of human immunodeficiency virus type 1 gp41 is required for optimal viral infectivity. J Virol 78:1069 –1079. https://doi.org/10.1128/JVI.78.3.1069-1079.2004.

9. Deschambeault J, Lalonde JP, Cervantes-Acosta G, Lodge R, Cohen EA, Lemay G. 1999. Polarized human immunodeficiency virus budding in lymphocytes involves a tyrosine-based signal and favors cell-to-cell viral transmission. J Virol 73:5010 –5017.

10. Lodge R, Lalonde JP, Lemay G, Cohen EA. 1997. The membrane-proximal intracytoplasmic tyrosine residue of HIV-1 envelope glycoprotein is critical for basolateral targeting of viral budding in MDCK cells. EMBO J 16:695–705. https://doi.org/10.1093/emboj/16.4.695.

11. Wyss S, Berlioz-Torrent C, Boge M, Blot G, Honing S, Benarous R, Thali M. 2001. The highly conserved C-terminal dileucine motif in the cytosolic domain of the human immunodeficiency virus type 1 envelope glycoprotein is critical for its association with the AP-1 clathrin adaptor. J Virol 75:2982–2992. https://doi.org/10.1128/JVI.75.6.2982-2992.2001.

12. Bhakta SJ, Shang L, Prince JL, Claiborne DT, Hunter E. 2011. Mutagenesis of tyrosine and di-leucine motifs in the HIV-1 envelope cytoplasmic domain results in a loss of Env-mediated fusion and infectivity. Retrovirology 8:37. https://doi.org/10.1186/1742-4690-8-37.

13. Qi M, Williams JA, Chu H, Chen X, Wang JJ, Ding L, Akhirome E, Wen X, Lapierre LA, Goldenring JR, Spearman P. 2013. Rab11-FIP1C and Rab14 direct plasma membrane sorting and particle incorporation of the HIV-1 envelope glycoprotein complex. PLoS Pathog 9:e1003278. https://doi.org/10.1371/journal.ppat.1003278.

14. Wallace DM, Lindsay AJ, Hendrick AG, McCaffrey MW. 2002. The novel Rab11-FIP/Rip/RCP family of proteins displays extensive homo- and hetero-interacting abilities. Biochem Biophys Res Commun 292: 909–915. https://doi.org/10.1006/bbrc.2002.6736.

15. Lall P, Lindsay AJ, Hanscom S, Kecman T, Taglauer ES, McVeigh UM, Franklin E, McCaffrey MW, Khan AR. 2015. Structure-function analyses of the interactions between

Rab11 and Rab14 small GTPases with their shared effector Rab coupling protein (RCP). J Biol Chem 290: 18817–18832. https://doi.org/10.1074/jbc.M114.612366.

16. Lindsay AJ, Hendrick AG, Cantalupo G, Senic-Matuglia F, Goud B, Bucci C, McCaffrey MW. 2002. Rab coupling protein (RCP), a novel Rab4 and Rab11 effector protein. J Biol Chem 277:12190–12199. https://doi.org/10.1074/jbc.M108665200.

17. Hales CM, Griner R, Hobdy-Henderson KC, Dorn MC, Hardy D, Kumar R, Navarre J, Chan EK, Lapierre LA, Goldenring JR. 2001. Identification and characterization of a family of Rab11-interacting proteins. J Biol Chem 276:39067–39075. https://doi.org/10.1074/jbc.M104831200.

18. Qi M, Chu H, Chen X, Choi J, Wen X, Hammonds J, Ding L, Hunter E, Spearman P. 2015. A tyrosine-based motif in the HIV-1 envelope glycoprotein tail mediates cell-type- and Rab11-FIP1C-dependent incorporation into virions. Proc Natl Acad Sci U S A 112:7575–7580. https://doi.org/10.1073/pnas.1504174112.

19. Lindsay AJ, McCaffrey MW. 2002. Rab11-FIP2 functions in transferrin recycling and associates with endosomal membranes via its COOH terminal domain. J Biol Chem 277:27193–27199. https://doi.org/10.1074/jbc.M200757200.

20. Damiani MT, Pavarotti M, Leiva N, Lindsay AJ, McCaffrey MW, Colombo MI. 2004. Rab coupling protein associates with phagosomes and regulates recycling from the

phagosomal compartment. Traffic 5:785–797. https://doi.org/10.1111/j.1600-0854.2004.00220.x.

21. Boge M, Wyss S, Bonifacino JS, Thali M. 1998. A membrane-proximal tyrosine-based signal mediates internalization of the HIV-1 envelope glycoprotein via interaction with the AP-2 clathrin adaptor. J Biol Chem 273:15773–15778. https://doi.org/10.1074/jbc.273.25.15773.

22. Yan Q, Schmidt BF, Perkins LA, Naganbabu M, Saurabh S, Andreko SK, Bruchez MP. 2015. Near-instant surface-selective fluorogenic protein quantification using sulfonated triarylmethane dyes and fluorogen activating proteins. Org Biomol Chem 13:2078 –2086. https://doi.org/10.1039/C4OB02309A.

23. Szent-Gyorgyi C, Schmidt BF, Creeger Y, Fisher GW, Zakel KL, Adler S, Fitzpatrick JA, Woolford CA, Yan Q, Vasilev KV, Berget PB, Bruchez MP, Jarvik JW, Waggoner A. 2008. Fluorogen-activating single-chain antibodies for imaging cell surface proteins. Nat Biotechnol 26:235–240. https://doi.org/10.1038/nbt1368.

24. Earl PL, Doms RW, Moss B. 1990. Oligomeric structure of the human immunodeficiency virus type 1 envelope glycoprotein. Proc Natl Acad Sci U S A 87:648–652. https://doi.org/10.1073/pnas.87.2.648.

25. Earl PL, Koenig S, Moss B. 1991. Biological and immunological properties of human immunodeficiency virus type 1 envelope glycoprotein: analysis of proteins with truncations and deletions expressed by recombinant vaccinia viruses. J Virol 65:31– 41.

26. Otteken A, Earl PL, Moss B. 1996. Folding, assembly, and intracellular trafficking of the human immunodeficiency virus type 1 envelope glycoprotein analyzed with monoclonal antibodies recognizing maturational intermediates. J Virol 70:3407–3415.

27. Pinter A, Honnen WJ, Tilley SA, Bona C, Zaghouani H, Gorny MK, Zolla Pazner S. 1989. Oligomeric structure of gp41, the transmembrane protein of human immunodeficiency virus type 1. J Virol 63:2674 –2679.

28. Schawaller M, Smith GE, Skehel JJ, Wiley DC. 1989. Studies with crosslinking reagents on the oligomeric structure of the env glycoprotein of HIV. Virology 172:367–369. https://doi.org/10.1016/0042-6822(89)90142-6.

29. Hallenberger S, Bosch V, Angliker H, Shaw E, Klenk HD, Garten W. 1992. Inhibition of furin-mediated cleavage activation of HIV-1 glycoprotein gp160. Nature 360:358 –361. https://doi.org/10.1038/360358a0.

30. McCune JM, Rabin LB, Feinberg MB, Lieberman M, Kosek JC, Reyes GR, Weissman IL. 1988. Endoproteolytic cleavage of gp160 is required for the activation of

human immunodeficiency virus. Cell 53:55– 67. https://doi.org/10.1016/0092-8674(88)90487-4.

31. Ono A. 2010. HIV-1 assembly at the plasma membrane. Vaccine 28(Suppl 2):B55–B59. https://doi.org/10.1016/j.vaccine.2009.10.021.

32. Ono A, Freed EO. 2001. Plasma membrane rafts play a critical role in HIV-1 assembly and release. Proc Natl Acad Sci U S A 98:13925–13930. https://doi.org/10.1073/pnas.241320298.

33. Saad JS, Miller J, Tai J, Kim A, Ghanam RH, Summers MF. 2006. Structural basis for targeting HIV-1 Gag proteins to the plasma membrane for virus assembly. Proc Natl Acad Sci U S A 103:11364–11369. https://doi.org/10.1073/pnas.0602818103.

34. Freed EO, Martin MA. 1995. Virion incorporation of envelope glycoproteins with long but not short cytoplasmic tails is blocked by specific, single amino acid substitutions in the human immunodeficiency virus type 1 matrix. J Virol 69:1984 –1989.

35. Freed EO, Martin MA. 1996. Domains of the human immunodeficiency virus type 1 matrix and gp41 cytoplasmic tail required for envelope incorporation into virions. J Virol 70:341–351.

36. Tedbury PR, Freed EO. 2014. The role of matrix in HIV-1 envelope glycoprotein incorporation. Trends Microbiol 22:372–378. https://doi.org/10.1016/j.tim.2014.04.012.

37. Cosson P. 1996. Direct interaction between the envelope and matrix proteins of HIV-1. EMBO J 15:5783–5788. 38. Vincent MJ, Melsen LR, Martin AS, Compans RW. 1999. Intracellular interaction of simian immunodeficiency virus Gag and Env proteins. J Virol 73:8138–8144.

39. Tedbury PR, Ablan SD, Freed EO. 2013. Global rescue of defects in HIV-1 envelope glycoprotein incorporation: implications for matrix structure. PLoS Pathog 9:e1003739. https://doi.org/10.1371/journal.ppat.1003739.

40. Tedbury PR, Novikova M, Ablan SD, Freed EO. 2016. Biochemical evidence of a role for matrix trimerization in HIV-1 envelope glycoprotein incorporation. Proc Natl Acad Sci U S A 113:E182–E190. https://doi.org/10.1073/pnas.1516618113.

41. Baetz NW, Goldenring JR. 2014. Distinct patterns of phosphatidylserine localization within the Rab11a-containing recycling system. Cell Logist 4:e28680. https://doi.org/10.4161/cl.28680.

42. Kelly EE, Horgan CP, Adams C, Patzer TM, Ni Shuilleabhain DM, Norman JC, McCaffrey MW. 2009. Class I Rab11-family interacting proteins are binding targets for the Rab14 GTPase. Biol Cell 102:51– 62. https://doi.org/10.1042/BC20090068.

43. Chakrabarti L, Guyader M, Alizon M, Daniel MD, Desrosiers RC, Tiollais P, Sonigo P. 1987. Sequence of simian immunodeficiency virus from macaque and its relationship to other human and simian retroviruses. Nature 328:543–547. https://doi.org/10.1038/328543a0.

44. Zingler K, Littman DR. 1993. Truncation of the cytoplasmic domain of the simian immunodeficiency virus envelope glycoprotein increases env incorporation into particles and fusogenicity and infectivity. J Virol 67:2824 –2831.

45. LaBranche CC, Sauter MM, Haggarty BS, Vance PJ, Romano J, Hart TK, Bugelski PJ, Marsh M, Hoxie JA. 1995. A single amino acid change in the cytoplasmic domain of the simian immunodeficiency virus transmembrane molecule increases envelope glycoprotein expression on infected cells. J Virol 69:5217–5227.

46. Sauter MM, Pelchen-Matthews A, Bron R, Marsh M, LaBranche CC, Vance PJ, Romano J, Haggarty BS, Hart TK, Lee WM, Hoxie JA. 1996. An internalization signal in the simian immunodeficiency virus transmembrane protein cytoplasmic domain modulates expression of envelope glycoproteins on the cell surface. J Cell Biol 132:795–811. https://doi.org/10.1083/jcb.132.5.795.

47. Bowers K, Pelchen-Matthews A, Honing S, Vance PJ, Creary L, Haggarty BS, Romano J, Ballensiefen W, Hoxie JA, Marsh M. 2000. The simian immunodeficiency virus envelope glycoprotein contains multiple signals that regulate its cell surface

expression and endocytosis. Traffic 1:661– 674. https://doi.org/10.1034/j.1600-0854.2000.010810.x.

48. Byland R, Vance PJ, Hoxie JA, Marsh M. 2007. A conserved dileucine motif mediates clathrin and AP-2-dependent endocytosis of the HIV-1 envelope protein. Mol Biol Cell 18:414–425. https://doi.org/10.1091/mbc.E06-06-0535.

49. Jin M, Goldenring JR. 2006. The Rab11-FIP1/RCP gene codes for multiple protein transcripts related to the plasma membrane recycling system. Biochim Biophys Acta 1759:281–295. https://doi.org/10.1016/j.bbaexp.2006.06.001.

50. Huang Y, Kong WP, Nabel GJ. 2001. Human immunodeficiency virus type 1-specific immunity after genetic immunization is enhanced by modification of Gag and Pol expression. J Virol 75:4947– 4951. https://doi.org/10.1128/JVI.75.10.4947-4951.2001.

51. Hammonds JE, Beeman N, Ding L, Takushi S, Francis AC, Wang JJ, Melikyan GB, Spearman P. 2017. Siglec-1 initiates formation of the virus-containing compartment and enhances macrophage-to-T cell transmission of HIV-1. PLoS Pathog 13:e1006181. https://doi.org/10.1371/journal.ppat.1006181.

52. Dunn KW, Kamocka MM, McDonald JH. 2011. A practical guide to evaluating colocalization in biological microscopy. Am J Physiol Cell Physiol 300:C723–C742. https://doi.org/10.1152/ajpcell.00462.2010.

53. Hammonds J, Wang JJ, Yi H, Spearman P. 2010. Immunoelectron microscopic evidence for Tetherin/BST2 as the physical bridge between HIV-1 virions and the plasma membrane. PLoS Pathog 6:e1000749. https://doi.org/10.1371/journal.ppat.1000749.

54. Ueno H, Huang X, Tanaka Y, Hirokawa N. 2011. KIF16B/Rab14 molecular motor complex is critical for early embryonic development by transporting FGF receptor. Dev Cell. 20(1):60-71. doi: 10.1016/j.devcel.2010.11.008. DOI: 10.1016/j.devcel.2010.11.008

55. Masuyama, N., Kuronita, T., Tanaka, R., Muto, T., Hirota, Y., Takigawa, A., Fujita, H., Aso, Y., Amano, J., and Tanaka, Y. (2009). HM1.24 is internalized from lipid rafts by clathrin-mediated endocytosis through interaction with alpha-adaptin. J. Biol. Chem. 284, 15927–15941. DOI: 10.1074/jbc.M109.005124

56. Rollason R, Korolchuk V, Hamilton C, Jepson M, Banting G. 2009. A CD317/tetherin-RICH2 complex plays a critical role in the organization of the subapical actin cytoskeleton in polarized epithelial cells. J Cell Biol. 184(5):721-36. doi: 10.1083/jcb.200804154. DOI: 10.1083/jcb.200804154

57. Chu H, Wang JJ, Qi M, Yoon JJ, Chen X, Wen X, Hammonds J, Ding L, Spearman P. 2012. Tetherin/BST-2 is essential for the formation of the intracellular virus-containing compartment in HIV-infected macrophages. Cell Host Microbe. 12(3):360-72. doi: 10.1016/j.chom.2012.07.011.

58. Bobadilla S, Sunseri N, Landau NR. 2013. Efficient transduction of myeloid cells by an HIV-1-derived lentiviral vector that packages the Vpx accessory protein. Gene Ther. 20(5):514-20. doi: 10.1038/gt.2012.61.

59. Bruce EA, Digard P, Stuart AD. The Rab11 pathway is required for influenza A virus budding and filament formation. 2010. J Virol. 84(12):5848-59. doi: 10.1128/JVI.00307-10. DOI: 10.1128/JVI.00307-10

60. Vale-Costa S, Amorim MJ. 2017. Clustering of Rab11 vesicles in influenza A virus infected cells creates hotspots containing the 8 viral ribonucleoproteins. Small GTPases. 8(2):71-77. doi: 10.1080/21541248.2016.1199190.

61. Jing J, Tarbutton E, Wilson G, Prekeris R. 2009. Rab11-FIP3 is a Rab11-binding protein that regulates breast cancer cell motility by modulating the actin cytoskeleton. Eur J Cell Biol. 88(6):325-41. doi: 10.1016/j.ejcb.2009.02.186.

62. Dong W, Qin G, Shen R. 2016. Rab11-FIP2 promotes the metastasis of gastric cancer cells. Int J Cancer. 138(7):1680-8. doi: 10.1002/ijc.29899.

## Chapter III: The mechanism of HIV-1 restriction by SERINC5

Jung Hwa Kirschman[1], Mariana Marin[1], Armando Stano[2], Michael Zwick[2], Gregory Melikian[1,3]

[1] Department of Pediatrics, Emory University, Atlanta, Georgia, USA

[2] The Scripps Research Institute, La Jolla, CA, USA

[3] Children's Healthcare of Atlanta, Atlanta GA, USA

Submitted to Plos One in August 2018

Abstract

SERINC5 incorporates into HIV-1 virions and inhibits viral fusion with target cells, and this effect is counteracted by Nef. Different Envs exhibit a broad range of sensitivities to SERINC5. The resistance to this restriction factor has been mapped to the variable loops V1-V3 of gp120 located at the apex of Env trimer. Our laboratory has previously shown that, in the absence of Nef, SERINC5 accelerates spontaneous functional inactivation of sensitive Envs, potentiates the neutralizing activity of anti-gp41 antibodies and, ultimately, inhibits the formation of small Env-mediated fusion pores (17). Here, we attempted to elucidate a link between SERINC5 sensitivity and functional inactivation of Envs. Toward this goal, we measured the rates of functional inactivation of a panel of HIV-1 Envs consisting of sensitive lab adapted strains, as well as resistant primary isolates and transmitted/founder viruses. We found a reasonable correlation between HIV-1 sensitivity to SERINC5, as measured by fold-reduction in infectivity, and the extent to which this factor accelerated Env inactivation (measured as reduction in half-time, $T_{50}$). The effect of SERINC5 on the rate of inactivation of sensitive Envs was more profound than on resistant strains. Increasing the density of Env in the virions did not noticeably affect SERINC5 incorporation, but rendered viruses more resistant to restriction. We also found that one of the Env conformational blocker, BMS-378806, delayed SERINC5-mediated Env inactivation. In addition, we showed that CD4 mimetics potentiated the SERINC5 effect. These results support the model that SERINC5 drives structural reorganization of Env and thereby favors its inactivation and a CD4-bound conformation is more prone to inactivation.

# Introduction

## *Virus accessory protein, Nef*

HIV-1 encodes for the structural viral proteins Gag, Pol and Env, as well as regulatory and accessory proteins Tat, Rev, Vif, Vpr, Vpu (Vpx in SIV) and Nef. Accessory proteins help dampen the host immune responses. The role of Nef in HIV-1 replication has not been fully understood until two recent papers revealed that Nef counteracts the HIV-1 restriction factor, SERINC5 (1, 2).

Nef was originally named ‘negative regulatory factor’ after the clinical observation of patients that were seropositive for HIV-1, who happened to be infected with Nef-negative virus (91). Long-term non-progressing HIV-1 infection (patients that maintained normal CD4 lymphocyte counts and very low virus blood titer) was found to be related to a lack of intact Nef genes. Slow disease progression in those patients was surprisingly similar to rhesus macaques infected with SIV strains lacking functional Nef, and presented slow clinical progression and lower viral load.

Nef can cause rapid endocytosis of major histocompatibility complex class I (MHC-I) from the surface of infected lymphoid cells, antigen presenting cells, and epithelial cells. This can prevent the recognition and clearance of infected cells by cytotoxic CD8 T cells. Natural killer cells (NK cells) are also involved in killing of virus-infected cells, but their function is impaired in the presence of Nef, which inhibits degranulation by lytic enzymes (3, 4). Nef from most SIV and HIV-2 strains can downregulate TCR-CD3 from infected T cells, thereby blocking activation-induced cell death. More importantly, Nef can also downregulate CD4 from the cell surface by

inducing its endocytosis and degradation, thereby preventing premature Env activation in infected cells and avoiding ADCC. The activation of Src kinases, such as Hck and Lyn, is also targeted by Nef, which impairs the function of downstream effectors in the signaling cascade during immune cell activation. In addition, Nef can disrupt actin dynamics via downregulation of cofilin, cellular motility, the formation of immunological synapse, and causes massive secretion of exosomes from T-cells which leads to apoptosis. Nef is also known to modulate protein expression and trafficking through binding and hijacking Dyn2 and AP-2.

Interestingly, SIV Nef can still actively increase HIV-1 infectivity in human cells (about two to ten times) (5). An unrelated murine leukemia virus protein referred to as glycoGag has been found to enhance infection, similar in effect of Nef on HIV-1 infection. Even though replacing HIV-1 Env with unrelated VSV G protein overcomes the Nef requirement, the exact molecular mechanisms of Nef-mediated infectivity increase has not been understood (6).

*Serine incorporators, 'SERINCs'*

An important function of Nef has been revealed in 2015 when two groups discovered a novel restriction factor "SERINC5" as a target of Nef (1, 2). The abbreviation SERINC comes from a study by the Inuzuka group (7) showing that this protein helps to incorporate serine during phosphatidylserine and sphingolipids biosynthesis in *E. Coli,* yeast and COS-7 cells. SERINC5 belongs to a unique family of 10 transmembrane domain proteins (Type III) that has no amino acid homology to other proteins, but is highly conserved among eukaryotes and contains five members.

SERINC5 has been shown to reduce fusion and late reverse transcription products in infected cells by ~4 fold, whereas infectivity was inhibited by ~20 fold (1, 2). SERINC5 knock-down (by siRNA) or knock-out (by CRISPR/Cas9) in CD4 T cells restores the infectivity. The counteracting effect of Nef against SERINC5 is saturable, since SERINC5 can still inhibit infection by 2-3 fold in the presence of Nef, as compared to 20-30 times in the absence of Nef, depending on the Env strain and producer cells. The Gottlinger group has shown that Nef counteracts SERINC5 by inducing its translocation from the PMto the large perinuclear compartment, likely late endosomes. Both Usami and Rosa et al. papers suggested a possibility that SERINC5 may interfere with fusion pore expansion and thereby block delivery of the core into the cytoplasm (1, 2).

*Nef and SERINC in an evolutionary arms race*

Analysis of Nef alleles derived from a broad panel of diverse HIV and SIV isolates have proven that the effect on infectivity is phylogenetically highly conserved (8). HIV-1 Env alleles are known to differ significantly in their Nef requirement (9). Nef is much less effective at increasing infectivity of primary isolates, such as ADA, YU2, and JRFL (9), and this effect has been mapped to Env.

There is a strong correlation between anti-SERINC5 potency of Nef and SIV prevalence in both primate and non-human primate species (10). Studies from the Murrell group (11) support the idea that SERINC5 and SERINC3 are unique retrovirus restriction factors in that these are not under positive selection. Compared to other restriction factors, such as APOBEC3, TRIM5-α, SAMHD-1 and BST-2 (Tetherin), SERINC5 and SERINC3 have lower proportions of codon sites under positive selection.

The Gottlinger group has shown that the intracellular loop 4 (ICL4) of SERINC5 determines its sensitivity Nef (12).

*SERINC5 antiviral activity*

As the name "serine incorporator" suggests, a possible mechanism by which SERINC5 inhibits HIV-1 infection is the altered lipid composition of the virus assembly sites (lipid rafts) on the plasma membrane. However, in contrast to the original findings by the Inuzuka group, the Trautz group has reported that SERINC5 expression neither alters the lipid composition of progeny virions nor changes the lipid content of virus-producing cells (13). SERINC5 restricted HIV-1 infectivity without altering the lipid composition and organization of virions (13). Trautz et al. also reported that Nef can increase infectivity in spite of SERINC5 incorporation into virions, suggesting a possible cryptic mechanism for HIV-1 infectivity regulation by these proteins.

The Gottlinger group has mapped the Nef sensitivity to the gp120 V1/V2 loops that are known to contribute to the trimer stability and neutralization sensitivity of Env (1). Compared to the NL4-3 and 89.6 Env, which are strongly inhibited by SERINC5, all transmitted/founder viruses are much less sensitive, and viruses like AD8 and YU-2 are highly resistant to SERINC5 (1). Fusion of HIV-1 particles pseudotyped with VSV-G protein or Ebola virus glycoproteins is also resistant to SERINC5 (14, 1, 2). SERINC5 is likely to inhibit other retroviruses, since the GlycoGag protein of murine leukemia virus and the S2 protein of equine infectious anemia virus counteract SERINC5 (1, 2, 15). The NL(AD8Env) chimera with AD8 Env cloned into the NL4-3 backbone showed resistance against SERINC5 inhibition (16). Interestingly, SERINC5 sensitizes both sensitive

HXB2 Env and resistant JRFL and BaL26 Env to the gp41-derived inhibitory peptides (e.g., C34) and neutralizing antibodies targeting the gp41 MPER (e.g., 4E10) and heptad repeat domain 1 (8k8) (16, 17). This shows that SERINC5 alters accessibility of certain epitopes on HIV-1 Env to neutralizing antibodies through inducing conformational changes in Env.

Sood et al. have shown by live cell imaging that SERINC5 blocks small fusion pore formation between single viruses and cells (17). This is in contrast to the original model proposed by Usami et al. and Rosa et al. that SERINC5 impairs the enlargement of a fusion pore (1, 2). An additional antiviral activity has been discovered by measuring the rates of spontaneous inactivation of HIV-1 Env in control and SERINC5 containing viruses (17). The accelerated inactivation of sensitive, but not resistant Env strains upon SERINC5 incorporation suggests an additional mechanism of antiviral activity and it is consistent with SERINC5-induced conformational changes in Env.

*Structure of Env*

The first structure of a monomeric HIV-1 gp120 core in complex with soluble CD4 and 17b Fab (a surrogate for co-receptor) has been solved in 1998. (18). The gp120 core consists of an inner domain and outer domain connected by a bridging sheet. The gp120 subunit contains highly variable loops V1-V5 that are largely exposed. The gp120 subunit is non-covalently associated with the gp41 subunit, masking the more conserved functional domains of gp41 involved in viral fusion. The gp41 membrane-proximal external region (MPER) links the C-terminal portion of the HR2 domain to the transmembrane domain. The gp120 and gp41 subunits within the Env trimer form a

lollipop -like structure that contains unique neutralizing antibody binding sites (19). More recently, the native unliganded Env structure has been reported (20). The structure of stabilized trimeric Env ectodomain has also been reported (21, 22). The three HR1 helices form a coiled-coil structure along the trimer symmetry axis. The V1, V2 and V3 loops of gp120 stabilize quaternary interactions between protomers, with the V3 loop sitting beneath V1/V2 and behind the glycan moiety N197. The V3 loop determines co-receptor usage and contains of high-mannose patch. The V4 and V5 loops project to the periphery and do not make contacts with other variable loops. Multiple broadly neutralizing antibodies (bnAbs) can recognize the N332 site, but bind at different angles (23, 24). The N332 site is composed of a number of overlapping glycan-dependent epitopes (25). The V3 epitope is structurally proximal to the V2 site (21), is located within the N332 supersite. V3-targeting antibodies show a similar mechanism to V2 site recognition, in that they access a minimal eight-residue peptide epitope between the positions 323 and 330 via long CDR-H3s (26). Two antibodies, PGT121 and PGT128, are highly dependent on the glycans at positions N301 and N332 (27). Studies with bnAb PG9 demonstrated its binding to the cluster of glycans including N156, N173, N160 at the apex of a trimer (28).

The Env molecule is meta-stable and readily dissociates into gp120 and gp41 subunits (gp120 shedding) upon soluble CD4 (sCD4) binding or interaction with some neutralizing antibodies (19, 30, 31). This property of Env has been a big hurdle for structural studies. A native-like trimeric Env has been engineered by insertion of a disulfide bind (SOS) at the gp120/gp41 interface with an additional mutation of Isoleucine to Proline in the $559^{th}$ amino acid in gp41 (IP) to stabilize the gp41 against

refolding and enhance proper trimerization (SOS+IP=SOSIP) (32, 33. 34). SOSIP appears to maintain proper antigenic and structural features of Env, as judged by cryo-electron tomography, single particle EM, and broadly neutralizing antibody binding (19, 35, 36).

The CD4 binding site (CD4bs) is located inside the gp120 protomer with limited accessibility in the contest of a trimer, which dictates the angle of bnAb binding to this site. The CD4bs is further restricted by surrounding glycans (37). Tier-1 viruses are more susceptible to CD4bs -targeting antibodies because of their more open structure and dissociated V1/V2 loops, while Tier-2 viruses less avidly bind CD4 due to a more compact trimer conformation that restricts access of CD4bs-targeting bnAbs (38).

Exposure of the gp41 MPER is induced by the CD4 binding, so this important neutralization epitope is only transiently exposed during the fusion process (39, 40, 41). Two human autoreactive bNAbs, 2F5 and 4E10, interact with a conserved region in the MPER (42, 43). They block viral infection by attacking an intermediate pre-hairpin conformation of gp41, and their binding to the viral membrane enhances the neutralizing activity (44, 45). Another MPER-specific antibody, 10E8, has recently been reported to neutralize HIV-1 with potency and breadth much greater than those of 2F5 or 4E10, but it appeared not to bind phospholipids and might target the native envelope spikes (46)

*Conformational dynamics of Env*

Envs from primary HIV-1 isolates are resistant to neutralizing antibodies. This is accomplished by the “closed” neutralization-resistant ground-state conformation and extensive N-glycosylation that masks conserved epitopes. Once Env engages the CD4

receptor on the host cell, it undergoes structural transformations, which expose the coreceptor binding site (47). Subsequent coreceptor engagement induces sequential rearrangement of the gp41 region, which exposes/forms the HR1 and HR2 domains, and refolds into the final six-helix bundle structure that brings the viral membrane and the cell membrane into close proximity and induces their fusion (48).

Recent groundbreaking studies by the Mothes group have directly measured the dynamic characteristics of the Env trimer in its native and CD4-bound states. These authors applied a single-molecule FRET assay to visualize conformational transitions in dual-labeled Env trimers. Donor and acceptor fluorescent dyes were introduced into different variable loops of gp120 from the neutralization-sensitive lab adapted strain NL4-3 or neutralization-resistant primary isolate JRFL. Single-molecule FRET experiments have shown the existence of three distinct conformations corresponding to low, intermediate and high FRET signal in the unliganded HIV-1 NL4-3 Env and JRFL Envs.. The major population in both unliganded Envs is low FRET, suggesting that Env preferentially remains in a closed, ground state conformation, which is masked from antibodies. Transitions into high and intermediate FRET levels corresponding to intermediate and CD4-bound structure, respectively, have been identified. The CD4 mimetic JRC-II-191, which promotes receptor-bound conformation, stabilizes the intermediate FRET level. When the small molecule entry inhibitor BMS-626529 was used as a conformational blocker (49), it stabilized the native-ground state in both HIV-1 NL4-3 Env and JRFL Envs. This work strongly suggests that locking Env in a ground state could be the mechanism of Env to evade antibody neutralization.

*Small molecule inhibitors of HIV-1 entry*

1. BMS-378806

BMS-378806 (aka BMS-806) is active against HIV-1, but not HIV-2 or SIV. BMS378806 stabilizes the prefusion ground state and blocks the Env conformational transitions induced by CD4, such as exposure of the gp41 HR1 coiled coil (50). It has been demonstrated that BMS-806 selectively affects regions around the gp120/gp41 interface, whereas the CD4 mimetic, NBD-556, destabilizes the V1/V2 and V3 crown loops (47). However, at higher concentration, the BMS-806 compound binds a distinct pocket under the ß20- ß21 loop where CD4 binds, leading to allosteric blockage of CD4 engagement (51). In summary, BMS-806 can indirectly block CD4-induced Env conformational changes, impeding the exposure of the gp41 HR1 coiled coil, but not gp120 V1/V2 relocation.

2. 484 (18A) inhibitor

484 (an analog of 18A inhibitor (Herschhorn 2014 Nature Chem Bio)) inhibits the entry of a wide range of HIV-1 isolates. 18A does not interfere with CD4 or CCR5 binding, but can block the CD4-induced disruption of quaternary structures at the trimer apex and the exposure of the gp41 HR1 region. In a recent paper, Herschhorn et al. found that 484 inhibits the following CD4-induced structural changes in a dose-dependent manner: (1) the movement of the V1/V2 region, detected by the quaternary PG9 antibody interaction, and (2) the exposure of the gp41 HR1, detected with the C34-Ig fusion protein, consisting of the Fc portion of human IgG1 linked to the HR2 region of the HXB2 Env (51). Thus,

484 inhibits CD4-induced Env transitions to downstream conformations that are critical for virus entry (51).

*Nef-SERINC5 interaction as a drug target*

There is one FDA-approved drug that blocks the HIV-1 entry steps (Enfuvirtide, Fuzeon; T20), which is used as salvage therapy in patients failing to respond to the current antiviral drugs. However, its clinical application is limited because of low efficiency, drug resistance and cross-reactivity with the preexisting antibodies in HIV-infected patients (85, 86, 87, 88, 89). For this reason, new HIV-1 fusion inhibitors are urgently needed. In this regard, studies of SERINC5-mediated HIV-1 restriction may provide important clues about Env vulnerability. An important aspect of SERINC5's activity is altering the Env structure which sensitizes Env to neutralizing antibodies (12). In addition, structural studies of Nef-SERINC5 interactions may lead to development of drugs targeting this interaction and thus counteracting the Nef activity.

Summary

In this chapter, we aimed to define the mechanism of SERINC5 restriction on HIV-1 entry/fusion. Recent studies revealed the important role of SERINC5 in inhibiting HIV-1 Env fusion, which can be counteracted by the viral protein Nef. However, the exact mechanism of inhibition of HIV-1 fusion by SERINC5 remains a mystery. In our study, I aimed to define the factors that can affect the Env resistance to SERINC5 restriction. I will mainly focus on functional inactivation of a panel of HIV-1 Env in the presence of

SERINC5 in order to assess the correlation between diverse Env conformations and SERINC5 sensitivity.

Results

*Functional inactivation of both sensitive and resistant HIV-1 strains is accelerated by SERINC5.*

A metastable structure of HIV-1 Env is spontaneously inactivated at 37$^{o}$C or even at 0$^{o}$C (17, 52). Other physical or chemical agents can affect the Env conformational preference, favoring a more "open" states that could be prone to functional inactivation (51, 52, 53). The relationship between the Env conformations and spontaneous inactivation is unclear. A paper by the Melikian lab (17) has reported that, in the absence of Nef, SERINC5 incorporated into virions enhances spontaneous inactivation of the susceptible strain HXB2, but not of the resistant JRFL Env. Strains that exhibited intermediate resistance to SERINC5 (BaL and R3A) showed moderate acceleration of spontaneous inactivation. SERINC5 has been reported to alter the native conformation of Env, leading to exposure of cryptic gp41 domains, such as the Membrane Proximal External Region (MPER) and HR1 domain (16, 17). We hypothesized that the Env's preference for the native (closed/State 1 (51, 54) conformation, as opposed for an intermediate or a CD4-bound conformation, confers resistance to SERINC5.

To assess the effect of SERINC5 on Env without Nef and to test the link between the Env stability and SERINC5 resistance, we generated a panel of pseudotyped viruses using a number of diverse Envs. We found that SERINC5 accelerates spontaneous inactivation of sensitive and, to a lesser extent, resistant Env (Fig. 1). As expected, sensitivity to SERINC5 greatly varied among HIV-1 isolates. Sensitive lab-adapted strains, such as HXB2 and ADA, that were more strongly inhibited by incorporated

SERINC5 exhibited faster decay of infectivity at 37ºC (shorter half-time of decay, $T_{50}$). Overall, we found that both susceptible and resistant Env strains were largely inactivated within 24 hours at 37ºC (Fig. 1). The relationship between fold-restriction of infectivity and fold-acceleration of infectivity loss over time (expressed as the ratio between $T_{50}$ for control and SERINC5 viruses) are shown in Table 1. As in our previous study, the infectivity decay of the Tier-1 HXB2 and ADA Env, which tend to sample more open conformations, was more strongly accelerated by SERINC5 than the infectivity decay of the Tier-2 primary isolates, JR2 or JRFL (17). In control experiments, and in agreement with our previous results (17), incorporation of the inactive SERINC2 into virions did not exhibit any antiviral effects, even for the most sensitive HXB2 Env (Fig. 1A). As expected, pseudoviruses bearing a non-HIV VSV G protein, were hardly affected by SERINC5 (Fig. 1C, Table 1).

To determine whether the observed loss of infectivity over time for all pseudoviruses tested was due to the loss of Env function, we measured decay of the viral fusion activity, using the enzyme-based BlaM assay (55). The BlaM assay is based on the incorporation of beta-lactamase-Vpr proteins (BlaM-Vpr) into HIV-1 virions. Upon viral fusion, BlaM-Vpr is delivered into the cytoplasm of a target cell and cleaves the fluorescent substrate CCF2-AM, changing its fluorescence emission spectrum from green (520 nm) to blue (447 nm). Blue/Green was calculated as a measure of viral fusion with TZM-bl cells after subtracting the background signal, as described in (55). As shown in Fig. 1D, decay in the fusion activity over time mirrored the SERINC5 effect on infectivity decay, showing that loss of infectivity was due to the loss of the Env function. Importantly, we found poor correlation between the fold-restriction and the $T_{50}$ ratio for

various HIV-1 strains (Fig. 2, Table 1). Exclusion of the HXB2 Env, which appears to be an outlier, further reduces correlation between the fold-restriction and the $T_{50}$ ratio (Fig. 2B).

*Stabilizing and destabilizing mutations in Env do not consistently alter SERINC5 activity.* We next compared the effects of mutations known to stabilize or destabilize the native structure of Env on SERINC5 sensitivity (fold-restriction and fold-acceleration of infectivity loss). We hypothesized that inducing a more open Env conformation will aid the SERINC5 activity due to exposure of cryptic epitopes, perhaps the gp41 MPER.

Among destabilizing mutations, the JRFL I423A mutation favors an open Env conformation (51). The I423A and L193A mutations in the β20–β21 base lead to open Env conformations, recapitulating the structural changes induced by CD4. These mutants require less CD4 to infect cells and are relatively resistant to Tier-2 preferring broadly neutralizing antibodies. However, the I423A mutant exhibited the same rate of Env inactivation or the fold-restriction in the presence of SERINC5 as wild-type JRFL (Fig. 2, Fig 3A-B).

The JR2 gp41 MPER destabilizing mutant K683Q is known to be partially neutralized by the MPER targeting antibody 10E8 (56). We expected it to exhibit a greater sensitivity to SERINC5, along with other MPER destabilizing mutants, such as F673L and W680G (56). However, only JR2 K683Q showed a moderate increase both in the SERINC5 fold-restriction and the $T_{50}$ ratio, while the other MPER destabilizing mutants only slightly affected the SERINC5 sensitivity (Fig. 4).

The gp120 Phe43 cavity accommodates CD4 residues and CD4-mimetic miniproteins (58). This cavity is thus critical for the CD4-gp120 interaction. In the AD8 S375W mutant, this cavity is already occupied by the bulky indole ring of Trp, which creates a CD4-bound-like conformation and thereby allows the binding of antibodies against the coreceptor binding site (58). The AD8 Env S375W mutant is also known to be sensitive to spontaneous Env inactivation in the cold (52). However, no significant differences in either the $T_{50}$ ratio or fold-restriction were observed between this mutant and wild-type AD8.

Next, we looked at stabilizing mutants of Env, hoping to confer SERINC5 resistance to sensitive Env strains (Fig. 3 C, D). The ADA V1-alt variant contains multiple mutations, including N139/I140 deletion and N142S substitution, that appear to stabilize the native conformation of the gp120 V1 loop region (59). The V1-alt Env exhibits resistance to heat inactivation (59). We also tested the N302Y and R315Q mutants that stabilize the gp120 V3 region of ADA Env. (60). The N302Y mutation converts the V3 crown from the consensus motif of clade B to that of clades A and C (i.e., GPGR-GPGQ) and is known to decrease in the potency of CCR5 antagonist maraviroc, and abrogates virus neutralization by both 447-52D and F425-B4e8 antibodies against the V3 loop (60). R315Q also increases the Maximum percent neutralization (MPN) of the PG9 bnAb against ADA and increases the thermal stability of ADA Env (60). We also tested the HXB2 3.2P variant which has been isolated from rhesus macaques after infection with a SHIV construct. The HXB2 3.2P has a dozen mutations in variable regions of gp120 and gp41 and is not only more resistant to neutralizing antibodies and cold inactivation (61, 62, 63), but also to cholesterol depletion (61).

Another stabilizing mutation tested was the H66N mutant in AD8 Env that exhibits reduced sampling of a CD4-bound conformation and reduced virus inactivation in the cold (52, 65). We found that neither of the above ADA stabilizing Env mutations exhibited decreased functional inactivation by SERINC5 (Fig. 3 and Table 1). The stabilizing mutants didn't show notable decreases in $T_{50}$ ratio except for the HXB2 3.2P mutant which was more resistant than wild type HXB2. Based on the overall results for both stabilizing and destabilizing Env mutants, we conclude that there is no clear correlation between the apparent Env stability or propensity to sample an open conformation and sensitivity to SERINC5-mediated loss of Env function.

*A higher density of Env resists SERINC5 restriction.*

We asked if the Env density can modulate the HIV-1 resistance to SERINC5. The Zwick group recently reported successful generation of cell lines that allow packaging high densities of ADA-derived Env expressed on their surface into HIV-1 particles (66). These sequentially selected cell lines termed V1, V2, V3, and V4 allow the incorporation of up to 15-fold more Env compared to parental 293T cells. Env expressed in these cell lines has a stop codon after amino acid 755 in the gp41 cytoplasmic tail, known as 755 stop, which itself does not ensure high Env expression on the cell surface. The Zwick group also confirmed that the CT truncation did not alter the antigenicity of high density Env-containing VLPs (hVLPs) that remained sensitive to neutralization by bnAbs, but not by Abs against the CD4-induced Env conformation, supporting the notion that mutant Env maintained the native Env structure.

We produced pseudoviruses carrying high density Env in the V1 and V4 cell lines (Fig. 5A). First, the expression levels of Env and SERINC5-HA was compared in control, V1 and V4 viruses by Western blotting. These analyses confirmed the abundance of Env in virions generated from V1 and V4 cells, as reported previously (Fig. 5B). SERINC5 was efficiently incorporated into V1 and V4 viruses. Functional analysis of the pseudoviruses produced in V1 and V4 cell lines revealed decreased susceptibility to SERINC5 inhibition compared to the sensitive ADA Env and its mutants, including Comb-mut and 755-stop produced in parental 293T cells (Fig. 5C). The V1 and V4 viruses were equally resistant to SERINC5, as measured by fold-restriction. The $T_{50}$ ratio for the V1 cell-produced viruses was even less affected by SERINC5 than V4 derived particles (**P=0.0033). This was unexpected, since V4 cell-produced viruses incorporate more Env than V1 cell-produced ones ((66) and Fig. 5B). Since, SERINC5 is efficiently incorporated into V1 and V4 virions (Fig. 5B), the reduced SERINC5 activity in these viruses is not due to exclusion of SERINC5. The rate of infectivity decay in control, V1, and V4 viruses showed minor differences in the $T_{50}$ values (Fig. 5C). In conclusion, the high density of Env on viruses resists SERINC5 restriction without affecting the fundamental Env inactivation rate.

*A small molecule inhibitor targeting closed conformation of Env does not significantly modulate the effect of SERINC5*

The 484 (a derivative of 18A) fusion inhibitor does not interfere with the CD4 or CCR5 binding and appears to block HIV-1 fusion by locking Env in the native conformation (67). In other words, 484 inhibits CD4-induced disruption of the quaternary structure at

the trimer apex and the exposure of the gp41 HR1 coiled coil after CD4 binding. Since 484 targets the closed Env conformation, Tier-1 strains, such as ADA and HXB2, that reside primarily in intermediate or open conformation are resistant to this compound. In contrast, Tier-2 strains, including JR2 and JRFL, are generally sensitive to this compound. We sought to test the effect of this conformational inhibitor on sensitivity of Env to SERINC5 under conditions disfavoring Env's exit from the native conformation. Since JRFL is known to be hyper-sensitive to 484 (67) we selected JRFL virus to test the effect of 484 on SERINC5's antiviral activity. Control and SERINC5-containing JRFL pseudoviruses were pre-incubated for varied times with a fully inhibitory concentration of 484 to block the Env transition from the "closed" to "open" state. Viruses were then bound to cells, washed to remove excess compound, and the effect of SERINC5 on infectivity was measured. We found that SERINC5 activity was not altered in 484 treated viruses compared to untreated samples (Fig. 5A-B), as judged by the $T_{50}$ ratio and fold restriction. The caveat of this approach is that, although JRFL Env is sensitive to 484 inhibition, it is resistant to SERINC5 inhibition (Table 1). This may mask the SERINC5 effect following the 484 pretreatment. In summary, attempts to lock Env in a closed conformation, which are less feasible for viruses that already prefer the native conformation, did not noticeably affect the SERINC5-mediated decay in infectivity.

*Probing the Env's closed conformation preference using 484 inhibitor*

Since the Env sensitivity to the 484 inhibitor is thought to be proportional to the time spent in the native state (66), we sought to use this inhibitor as a probe the effects of SERINC5 and Env mutations on the closed conformation preference. We found that the

484 potency correlated with the greater stability of native Envs (Fig. 6 and Table 2). By and large, the antiviral activity of 484 increased for Env-stabilizing mutations and decreased for destabilizing mutations. Also, incorporation of SERINC5 tended to potentiate the 484 inhibition of ADA and HXB2 Env-mediated fusion (Table 2). The exception was the increased 484 potency against the highly stable JR2 Env containing SERINC5. This indicates that, strangely, SERINC5 can stabilize the native quaternary structure of the Env apex, while exposing the MPER (Fig. 7) (16, 17).

All ADA Env stabilizing mutants exhibited reduced IC50 for 484, while the MPER destabilizing JR2 mutants increased IC50 in control viruses (Table 2). We did not observe any strong enhancement of the 484 potency by SERINC5 incorporation (Fig. 7), in contrast to the effect reported in (68). The IC50 ratios for the control and SERINC5 viruses were between 1 and 2 (Table 2). Overall, the IC50 was slightly decreased by SERINC5 and by stabilizing mutations while it was increased by SERINC5 in destabilizing mutations (Fig. 7A, B).

*CD4 mimetic enhances SERINC5 activity.*

Soluble CD4 (sCD4) and CD4 mimetics (CD4m) can irreversibly inactivate most of HIV-1 Env strains at high concentrations, while low concentrations can promote infection, especially in CD4-deficient target cells (69, 70). CD4m are also known to sensitize Env to antibody-dependent cell-mediated cytotoxicity (ADCC) by promoting an open conformation of Env. Recent studies revealed that CD4m can induce a short-lived active conformation of Env, which irreversibly leads to loss of fusion competence. In contrast, cell-surface CD4 induces long-lived active Env conformation (30). To investigate if HIV-

1 is sensitized to SERINC5 in the presence of the CD4 mimetic BNM-III-170 (71, 72), we tested control and SERINC5-containing JRFL viruses for synergy between the restriction factors and CD4 mimetic in promoting spontaneous inactivation of Env (Fig. 8). Incubating with BNM-III-170 for 2 or 8 hours revealed that BNM-III-170 significantly accelerated functional inactivation of JRFL-SERINC5 viruses compared to no treatment control, as determined by the $T_{50}$ ratio (*P=0.0123, Fig. 8A). The ratio of $T_{50}$ between Vector and SERINC5 was also increased by CD4m (*P=0.0157, Fig. 8B). Vector versus SERINC5 virus clearly showed that SERINC5 potently inhibited JRFL virus by 8 hours of CD4m treatment (Fig. 8C). We conclude that CD4m itself accelerates functional inactivation and SERINC5 acts synergistically to further promote loss of function.

*A conformational blocker slows down inactivation of Env by SERINC5*

BMS-378806 is known to bind to a gp120 pocket that is distinct from the CD4 binding site and allosterically stabilize the native Env structure (73). This compound has been shown to shift the Env conformational transitions toward the closed/State 1 conformation (74). We asked whether this compound affects SERINC5-mediated inactivation of Env. These experiments rely on the ability to wash out the drug after pre-incubation and probe the resulting infectivity, which proved difficult due to the poor reversibility of BMS-378806 binding to gp120 (75). Hence we used an intermediate concentration of BMS-378806 and a “reverse infection system” adapted from previous literatures (73, 76) (Fig. 9A). In this system, viruses are first adhered to the bottom of poly-lysine coated multi-well plates, treated with drugs, washed and overlaid with cells (76). After incubating the

virus with BMS-378806, we measured the fold decrease of infectivity between 2 and 6 hours of BMS-378806 pretreatment at 37ºC. Only SERINC5+ virus and not Vector virus showed a significant fold decrease in $T_{50}$ (2.1 ± 0.39 to 1.4 ± 0.26, **P=0.0059) (Fig. 9B). Likewise, the infectivity decay of SERINC5 virus over time without the drug was accelerated compared to control, while BMS-378806-treated SERINC5 virus exhibited a significantly delayed functional decay. We assume that stabilizing the native conformation of Env by BMS-378806 prevents SERINC5 access to more vulnerable open conformations. In summary, conformational blocker BMS-378806 decelerated SERINC5 inhibition of ADA virus.

## Discussion

We hypothesized that an inherent stability of Env and its propensity to sample different conformations may modulate the sensitivity to SERINC5. We also speculated that mutations, physical factors and chemical agents that promote transition from the native conformation may modulate resistance to SERINC5. Our result showed that spontaneous inactivation of both susceptible and resistant HIV-1 Envs is accelerated in the presence of SERINC5, but that the resistant strains were less affected by this factor. In addition, most stabilizing and destabilizing mutations in Env did not alter the SERINC5's antiviral activity. We demonstrated a moderate correlation between the propensity of Env to assume an open conformation and SERINC5 restriction. Modulation of the Env conformational preference by some mutations or by fusion inhibitors is consistent with the notion that SERINC5 targets a transient intermediate Env conformation.

A much weaker SERINC5 effect on the $T_{50}$ ratio was observed for SERINC5-resistant Envs compared to sensitive Envs, consistent with our previous paper (Fig. 1) (17). HXB2 showed the far greater fold-restriction and the $T_{50}$ ratio by SERINC5 compared to other strains. Unfortunately, another sensitive strain, ADA, had only a moderately larger fold-restriction and the $T_{50}$ ratio compared to resistant strains. A relatively weak correlation between fold-restriction and $T_{50}$ ratio suggests that acceleration of functional Env inactivation is not the main mechanism of SERINC5 activity, except for the HXB2 strain.

Comparison of various Env stabilizing and destabilizing mutants did not reveal a strong correlation between the preference for the closed Env structure, SERINC5

sensitivity and fold-restriction, especially in regards to the $T_{50}$ ratio. There were, however, a few mutations that showed a predicted phenotype. The stabilization of the hyper-sensitive HXB2 Env by selecting for a stable HXB2 3.2P variant significantly reduced the virus sensitivity to SERINC5 (Fig. 3C-D, Fig. 4C). Stabilization of another SERINC5-sensitive strain ADA by introducing a cold-resistance mutation H66N resulted in a significant decrease in the $T_{50}$ ratio compared to wild-type Env (Fig. 3C-D, Fig. 4D). Also, one destabilizing K683Q mutation in the JR2 MPER increased the inactivation rate by SERINC5. However, no significant effects on SERINC5 sensitivity were observed for other MPER-destabilizing mutations, JR2 W680G or F673L. Overall, most of the mutations in different regions of Env altering its stability failed to significantly modulate the effect of SERINC5.

The fact that a denser array of Env renders the virus resistant to SERINC5 (Fig. 5) is in line with the promotion of functional inactivation of Env by SERINC5, as proposed previously (17). Whereas the fundamental rate of Env inactivation appears to be independent of the Env density, a much greater number of functional Envs is expected to be retained by viruses that contain more copies of Env at any given time. Indeed, the average number of Env trimers required for entry is between 1 and 7 (82, 83), whereas V4 viruses pack around 150 trimers (66). We currently cannot explain the greater resistance of V1 viruses to SERINC5 as compared to V4 viruses that pack on average a greatest number of Envs per virion (66). It is possible that a gross overexpression of Envs in V4 cells comes at the cost of slightly altered Env processing and/or post-translational modifications. Usage of a different Envs, such as the sensitive HXB2 strain in V1/V4 packaging cells could be a good control.

We observed that a CD4 mimetic can enhance the SERINC5 effect on functional inactivation of the resistant JRFL Env. Conversely, BMS-378806 decreased the rate of SERINC5-mediated inactivation of sensitive ADA Env. These findings are consistent with the hypothesis that SERINC5 targets transient epitopes that are exposed in an intermediate or open (CD4-bound) structure of Env. Previous study showed that SERINC5 renders HIV-1 Env become sensitive to CCR5 co-receptor antagonist maraviroc (17). Unlike BMS-378806, incubation with 484 did not modulate the SERINC5-sensitivity of JRFL Env. The lack of 484 effect may be due to its ability to lock the ground conformation of Env (51) versus the BMS-378806's ability to drive conformational transitions from the intermediate/open states to the closed/ground state (84).

The ability of SERINC5 to inhibit infection did not exceed 20-fold under our conditions, even for the most sensitive strains, in contrast to the stronger SERINC5 effects reported in the literature (2). This is likely due to our explicit strategy not to over-incorporate SERINC5 into virions. One caveat is that we did not measure the incorporation of SERINC5 into virions. These issues can be addressed in the future experiments.

Coreceptor tropism does not appear to correlate with SERINC5 sensitivity, since both the lab-adapted HXB2 strain is CXCR4-tropic, while the ADA strain uses CCR5 for entry are sensitive to SERINC5. The Chou group (90) recently published the NMR structure of the prefusion state of the MPER and transmembrane domain. Their findings showed very slow bnAb binding with epitopes which indicates that infrequent fluctuations of the MPER structure give these antibodies occasional access to alternative

conformations of MPER epitopes. We speculate the epitope required for SERINC5 inhibition has very limited access to SERINC5 during fusion process which needs more mutation studies to probe spatiotemporal access in the presence of variable open Env conformations.

Through altering the native Env conformation, we obtained important clues regarding the mechanism of SERINC5-mediated acceleration of functional inactivation of Env. We found that a CD4 mimetic that promotes an open conformation of Env potentiates SERINC5 restriction of viral fusion. In contrast, the conformational blocker, BMS-378806, which favors the closed conformation of Env, delays SERINC5-mediated inactivation. Additionally, some mutations that stabilize the closed Env conformation (HXB2-3.2P, AD8 H66N) render Env more resistant to SERINC5. Even though we did not observe a clear correlation between the Env conformation and SERINC5 sensitivity, our results are consistent with be existence of cryptic sites within Env that may interact with SERINC5. Our results suggest that these putative epitopes are more accessible to SERINC5 in a CD4-bound state. While the exact conformation(s) targeted by SERINC5 is(are) unknown, it is possible that certain transient states other than the three main Env conformations depicted in the model (Fig. 1D in Introduction to SERINC5) interact with SERINC5. It is also possible that SERINC5 targets an Env conformation downstream of a CD4-bound state, such as the ternary complex of Env with CD4 and coreceptor. The inconsistent effects of stabilizing and destabilizing mutations indicate that a single substitution may not be sufficient to expose a cryptic epitope that may be targeted by SERINC5. We speculate that the JR2 K683Q mutation in the MPER, which is positioned at the hinge between the gp41 MPER and transmembrane domain (56), but not other

tested mutations in this region, may expose a SERINC5-targeted epitope. In future studies, SERINC5/Env co-IP can be performed in the presence of CD4 mimetics to favor SERINC5-interacting conformation of Env.

## Materials and Methods

### *Cell Lines, plasmids and reagents*

HEK293T/17 cells were purchased from ATCC (Manassas, VA) and TZM-bl cells from the AIDS Research and Reference Reagent Program (National Institutes of Health). HEK293T/17 cells and TZM-bl cells were passed in Dulbecco's Modified Eagle's Medium with L-glutamine (Lonza, MD), sodium pyruvate and glucose (Gibco, NY) supplemented with 10% fetal bovine serum and 100units/ml penicillin/streptomicin (Gemini Bio-Products, Sacramento, CA). The culture medium for HEK293T/17 cells included 0.5mg/ml Geneticin (G418) to keep selection of resistant cells over passage (Cellgro, Mediatech, Manassas, VA). Cells were incubated at 37°C in a humidified 5% $CO_2$ air environment.

Bright-Glo luciferase kit was purchased from Promega (Madison, WI). Fresh fetal bovine serum (FBS) was heat-inactivated in 55°C before added to the growth medium (Corning, NY). Poly-D-lysine was obtained from Sigma, Germany. The BMS-378806 compound (50, 78) was synthesized by ChemPacific Corp. (Baltimore, MD). 484 (18A) was a kind gift from Dr. Sodroski (Dana-Farber Cancer Institute, Harvard Medical School, Boston, MA).

The pCAGGS plasmids encoding HXB2, JRFL envelope glycoproteins were provided by Dr. J. Binley (Torrey Pines Institute, CA). pcRev (Dr. Bryan R. Cullen) (79); pMM310- BlaM-Vpr (Dr. Michael Miller, Merck Research Laboratories) (80); HIV immunoglobulin (HIV Ig) (Dr. Luiz Barbosa, NABI, NHLBI, National Institutes of Health); HIV monoclonal antibodies (mAbs) PG9 (from IAVI, La Jolla, CA); The

pMDG-VSV-G plasmid expressing VSV-G was kindly offered from J. Young (Roche Applied Science, Mannheim, Germany). The HIV-1-based packaging vector such as pR9ΔEnvΔNef was from Dr. Chris Aiken (Vanderbilt University). PBJ5, PBJ5-SER5-HA, PBJ5-SER2-HA expression plasmids were engineered and used as described previously. (2, 77).

*Pseudovirus production*

HIV-1 pseudoviruses were produced after transfection of packaging vectors and each Envelope-containing plasmids in HEK293T/17 cells. Cells were transfected with 4μg of pR9ΔEnvΔNef, 1.5μg of pBJ5 mock or pBJ5-SER5-HA or pBJ5-SER2-HA, 2ug of BlaM-vpr, and 1μg of pcRev per 100-mm dish as described in our previous paper (17). JetPrime transfection kit (Polyplus, NY) was used for transfection. For dense Env array experiments, 755 stop Comb-mut Env was transfected into 293T cells along with packaging vector pR9ΔEnvΔNef while in V1 and V4 cell lines only packaging vector was transfected with or without SERINC5-HA plasmid. After overnight transfection, the supernatant was replaced with phenol-red negative media (Gibco, NY) and at 48 hours post-transfection the supernatant was harvested and filtered through 0.45um syringe filter (VWR, PA). V1 and V4 Env packaging cell lines were a kind gift from Dr. Zwick (The Scripps Research Institute, La Jolla, CA) and were culture in the presence of 2 μg/ml puromycin (Life Technologies). Lenti-X concentrator (Clontech, Japan) was used for further concentration of virus (10x concentration). Virus stocks were stored in at -80°C before used in BlaM assay or single round infectivity in TZM-bl cells.

*Virus-cell fusion and infectivity assays*

Virus-cell fusion was quantified using BlaM assay, as described previously (Miyauchi, 2009 Cell). Briefly, TZM-bl cells were plated in 96-well clear-bottom pated (corning) a day before to reach minimum 90-100% confluency next day. Each virus was normalized with p24 measurement by ELISA before initiation of BlaM assay and infectivity assay. Viruses were attached to target cells by spinoculation method which involved chilling cells at 4°C while centrifuging for 30 minutes at 1650xg Cells were rested in incubator at 37°C for 90 minutes in phenol red negative growth medium before stopping fusion process by directly putting the plate on the ice (Sood, 2017 JBC). The growth medium was replaced with BlaM substrate, CCF4-AM (Invitrogen). BlaM activity was measured next morning after incubating cells at 12°C overnight using SpectraMaxi3 fluorescence plate reader (Molecular Devices, Sunnyvale, CA). The fold was quantified by calculating the ratio of coumarin versus fluorescein signal.

Infectivity assays were performed with normalized amount of virus, as in the BlaM assays in TZM-bl cells. In order to prevent the luciferase signal saturation in a given time window, viruses were serially diluted. Cells were plated a day before with $1x10^4$ cells per well in the 96 black clear well plates. Viruses were incubated in the 96 well tissue-treated plate for indicated times at 37°C in the presence of 20 mM of HEPES before spinoculated over target cells. After 48 hours of incubation at 37°C, the infectivity was measured using Bright-Glo luciferase substrate.

*P24 ELISA and Western blotting*

Mouse anti-p24 monoclonal CA-183 (provided by Bruce Chesebro and Kathy Wehrly through the NIH AIDS Research and Reference Reagent Program) was used for enzyme-linked immunosorbent assay (ELISA) to measure HIV-1 Gag in virus-containing culture supernatant and virus pellets; the capture ELISA was performed as previously described (81). Equal amount of virus measured by p24 (10pg) in 1X SDS-containing loading buffer (Biorad) was loaded onto 4-15% gradient premade gel (Biorad) and then transferred on to a nitrocellulose membrane, blocked with 10% blotting grade Blocker (Biorad) for 30minutes to 1 hour. Precision Pus protein standards (10kb, Biorad) was used as protein size markers. HIV-Ig (1:2000 dilution) was used to blot gag and rabbit anti-HA (sigma, 1:500 dilution) was used to blot SERINC5. PG9 human antibody (NIH) was used to blot gp120 and gp160 of HIV-1 Env. Horseradish peroxidase-conjugated (HRP) goat anti-rabbit antibody (Santa Cruz Biotechnology, 1:500 dilution), HRP-rabbit anti mouse (Millipore) and a chemiluminescence reagent (GE Healthcare) were used for chemiluminescence detection.

*Graphs and equations*

The $T_{50}$ ratio was calculated by dividing $T_{50}$ for the Vector control by $T_{50}$ for SERINC5-containing viruses as a measure of the extent of SERINC5-mediated acceleration of infectivity decay. The less stable or more prone to inactivation Env glycoproteins exhibit larger is $T_{50}$ ratios. Fold-restriction was calculated by dividing the infectivity of freshly thawed virus without SERINC5 by that of virus with SERINC5. Greater values show a more potent effect of SERINC5 on infectivity.

The equation used for inactivation in $T_{50}$ is (Fig. 3A, C); Mut stands for ‘mutation’.

$$y = \frac{\text{T50 vec mut/T50 SER5 mut}}{\text{T50 vec WT/T50 SER5 WT}}$$

The equation used for inactivation in Fold restriction is (Fig. 3B, D);

$$y = \frac{\text{FR vec mut/FR SER5 mut}}{\text{FR vec WT/FR SER5 WT}}$$

‘Mut’ stands for ‘mutation’.

Figures

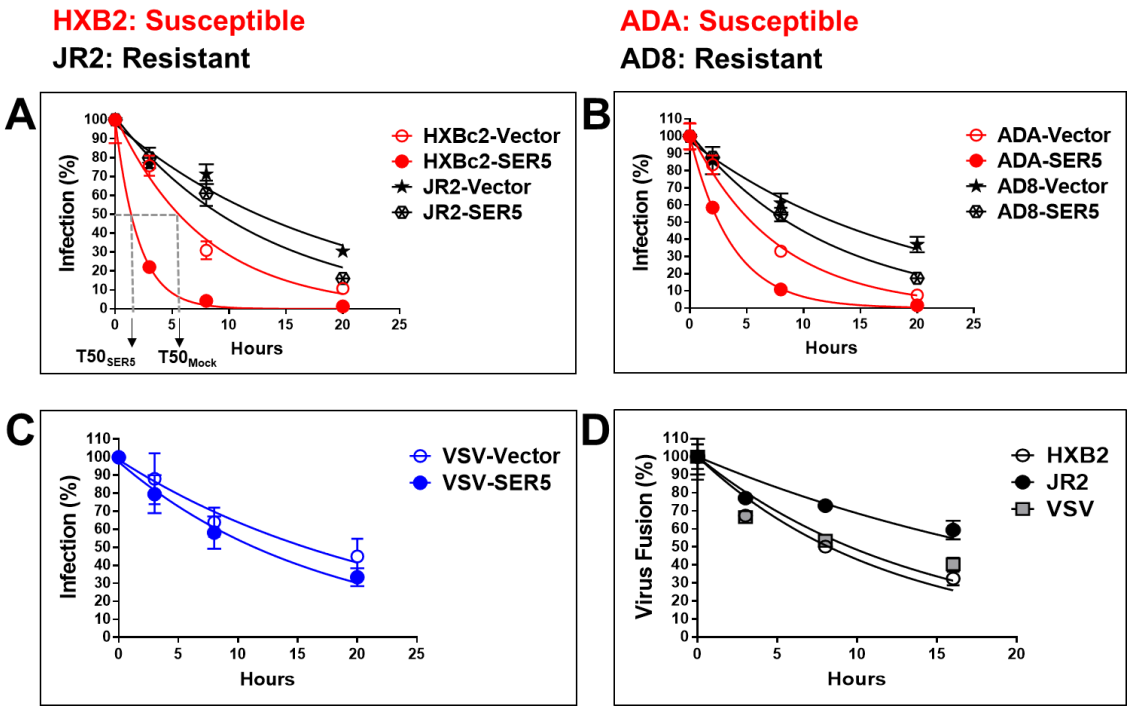


**Fig. 1. SERINC5 accelerates spontaneous inactivation of sensitive and, to a lesser extent, of resistant Env**

(A, B) Loss of infectivity of pseudoviruses bearing sensitive or resistant Env strains over time at 37ºC. (C) Non-HIV VSV-G pseudoviruses inactivate slowly and are resistant to SER5. (D) Drop in infectivity at 37°C is related to loss of fusion competence. The T50 ratio was calculated by measuring the time at which 50% of infectivity was lost using a single-exponential curve fit (non-linear curve fit) in Graph Pad Prism 6 software. T50 Mock and T50 Serinc5 are marked in (A). Representative graphs are shown as means ± SD from at least 2 independent experiments.

| Env | T50 | SD | T50 Ratio (mock/SER5) | Fold restriction | Phenotype | P value (T50) |
|---|---|---|---|---|---|---|
| HXB2-mock | 5.4 | 0.36 | 5.3 ± 1.69 | 10.7 ± 0.74 | Tier-1 like | stats with HXB2 |
| HXB2-SER5 | 1.1 | 0.34 | | | | |
| HXB2 3.2P-mock | 12.7 | 1.65 | 1.8 ± 0.30 | 3.3 ± 0.23 | Resistant to Abs and cold | *P = 0.0467 |
| HXB2 3.2P-SER5 | 7.1 | 0.77 | | | | |
| HXB2-mock | 3.3 | 0.08 | 1.23 ± 0.02 | 0.7 ± 0.07 | Tier-1 like | *P = 0.0326 |
| HXB2-SER2 | 2.6 | 0.27 | | | | |
| ADA-mock | 4.9 | 1.16 | 1.8 ± 0.65 | 6.5 ± 0.82 | Tier-1 like | |
| ADA-SER5 | 2.8 | 0.76 | | | | |
| ADA-V1 alt-mock | 11.1 | 2.98 | 2.3 ± 0.87 | 6.0 ± 0.52 | N139/I140 deletion, N142S | |
| ADA-V1 alt-SER5 | 4.9 | 1.34 | | | GP120 V1 stabilizing | |
| ADA-N302Y-mock | 7.3 | 0.27 | 2.0 ± 0.26 | 6.0 ± 0.99 | GP120 V3 Stabilizing | |
| ADA-N302Y-SER5 | 3.7 | 0.45 | | | | |
| ADA-R315Q-mock | 8.4 | 0.13 | 1.8 ± 0.41 | 3.7 ± 0.01 | GP120 V3 Stabilizing | P = 0.0522 |
| ADA-R315Q-SER5 | 4.8 | 1.11 | | | | |
| Comb-mock | 14 | 4 | 1.7 ± 0.8 | 4.7 ± 1.45 | 8 Stabilizing mutations on ADA | |
| Comb-SER5 | 8 | 2.99 | | | More thermostable | |
| JRFL-mock | 12 | 1.3 | 1.5 ± 0.16 | 2.6 ± 0.11 | Tier-2 like isolate | *P = 0.0128 |
| JRFL-SER5 | 8 | 0.34 | | | | |
| JRFL I423A-mock | 8.3 | 0.3 | 1.3 ± 0.11 | 1.7 ± 0.32 | Induced open structure (β20-β21 sheet) | *P = 0.0344 |
| JRFL I423A-SER5 | 8.1 | 0.48 | | | Sensitive to CD4m, sCD4, Abs in downstream | |
| AD8-mock | 13.5 | 0.57 | 1.6 ± 0.1 | 2.5 ± 0.25 | Tier-2 like | *P = 0.0434 |
| AD8-SER5 | 8.3 | 0.39 | | | | |
| AD8-S375W-mock | 14 | 1.05 | 1.2 ± 0.35 | 1.0 ± 0.09 | More CD4-bound-like | *P = 0.0325 |
| AD8-S375W-SER5 | 12.2 | 3.5 | | | Exposure of CoR binding site, Cold sensitive | |
| AD8 H66N-mock | 13.5 | 1.68 | 0.9 ± 0.25 | 2.1 ± 0.08 | More closed conformation | *P = 0.0258 |
| AD8 H66N-SER5 | 14.4 | 3.39 | | | Cold resistant | |
| AD8 N197S-mock | 14.2 | 2.91 | 1.2 ± 0.46 | 1.2 ± 0.46 | Shift in V1 V2 loops | *P = 0.0330 |
| AD8 N197S-SER5 | 11.9 | 3.82 | | | Exposure of CoR binding site | |
| JR2-mock | 12 | 2.15 | 1.6 ± 0.56 | 2.2 ± 0.45 | Tier-2 like isolate | *P = 0.0160 |
| JR2-SER5 | 7.7 | 2.26 | | | | |
| JR2-K683Q-mock | 17.7 | 1.44 | 3.0 ± 0.63 | 2.7 ± 0.22 | MPER destabilizing | |
| JR2-K683Q-SER5 | 6 | 1.18 | | | | |
| VSV-mock | 12.5 | 2.6 | 1.1 ± 0.25 | 2.2 ± 0.82 | non HIV G protein expression | **P=0.0027 |
| VSV-SER5 | 11.2 | 1 | | | | |

**Table 1. Spontaneous inactivation of sensitive Envs is more profoundly accelerated by SERINC5 than resistant Envs.**

**S**ensitive Env strains, such as lab-adapted strains HXB2 and ADA, are colored red, while resistant strains, including primary isolate JRFL, AD8 and JR2, are colored black; non-HIV control VSV-G pseudovirus is colored blue. The effects of SERINC5 on sensitive and resistant wild-type or mutant Envs were compared. The T50 ratio was calculated by measuring the time at which 50% of infectivity was lost using a single-exponential curve fit in Graph Pad Prism 6 software. Fold-restriction is the ratio of inhibition of infection by SER5 in freshly collected and frozen control and SERINC5-containing viruses. Results

are shown as means ± SD from at least 2 representative individual experiments. *, $\rho < 0.05$; **, $\rho < 0.01$, as determined by the Student's unpaired t test using GraphPad Prism 6.

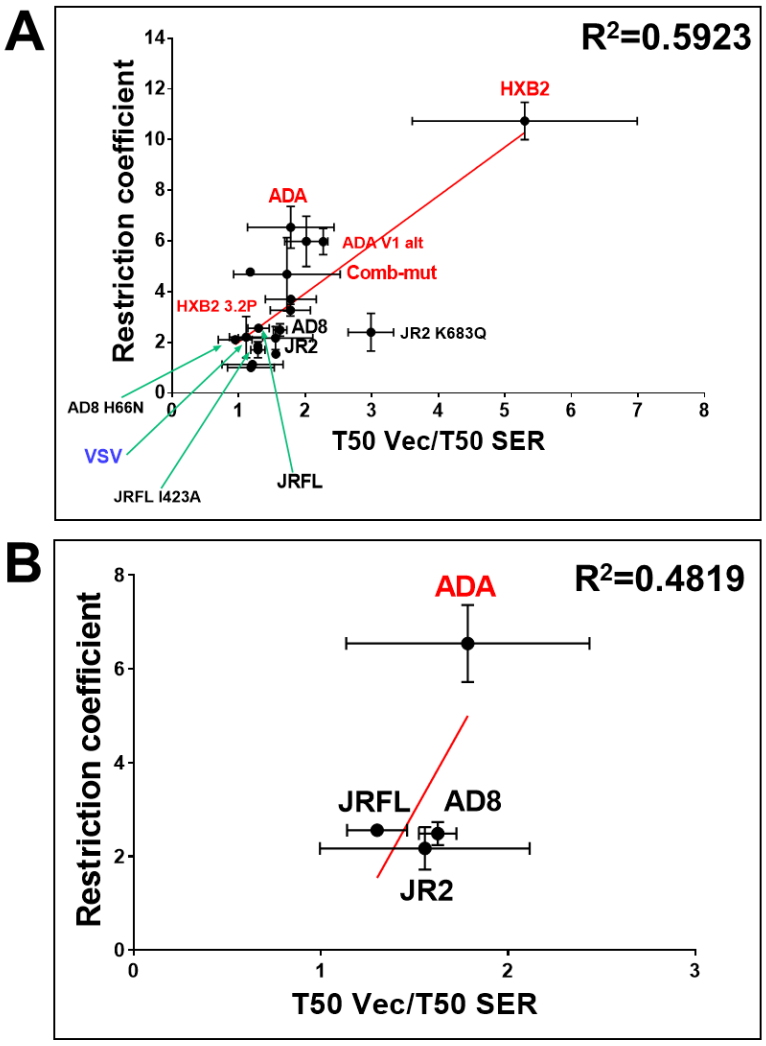


**Fig. 2. The rate of functional Env inactivation by SERINC5 at 37°C weakly correlates with sensitivity to restriction.**

The T50 ratio was calculated by measuring the time at which 50% of infectivity was lost using a single-exponential curve fit in Graph Pad Prism 6 software. Fold-restriction is the ratio of inhibition of infection by SER5 in freshly collected and frozen control and SERINC5-containing viruses. (A) Sensitive Env strains are colored red, while resistant strains are black; non-HIV control VSV-G is colored blue. The correlation between restriction coefficient and T50 ratio is relatively weak ($R^2$ is less than 0.70 but greater

than 0.50). (B) Exclusion of the “outlier” HXB2 further reduces the correlation efficient. Red line is the linear regression fit to the results.

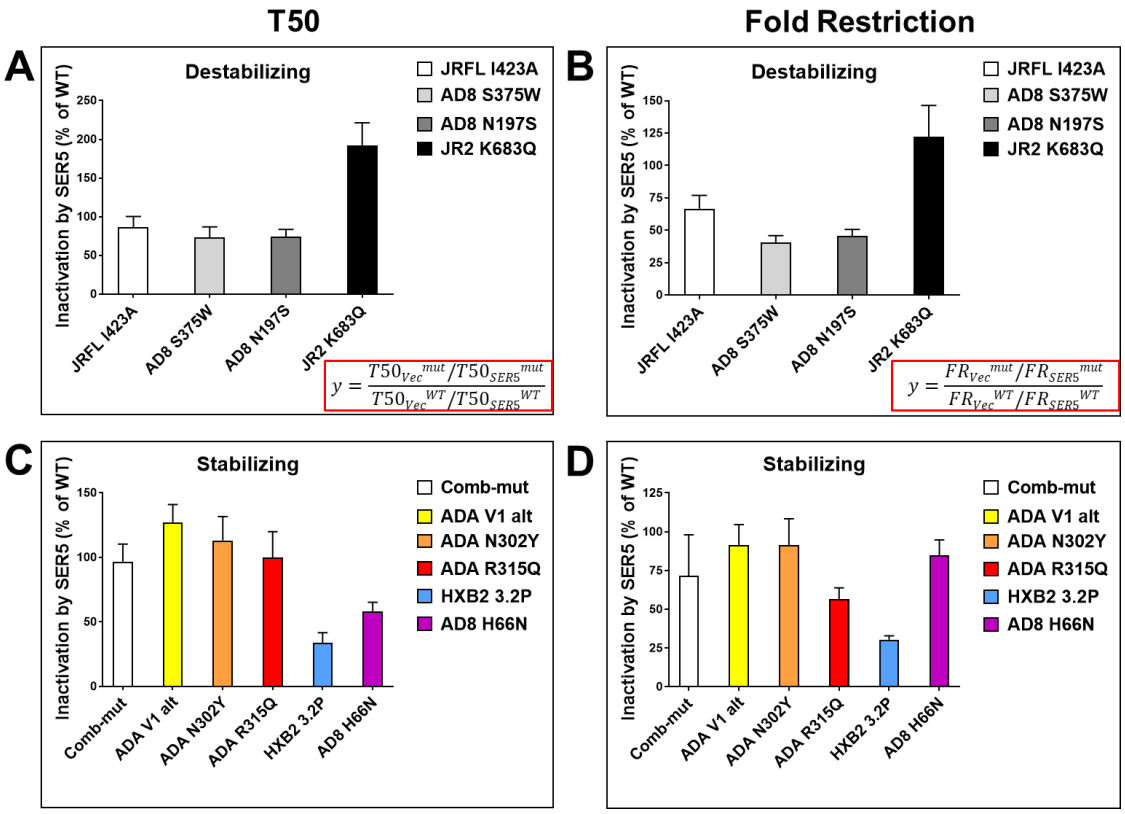


**Fig. 3. Mutations that destabilize or stabilize the native HIV-1 Env structure do not consistently alter the anti-viral activity of SERINC5.**

(A-B) Destabilizing mutations did not cause dramatic inactivation by SERINC5 as manifested in the T50 ratio and fold restriction. Equations used to calculate the T50 ratio (A) and fold-restriction (B) are shown in the bottom right. Functional inactivation of Env by SERINC5 is not accelerated by the I432A mutation that opens up the JRFL Env. (C-D) Stabilizing mutations did not considerably antagonize the functional inactivation of Env by SERINC5, as shown by the T50 ratio and fold-restriction. Results are means ± SD from at least 2 indipendent experiments.

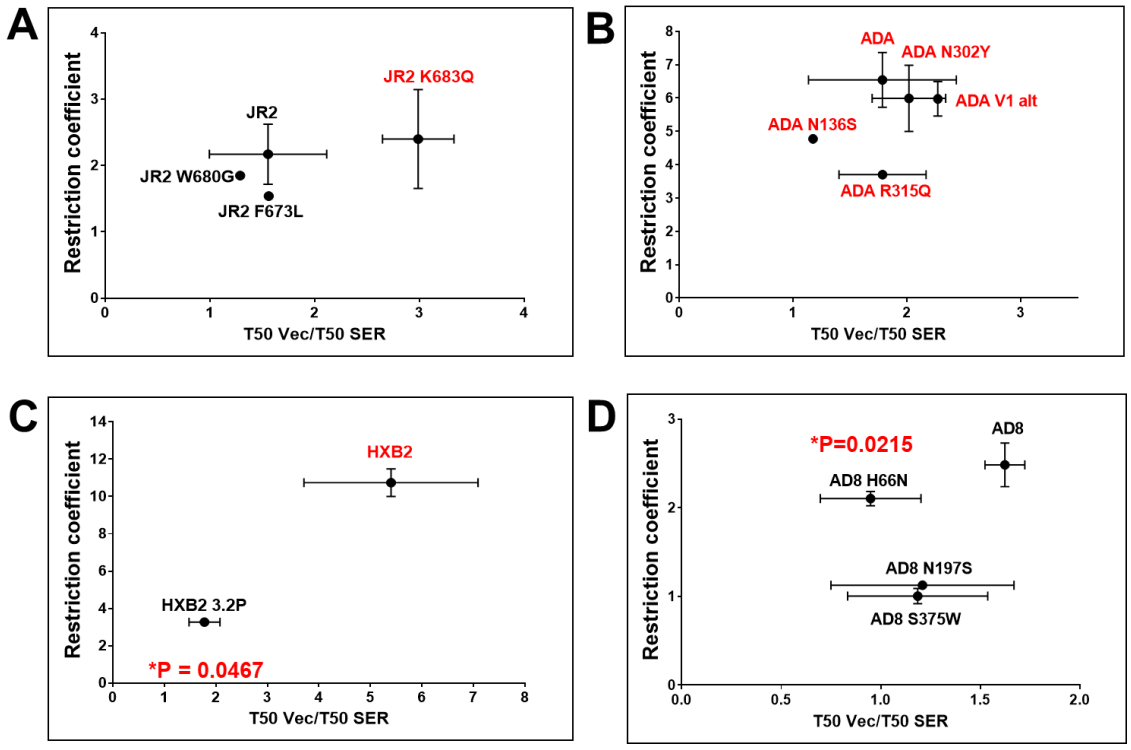


**Fig. 4. The effect of Env-stabilizing mutations the SERINC5 activity.**

(A) Two gp41 MPER destabilizing JR2 mutants did not significantly change either fold-restriction or the T50 ratio SERINC5 vs. control viruses. Only the third mutant JR2 K684Q was sensitized to SERINC5-mediated decay of infectivity. (B) gp120 V1-V3 stabilizing ADA mutations did not decrease SERINC5 sensitivity. (C) The stabilized HXB2 3.2P mutant was significantly more resistant to SERINC5 inactivation. (D) The cold-resistant AD8 H66N mutant was more slowly inactivated at 37$^{o}$C than wild-type Env. Results are shown as means ± SD from at least 2 independent experiments. *, $\rho < 0.05$

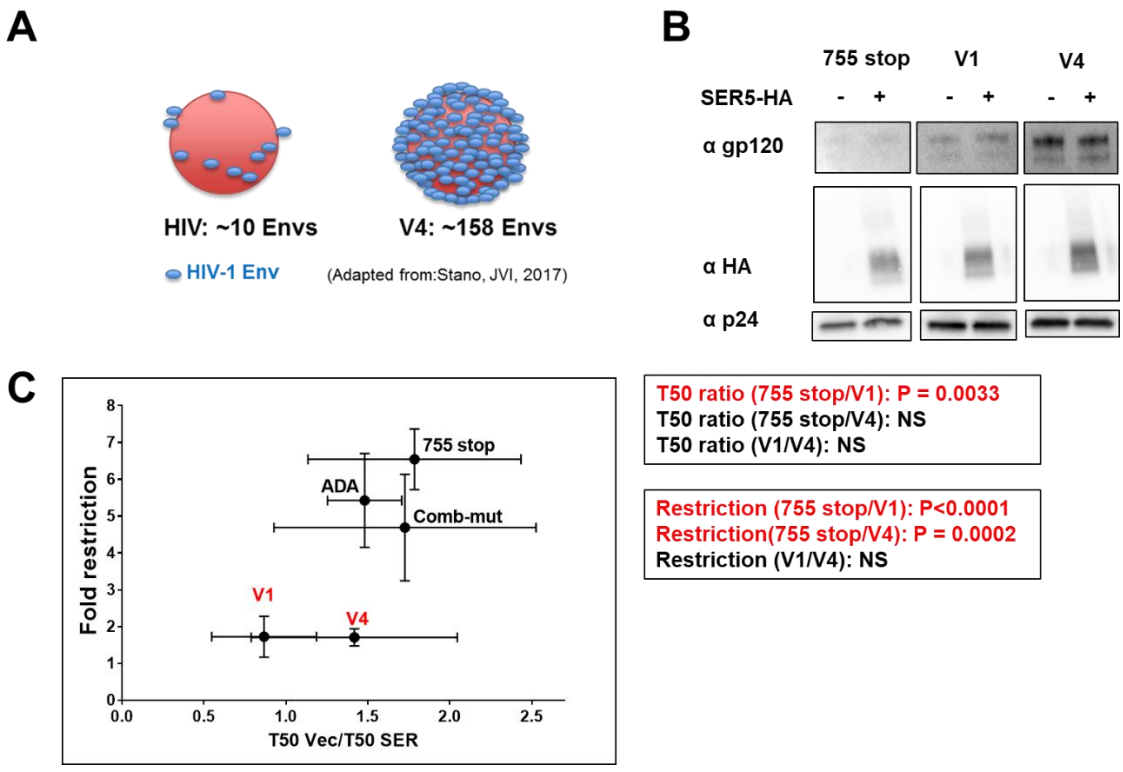


**Fig. 5. Increased density of HIV-1 Env reduces sensitivity to SERINC5**

(A) Schematic diagram of HIV-1 virions and V4 virions with increased Env density (B) Western blot analysis of Env and SERINC5 incorporation into V1, V4 and control 755-stop viruses. HIV-1 pseudoviruses were produced in the presence or absence of SERINC5-HA, normalized for p24 content by ELISA and loaded onto a 4-15% gradient polyacrylamide gel. Note that SERINC5-HA incorporation was not impeded by overexpressed Env on the virion surface. (C) Fold-restriction by SERINC5 is diminished for viruses produced in both V1 and V4 cell lines (755 stop/ V1: ****P <0.0001, 755 stop/ V4: ***P=0.0002). V1 cell line-produced viruses exhibit significantly decreased T50 ratio compared to control viruses produced in 293T cells (755-stop). Results are

shown as means ± SD from at least 2 independent experiments. P values were calculated using the Student's unpaired t test using GraphPad Prism 6.

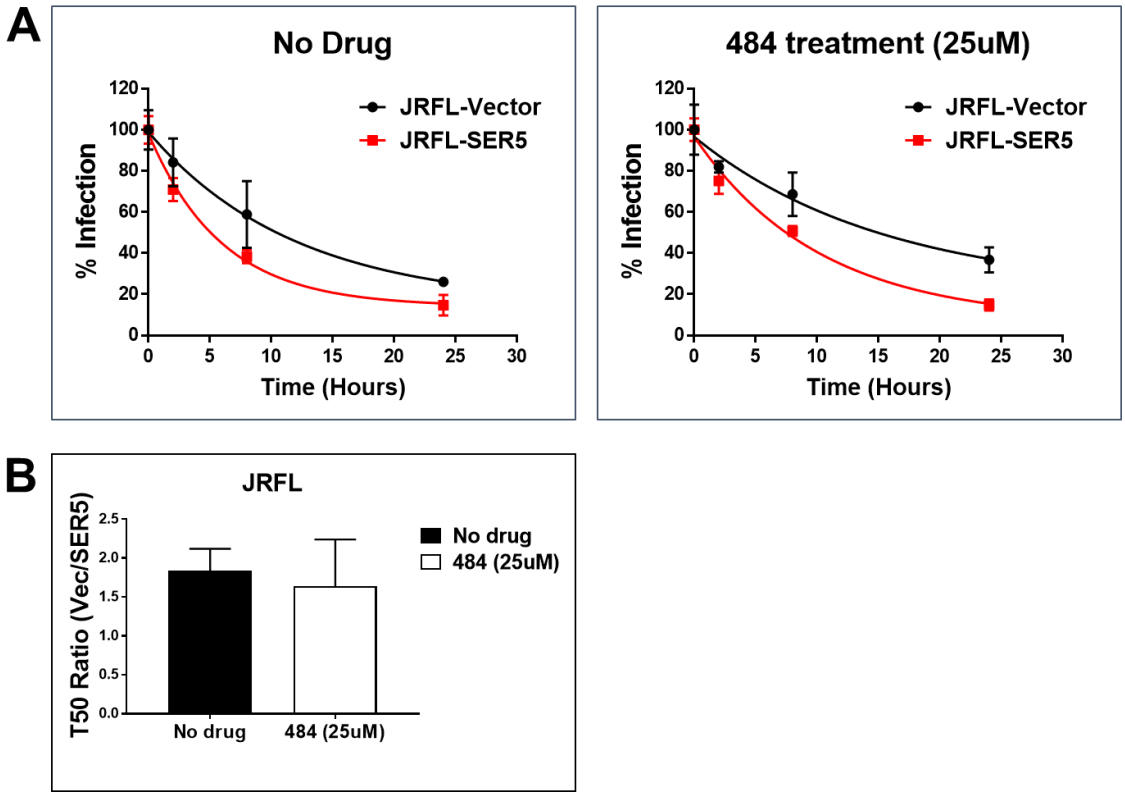


**Fig. 6. Constraining native/ground state of Env by 484 does not significantly change JRFL Env sensitivity to SERINC5.**

(A) JRFL Env pseudotyped viruses containing or lacking SERINC5 were preincubated at 37$^{o}$C with or without the small molecule inhibitor 484 for indicated times before binding on a poly-D-lysine coated plate. After virus binding, drug was washed away three times, and TZM-bl cells were overlaid onto viruses by spinoculation. There was no significant effect of 484 on SERINC5 inhibition. (B) Env inactivation by SERINC5 was not different between no drug control and drug treatment.

| Env | 484 IC50 (uM) | SD | IC50 Ratio(mock/SER5) | Phenotype |
|---|---|---|---|---|
| ADA-mock | 8.2 | 2.27 | 2.1 ± 0.86 | Tier-1 like |
| ADA-SER5 | 4 | 1.27 | | |
| ADA V1 alt-mock | 4.3 | 2.65 | 1.4 ± 0.98 | N139/I140 deletion, N142S |
| ADA V1 alt-SER5 | 3 | 1 | | GP120 V1 stabilizing |
| ADA R315Q-mock | 2.5 | | 1.1 | GP120 V3 Stabilizing |
| ADA R315Q-SER5 | 2.2 | | | |
| AD8 H66N-mock | 31.9 | | 1.1 | More closed conformation |
| AD8 H66N-SER5 | 29.8 | | | Cold resistant |
| HXB2-mock | 21.1 | 1.97 | 1.6 ± 0.70 | Tier-1 like |
| HXB2-SER5 | 14.7 | 6.52 | | |
| HXB2 3.2P-mock | 12.7 | | 1.8 | Resistant to Abs and cold |
| HXB2 3.2P-SER5 | 7.1 | | | |
| JR2-mock | 0.4 | 0.07 | 1.0 ± 0.17 | Tier-2 like isolate |
| JR2-SER5 | 0.4 | 0.007 | | |
| JR2 K683Q-mock | 0.6 | 0.12 | 2.0 ± 1.1 | MPER destabilizing |
| JR2 K683Q-SER5 | 0.3 | 0.15 | | |
| JR2 F673L-mock | 1.1 | | 1.0 | MPER destabilizing |
| JR2 F673L-SER5 | 1.1 | | | |
| JR2 W680G-mock | 2.2 | | 1.4 | MPER destabilizing |
| JR2 W60G-SER5 | 1.5 | | | |
| JRFL-mock | 1.8 | 0.36 | 1.1 ± 0.47 | Tier-2 like isolate |
| JRFL-SER5 | 1.6 | 0.61 | | |

**Table 2. Relationship between Env stability, SERINC5-sensitivity and sensitivity to 484 inhibition.**

SERINC5-sensitive strains, such as ADA and HXB2, are resistant to 484 inhibition compared to SERINC5-resistant strains, including JR2 and JRFL. Env-stabilizing mutants increase and destabilizing mutants decrease 484 potency. The IC50 values were measured using dose-response inhibition equation Y=100/(1+X/IC50), where X is the 484 concentration in µM in GraphPad Prism 6.

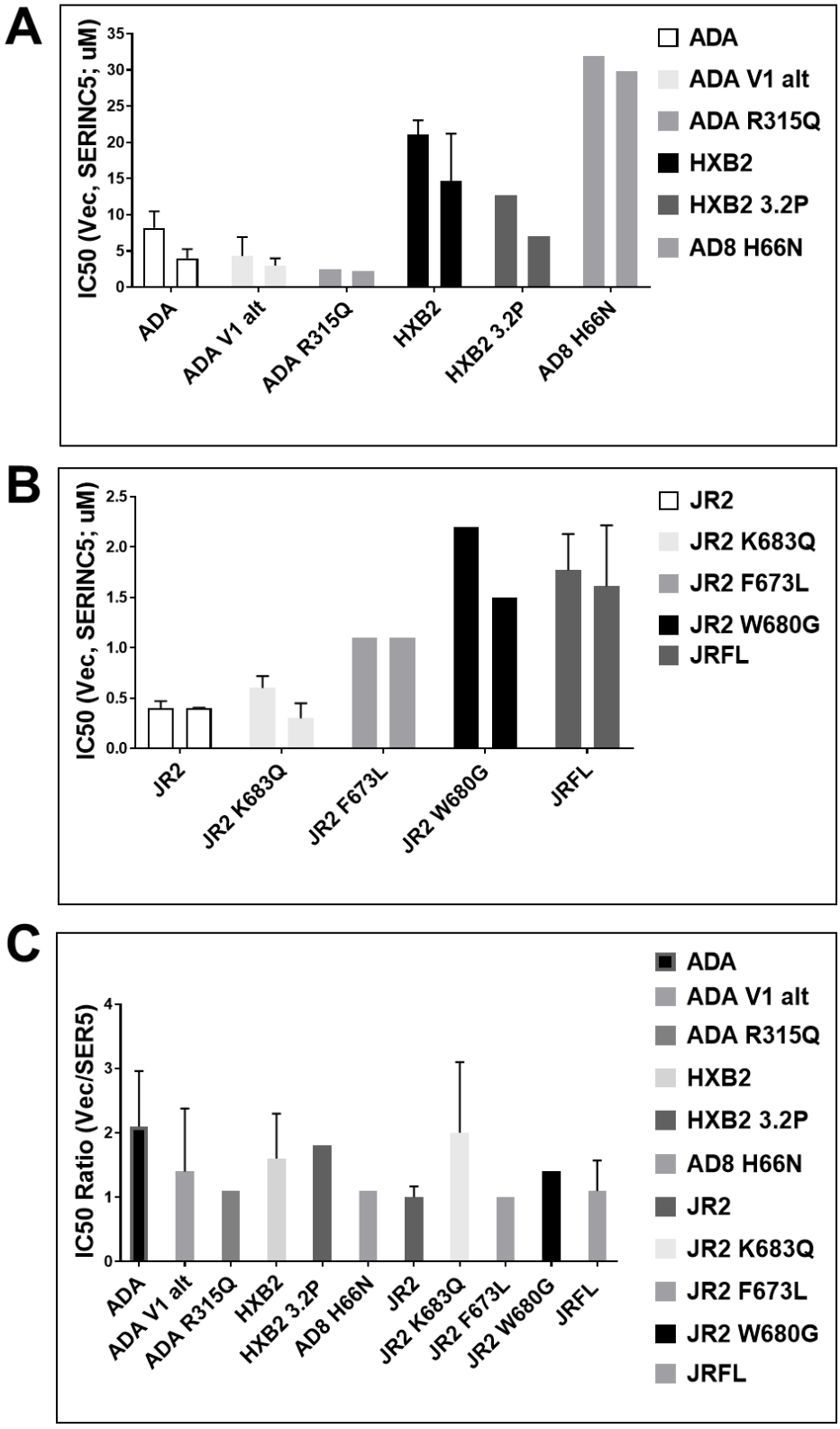
A
IC50 (Vec, SERINC5; uM)
35
30
25
20
15
10
5
0
ADA
ADA V1 alt
ADA R315Q
HXB2
HXB2 3.2P
AD8 H66N
B
IC50 (Vec, SERINC5; uM)
2.5
2.0
1.5
1.0
0.5
0.0
JR2
JR2 K683Q
JR2 F673L
JR2 W680G
JRFL
C
IC50 Ratio (Vec/SER5)
4
3
2
1
0
ADA
ADA V1 alt
ADA R315Q
HXB2
HXB2 3.2P
AD8 H66N
JR2
JR2 K683Q
JR2 F673L
JR2 W680G
JRFL

**Fig. 7. Effect of Env-stabilizing the destabilizing mutations on SERINC5- and 484-sensitivity**

(A) The IC50 values of 484-resistant SERINC5-sensitive strains, such as ADA and HXB2, are similar for Vector and SERINC5-containing viruses. Viruses were spinoculated onto TZM-bl cells in the presence of varied doses of 484 and cells were cultured for 48 hours before measuring infectivity by a luciferase assay. Env-stabilizing mutations tend to decrease the IC50 for 484. (B) “Closed” conformation-preferring Envs, JR2 and JRFL, are sensitive to 484. As with “open” conformation-preferring Envs, these the presence of SERINC5 does not noticeably affect the sensitivity to 484. Env-destabilizing mutations tend to increase the IC50 for 484. (C) IC50 ratios for Vector over SERINC5 viruses bearing different Env strains and their mutants do not show a consistent trend.

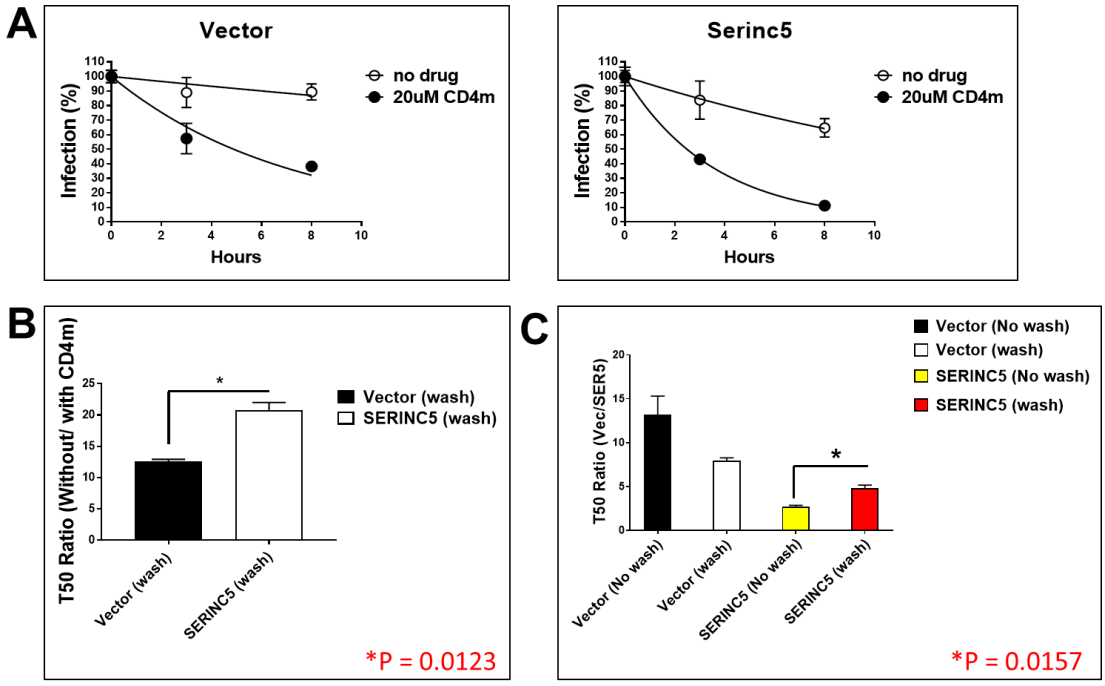


**Fig. 8. CD4 mimetic augments SERINC5-mediated acceleration of infectivity decay.** (A) Original graphs showing the effect of CD4 mimetic on T50.(B) Control JRFL or SERINC5-containing pseudoviruses were pre-incubated with 20 µM CD4m (BNM-III-170) for indicated time and washed 3 times before binding to a poly-D-lysine coated plate (reverse system). After TZM-bl cells were spinoculated onto the viruses, infectivity was measured after 48 hours of incubation. (C) Comparison of the infectivity decay rates for control and SERINC5-containing pseudoviruses after pretreatment with CD4m. In control experiments, the combined effects of CD4m and SERINC5 were assessed by not removing the drug after pre-incubation and performing infection in the presence of drug.

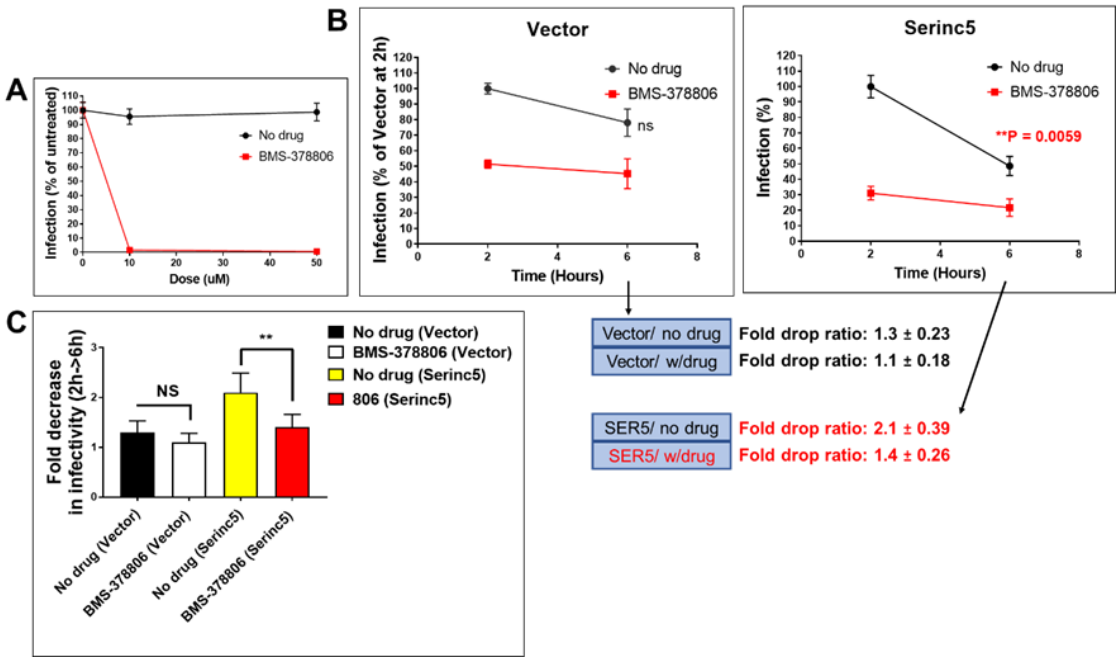


**Fig. 9. Conformational blocker BMS-378806 decelerates SERINC5-mediated decay of ADA infectivity.**

(A) BMS-378806 dose-response curve for ADA pseudovirus infection of TZM-bl cells. ADA pseudoviruses were pre-incubated with 20 µM BMS-378806 for an indicated time (2 or 6 h), bound to a poly-D-lysine coated plate before spinoculation with target cells (B-C). Favoring the closed conformation of Env by BMS-3788806 significantly delays SERINC5-mediated Env inactivation between 2 hours and 6 hours of pre-treatment. Fold decrease in infectivity from 2 to 6 h was calculated. **, $\rho < 0.01$. P values were calculated using the Student's unpaired t test (GraphPad Prism).

References

1. Usami Y, Wu Y, Göttlinger HG. 2015. SERINC3 and SERINC5 restrict HIV-1 infectivity and are counteracted by Nef. Nature. 526(7572):218-23. doi: 10.1038/nature15400.

2. Rosa A, Chande A, Ziglio S, De Sanctis V, Bertorelli R, Goh SL, McCauley SM3, Nowosielska A, Antonarakis SE, Luban J, Santoni FA, Pizzato M. HIV-1 Nef promotes infection by excluding SERINC5 from virion incorporation. Nature. 526(7572):212-7. doi: 10.1038/nature15399.

3. Collins KL, Chen BK, Kalams SA, Walker BD, Baltimore D. 1998. HIV-1 Nef protein protects infected primary cells against killing by cytotoxic T lymphocytes. Nature. 22;391(6665):397-401.

4. Shah AH, Sowrirajan B, Davis ZB, Ward JP, Campbell EM, Planelles V, Barker E. 2010. Degranulation of natural killer cells following interaction with HIV-1-infected cells is hindered by downmodulation of NTB-A by Vpu. Cell Host Microbe. 8(5):397-409. doi: 10.1016/j.chom.2010.10.008.

5. Sinclair E, Barbosa P, Feinberg MB. 1997. The nef gene products of both simian and human immunodeficiency viruses enhance virus infectivity and are functionally interchangeable. J Virol. 71(5):3641-51. PMID: 9094638

6. Aiken C. 1997. Pseudotyping human immunodeficiency virus type 1 (HIV-1) by the glycoprotein of vesicular stomatitis virus targets HIV-1 entry to an endocytic pathway and suppresses both the requirement for Nef and the sensitivity to cyclosporin A. J Virol. 71(8):5871-7. PMID: 9223476

7. Inuzuka M, Hayakawa M, Ingi T. 2005. Serinc, an activity-regulated protein family, incorporates serine into membrane lipid synthesis. J Biol Chem. 280(42):35776-83. DOI: 10.1074/jbc.M505712200

8. Münch J, Rajan D, Schindler M, Specht A, Rücker E, Novembre FJ, Nerrienet E, Müller-Trutwin MC, Peeters M, Hahn BH, Kirchhoff F. 2007. Nef-mediated enhancement of virion infectivity and stimulation of viral replication are fundamental properties of primate lentiviruses. J Virol. 81(24):13852-64. DOI: 10.1128/JVI.00904-07

9. Usami Y, Göttlinger H. 2013. HIV-1 Nef responsiveness is determined by Env variable regions involved in trimer association and correlates with neutralization sensitivity. Cell Rep. 5(3):802-12. doi: 10.1016/j.celrep.2013.09.028.

10. Heigele A, Kmiec D, Regensburger K, Langer S, Peiffer L, Stürzel CM, Sauter D, Peeters M, Pizzato M, Learn GH, Hahn BH, Kirchhoff F. 2016. The Potency of Nef-

Mediated SERINC5 Antagonism Correlates with the Prevalence of Primate Lentiviruses in the Wild. Cell Host Microbe. 20(3):381-391. doi: 10.1016/j.chom.

11. Murrell B, Vollbrecht T, Guatelli J, Wertheim JO. 2016. The Evolutionary Histories of Antiretroviral Proteins SERINC3 and SERINC5 Do Not Support an Evolutionary Arms Race in Primates. J Virol. 90(18):8085-9. doi: 10.1128/JVI.00972-16.

12. Dai W, Usami Y, Wu Y, Göttlinger H. 2018. A Long Cytoplasmic Loop Governs the Sensitivity of the Anti-viral Host Protein SERINC5 to HIV-1 Nef. Cell Rep. 22(4):869-875. doi: 10.1016/j.celrep.2017.12.082.

13. Trautz B, Wiedemann H, Lüchtenborg C, Pierini V, Kranich J, Glass B, Kräusslich HG, Brocker T, Pizzato M, Ruggieri A, Brügger B, Fackler OT. 2017. The host-cell restriction factor SERINC5 restricts HIV-1 infectivity without altering the lipid composition and organization of viral particles. J Biol Chem. 292(33):13702-13713. doi: 10.1074/jbc.M117.797332.

14. Pizzato M, Popova E, Göttlinger HG. 2008. Nef can enhance the infectivity of receptor-pseudotyped human immunodeficiency virus type 1 particles. J Virol. 82(21):10811-9. doi: 10.1128/JVI.01150-08.

15. Chande A, Cuccurullo EC, Rosa A, Ziglio S, Carpenter S, Pizzato M. 2016. S2 from equine infectious anemia virus is an infectivity factor which counteracts the retroviral inhibitors SERINC5 and SERINC3. Proc Natl Acad Sci U S A. 113(46):13197-13202. DOI: 10.1073/pnas.1612044113

16. Beitari S, Ding S, Pan Q, Finzi A, Liang C. 2017. Effect of HIV-1 Env on SERINC5 Antagonism. J Virol. 91(4). pii: e02214-16. doi: 10.1128/JVI.02214-16.

17. Sood C, Marin M, Chande A, Pizzato M, Melikyan GB. 2017. SERINC5 protein inhibits HIV-1 fusion pore formation by promoting functional inactivation of envelope glycoproteins. J Biol Chem. 292(14):6014-6026. doi: 10.1074/jbc.M117.777714.

18. Wyatt R, Kwong PD, Desjardins E, Sweet RW, Robinson J, Hendrickson WA, Sodroski JG. 1998. The antigenic structure of the HIV gp120 envelope glycoprotein.

19. Liu J, Bartesaghi A, Borgnia MJ, Sapiro G, Subramaniam S. 2008. Molecular architecture of native HIV-1 gp120 trimers. Nature. 455(7209):109-13. doi: 10.1038/nature07159.

20. Kwon M, Pavlov TS, Nozu K, Rasmussen SA, Ilatovskaya DV, Lerch-Gaggl A, North LM, Kim H, Qian F, Sweeney WE Jr, Avner ED, Blumer JB, Staruschenko A,

Park F. 2012. Kwon M1, Pavlov TS, Nozu K, Rasmussen SA, Ilatovskaya DV, Lerch-Gaggl A, North LM, Kim H, Qian F, Sweeney WE Jr, Avner ED, Blumer JB, Staruschenko A, Park F. Proc Natl Acad Sci U S A109(52):21462-7. doi: 10.1073/pnas.1216830110

21. Julien JP, Cupo A, Sok D, Stanfield RL, Lyumkis D, Deller MC, Klasse PJ, Burton DR, Sanders RW, Moore JP, Ward AB, Wilson IA. 2013. Crystal structure of a soluble cleaved HIV-1 envelope trimer. Science. 342(6165):1477-83. doi: 10.1126/science.1245625.

22. Bartesaghi A, Merk A, Borgnia MJ, Milne JL, Subramaniam S. 2013. Prefusion structure of trimeric HIV-1 envelope glycoprotein determined by cryo-electron microscopy. Nat Struct Mol Biol. 20(12):1352-7. doi: 10.1038/nsmb.2711.

23. Sok et al. 2014. Promiscuous glycan site recognition by antibodies to the high-mannose patch of gp120 broadens neutralization of HIV. Sci Transl Med. 6(236):236ra63. doi: 10.1126/scitranslmed.3008104.

24. Murin CD, Julien JP2, Sok D3, Stanfield RL2, Khayat R4, Cupo A5, Moore JP5, Burton DR6, Wilson IA7, Ward AB8. 2014. Structure of 2G12 Fab2 in complex with

soluble and fully glycosylated HIV-1 Env by negative-stain single-particle electron microscopy. J Virol. 88(17):10177-88. doi: 10.1128/JVI.01229-14.

25. Kong et al. 2013. Supersite of immune vulnerability on the glycosylated face of HIV-1 envelope glycoprotein gp120. Nat Struct Mol Biol. 20(7): 796–803. doi: 10.1038/nsmb.2594

26. Pejchal R et al. 2011. A potent and broad neutralizing antibody recognizes and penetrates the HIV glycan shield. Science. 2011 Nov 25;334(6059):1097-103. doi: 10.1126/science.1213256.

27. Walker LM. 2011. Broad neutralization coverage of HIV by multiple highly potent antibodies. Nature. 2011 Sep 22;477(7365):466-70. doi: 10.1038/nature10373.

28. Julien JP et al. 2013. Asymmetric recognition of the HIV-1 trimer by broadly neutralizing antibody PG9. Proc Natl Acad Sci U S A. 2013 Mar 12;110(11):4351-6. doi: 10.1073/pnas.1217537110.

29. JP Moore, JA McKeating, RA Weiss, QJ Sattentau. 1990. Dissociation of gp120 from HIV-1 virions induced by soluble CD4. Science Vol. 250, Issue 4984, pp. 1139-1142

DOI: 10.1126/science.2251501

30. Haim H et al. 2009. Soluble CD4 and CD4-Mimetic Compounds Inhibit HIV-1 Infection by Induction of a Short-Lived Activated State. PLoS Pathog 5(4): e1000360. doi: 10.1371/journal.ppat.1000360

31. Ruprecht CR et al. 2011. MPER-specific antibodies induce gp120 shedding and irreversibly neutralize HIV-1. J Exp Med. 208(3): 439–454. doi: 10.1084/jem.20101907

32. Binley, J.M. et al. 2000. A recombinant human immunodeficiency virus type 1 envelope glycoprotein complex stabilized by an intermolecular disulfide bond between the gp120 and gp41 subunits is an antigenic mimic of the trimeric virion-associated structure. J. Virol. 74, 627–643 PMID: 10623724

33. Sanders, R.W. et al. 2002. Stabilization of the soluble, cleaved, trimeric form of the envelope glycoprotein complex of human immunodeficiency virus type 1. J. Virol. 76, 8875–8889 DOI: 10.1128/JVI.76.17.8875-8889.2002

34. Sanders, R.W. et al. 2013. A next-generation cleaved, soluble HIV-1 Env trimer, BG505 SOSIP.664 gp140, expresses multiple epitopes for broadly neutralizing but not

non-neutralizing antibodies. PLoS Pathog. 9, e1003618 doi: 10.1371/journal.ppat.1003618.

35. Blattner, C. et al. 2014. Structural delineation of a quaternary, cleavage-dependent epitope at the gp41-gp120 interface on intact HIV-1 Env trimers. Immunity 40, 669–680 doi: 10.1016/j.immuni.2014.04.008

36. Falkowska, E. et al. 2014. Broadly neutralizing HIV antibodies define a glycan-dependent epitope on the prefusion conformation of gp41 on cleaved envelope trimers. Immunity 40, 657–668 doi: 10.1016/j.immuni.2014.04.009.

37. Jardine, J. et al. 2013. Rational HIV immunogen design to target specific germline B cell receptors. Science 340, 711–716 doi: 10.1126/science.1234150.

38. Tran, K. et al. 2014. Vaccine-elicited primate antibodies use a distinct approach to the HIV-1 primary receptor binding site informing vaccine redesign. Proc. Natl. Acad. Sci. U.S.A. 111, E738–E747 https://doi.org/10.1073/pnas.1319512111

39. Cardoso RM, Zwick MB, Stanfield RL, Kunert R, Binley JM, Katinger H, Burton DR, Wilson IA.2005. Broadly neutralizing anti-HIV antibody 4E10 recognizes a helical

conformation of a highly conserved fusion-associated motif in gp41. Immunity. 22(2):163-73. DOI: 10.1016/j.immuni.2004.12.011

40. Morris M, Koyama A, Masliah E, Mucke L. 2011. Tau reduction does not prevent motor deficits in two mouse models of Parkinson's disease. PLoS One. 6(12):e29257. doi: 10.1371/journal.pone.0029257.

41. Ofek G, Tang M, Sambor A, Katinger H, Mascola JR, Wyatt R, Kwong PD. 2004. Structure and mechanistic analysis of the anti-human immunodeficiency virus type 1 antibody 2F5 in complex with its gp41 epitope. J Virol. 2004 Oct;78(19):10724-37. DOI: 10.1128/JVI.78.19.10724-10737.2004

42. Muster T, Steindl F, Purtscher M, Trkola A, Klima A, Himmler G, Rüker F, Katinger H. 1993. A conserved neutralizing epitope on gp41 of human immunodeficiency virus type 1. J Virol 67(11):6642-7. PMID: 7692082

43. Stiegler G, Kunert R, Purtscher M, Wolbank S, Voglauer R, Steindl F, Katinger H. 2001. A potent cross-clade neutralizing human monoclonal antibody against a novel epitope on gp41 of human immunodeficiency virus type 1. AIDS Res Hum Retroviruses. 2001 Dec 10;17(18):1757-65. DOI: 10.1089/08892220152741450

44. Alam SM, Morelli M, Dennison SM, Liao HX, Zhang R, Xia SM, Rits-Volloch S, Sun L, Harrison SC, Haynes BF, Chen B. 2009. Proc Natl Acad Sci U S A. 2009 Dec 1;106(48):20234-9. doi: 10.1073/pnas.0908713106.

45. Frey G, Peng H, Rits-Volloch S, Morelli M, Cheng Y, Chen B. 2008. A fusion-intermediate state of HIV-1 gp41 targeted by broadly neutralizing antibodies. Proc Natl Acad Sci U S A. 105(10):3739-44. doi: 10.1073/pnas.0800255105.

46. Huang J et al. Broad and potent neutralization of HIV-1 by a gp41-specific human antibody. 2012. Nature. 491(7424):406-12. doi: 10.1038/nature11544.

47. Guttman M, Garcia NK, Cupo A, Matsui T, Julien JP, Sanders RW, Wilson IA, Moore JP, Lee KK. 2014. CD4-induced activation in a soluble HIV-1 Env trimer. Structure. 22(7):974-84. doi: 10.1016/j.str.2014.05.001.

48. Guenaga J, Wyatt RT. 2012. Structure-guided alterations of the gp41-directed HIV-1 broadly neutralizing antibody 2F5 reveal new properties regarding its neutralizing function. PLoS Pathog. 8(7):e1002806. doi: 10.1371/journal.ppat.1002806.

49. Li XS, Dong WC, Wang XM, Hu GZ, Wang YB, Cai BY, Wu CM, Wang Y, Du XD. 2013. Presence and genetic environment of pleuromutilin-lincosamide-streptogramin A

resistance gene lsa(E) in enterococci of human and swine origin. J Antimicrob Chemother. 69(5):1424-6. doi: 10.1093/jac/dkt502.

50. Si Z et al. 2004. Small-molecule inhibitors of HIV-1 entry block receptor-induced conformational changes in the viral envelope glycoproteins. Proc Natl Acad Sci U S A. 101(14):5036-41.

51. Herschhorn et al. 2017. The β20-β21 of gp120 is a regulatory switch for HIV-1 Env conformational transitions. Nat Commun. 8(1):1049. doi: 10.1038/s41467-017-01119-w.

52. A Kassa, A Finzi, M Pancera, JR. Courter, AB. Smith, J Sodroski. 2009. Identification of a Human Immunodeficiency Virus Type 1 Envelope Glycoprotein Variant Resistant to Cold Inactivation. J Virol. 2009 May; 83(9): 4476–4488. doi: 10.1128/JVI.02110-08

53. Pancheco B. 2017. Residues in the gp41 Ectodomain Regulate HIV-1 Envelope Glycoprotein Conformational Transitions Induced by gp120-Directed Inhibitors. J Virol. 91(5). pii: e02219-16. doi: 10.1128/JVI.02219-16.

54. Wang H, Cohen AA, Galimidi RP, Gristick HB, Jensen GJ, Bjorkman PJ.2016. Cryo-EM structure of a CD4-bound open HIV-1 envelope trimer reveals structural

rearrangements of the gp120 V1V2 loop. Proc Natl Acad Sci U S A. 113(46):E7151-E7158. DOI: 10.1073/pnas.1615939113

55. Marin M, Du Y, Giroud C, Kim JH, Qui M, Fu H, Melikyan GB. 2015. High-Throughput HIV-Cell Fusion Assay for Discovery of Virus Entry Inhibitors. Assay Drug Dev Technol. 13(3):155-66. doi: 10.1089/adt.2015.639.

56. Kim AS, Leaman DP1, Zwick MB1. 2014. Antibody to gp41 MPER alters functional properties of HIV-1 Env without complete neutralization. PLoS Pathog. 10(7):e1004271. doi: 10.1371/journal.ppat.1004271.

57. Dey B, Berger EA. 2014. Blocking HIV-1 gp120 at the Phe43 cavity: if the extension fits. Structure. 21(6):871-2. doi: 10.1016/j.str.2013.05.004.

58. Guo Q et al. 2013. Biochemical and genetic characterizations of a novel human immunodeficiency virus type 1 inhibitor that blocks gp120-CD4 interactions. J Virol. 77(19):10528-36. PMID: 12970437

59. DP. Leaman, MB. Zwick. 2013. Increased Functional Stability and Homogeneity of Viral Envelope Spikes through Directed Evolution. PLoS Pathog. 9(2): e1003184. doi: 10.1371/journal.ppat.1003184

60. SK Gift, DP. Leaman, L Zhang, AS. Kim, MB. Zwick. 2017. Functional Stability of HIV-1 Envelope Trimer Affects Accessibility to Broadly Neutralizing Antibodies at Its Apex. J Virol. 91(24): e01216-17. doi: 10.1128/JVI.01216-17

61. Z Si, M Cayabyab, J Sodroski. 2001. Envelope Glycoprotein Determinants of Neutralization Resistance in a Simian-Human Immunodeficiency Virus (SHIV-HXBc2P 3.2) Derived by Passage in Monkeys. J Virol. 75(9): 4208–4218. doi: 10.1128/JVI.75.9.4208-4218.2001

62. Herrera C, Klasse PJ, Michael E, Kake S, Barnes K, Kibler CW, Campbell-Gardener L, Si Z, Sodroski J, Moore JP, Beddows S. 2005. The impact of envelope glycoprotein cleavage on the antigenicity, infectivity, and neutralization sensitivity of Env-pseudotyped human immunodeficiency virus type 1 particles. Virology. 338(1):154-72. DOI: 10.1016/j.virol.2005.05.002

63. Johnson J et al. 2017. Induction of a Tier-1-Like Phenotype in Diverse Tier-2 Isolates by Agents That Guide HIV-1 Env to Perturbation-Sensitive, Nonnative States. J Virol. 91(15). pii: e00174-17. doi: 10.1128/JVI.00174-17.

64. Marin M, Rose KM, Kozak SL, Kabat D. 2003. HIV-1 Vif protein binds the editing enzyme APOBEC3G and induces its degradation. Nat Med9(11):1398-403 PMID: 14528301

65. Haim H et al. 2011. Contribution of intrinsic reactivity of the HIV-1 envelope glycoproteins to CD4-independent infection and global inhibitor sensitivity. PLoS Pathog. 7(6):e1002101. doi: 10.1371/journal.ppat.1002101.

66. Stano A et al. 2017. Dense Array of Spikes on HIV-1 Virion Particles. J Virol. 2017 Jun 26;91(14). pii: e00415-17. doi: 10.1128/JVI.00415-17.

67. Herschhorn A, Gu C, Espy N, Richard J, Finzi A, Sodroski JG. 2014. A broad HIV-1 inhibitor blocks envelope glycoprotein transitions critical for entry. Nat Chem Biol. 10(10):845-52. doi: 10.1038/nchembio.1623.

68. Schulte B, Selyutina A, Opp S, Herschhorn A, Sodroski JG, Pizzato M, Diaz-Griffero F. 2018. Localization to detergent-resistant membranes and HIV-1 core entry inhibition correlate with HIV-1 restriction by SERINC5. Virology. 515:52-65. doi: 10.1016/j.virol.2017.12.005.

69. Daar ES, Li XL, Moudgil T, Ho DD. 1990. High concentrations of recombinant soluble CD4 are required to neutralize primary human immunodeficiency virus type 1 isolates. Proc Natl Acad Sci U S A. 87(17):6574-8. PMID: 2395859

70. Sullivan N, Sun Y, Binley J, Lee J, Barbas CF 3rd, Parren PW, Burton DR, Sodroski J. 1998. Determinants of human immunodeficiency virus type 1 envelope glycoprotein activation by soluble CD4 and monoclonal antibodies. J Virol. 72(8):6332-8. PMID: 9658072

71. Madani N et al. 2016. Antibodies Elicited by Multiple Envelope Glycoprotein Immunogens in Primates Neutralize Primary Human Immunodeficiency Viruses (HIV-1) Sensitized by CD4-Mimetic Compounds. J Virol. 90(10):5031-5046. doi: 10.1128/JVI.03211-15.

72. Madani et al. 2018. A CD4-mimetic compound enhances vaccine efficacy against stringent immunodeficiency virus challenge. Nat Commun. 9(1):2363. doi: 10.1038/s41467-018-04758-9.

73. Pancera M et al. 2017. Crystal structures of trimeric HIV envelope with entry inhibitors BMS-378806 and BMS-626529. Nat Chem Biol. 13(10):1115-1122. doi: 10.1038/nchembio.2460.

74. Munro JB, Mothes W. 2015. Structure and Dynamics of the Native HIV-1 Env Trimer. J Virol. 89(11):5752-5. doi: 10.1128/JVI.03187-14.

75. Guo Q et al. 2003. Biochemical and genetic characterizations of a novel human immunodeficiency virus type 1 inhibitor that blocks gp120-CD4 interactions. J Virol 77(19):10528-36. PMID: 12970437

76. Giroud C, Marin M, Hammonds J, Spearman P, Melikyan GB. 2015. P2X1 Receptor Antagonists Inhibit HIV-1 Fusion by Blocking Virus-Coreceptor Interactions. J Virol. 89(18):9368-82. doi: 10.1128/JVI.01178-15.

77. Desai TM, Marin M, Sood C, Shi J, Nawaz F, Aiken C, Melikyan GB. 2015. Fluorescent protein-tagged Vpr dissociates from HIV-1 core after viral fusion and rapidly enters the cell nucleus. Retrovirology. 12:88. doi: 10.1186/s12977-015-0215-z.

78. Lin et al. 2003. A small molecule HIV-1 inhibitor that targets the HIV-1 envelope and inhibits CD4 receptor binding. Proc Natl Acad Sci U S A. 100(19):11013-8. DOI: 10.1073/pnas.1832214100

79. Malim MH, Hauber J, Fenrick R, Cullen BR. 1988. Immunodeficiency virus rev trans-activator modulates the expression of the viral regulatory genes. Nature. Nature. 335(6186):181-3. DOI: 10.1038/335181a0

80. Tobiume M, Lineberger JE, Lundquist CA, Miller MD, Aiken C. 2003. Nef does not affect the efficiency of human immunodeficiency virus type 1 fusion with target cells. J Virol. 77(19):10645-50. PMID: 12970449

81. Kirschman J, Qi M1, Ding L, Hammonds J, Dienger-Stambaugh K, Wang JJ, Lapierre LA, Goldenring JR, Spearman P. HIV-1 Envelope Glycoprotein Trafficking through the Endosomal Recycling Compartment Is Required for Particle Incorporation. J Virol. 92(5). pii: e01893-17. doi: 10.1128/JVI.01893-17

82. Brandenberg OF, Magnus C, Rusert P, Regoes RR, Trkola A. 2015. Different infectivity of HIV-1 strains is linked to number of envelope trimers required for entry. PLoS Pathog. 11(1):e1004595. doi: 10.1371/journal.ppat.1004595.

83. Yang X, Kurteva S, Ren X, Lee S, Sodroski J. 2006. Subunit stoichiometry of human immunodeficiency virus type 1 envelope glycoprotein trimers during virus entry into host cells. J Virol. 80(9):4388-95. DOI: 10.1128/JVI.80.9.4388-4395.2006

84. Munro JB et al. 2014. Conformational dynamics of single HIV-1 envelope trimers on the surface of native virions. Science. 346(6210):759-63. doi: 10.1126/science.1254426.

85. Mink M. et al. 2005. Impact of Human Immunodeficiency Virus Type 1 Gp41 Amino Acid Substitutions Selected During Enfuvirtide Treatment on Gp41 Binding and Antiviral Potency of Enfuvirtide in Vitro. J. Virol. 79, 12447–12454.

86. Lu J. et al. 2006. Rapid Emergence of Enfuvirtide Resistance in HIV-1-Infected Patients: Results of a Clonal Analysis. J. Acquir. Immune. Defic. Syndr. 43, 60–64.

87. Sista P. R. et al. 2004. Characterization of Determinants of Genotypic and Phenotypic Resistance to Enfuvirtide in Baseline and on-Treatment HIV-1 Isolates. AIDS 18, 1787–1794.

88. Rimsky L. T., Shugars D. C. & Matthews T. J. 1998. Determinants of Human Immunodeficiency Virus Type 1 Resistance to Gp41-Derived Inhibitory Peptides. J. Virol. 72, 986–993.

89. Vincent N. et al. 2005. Depletion in Antibodies Targeted to the HR2 Region of HIV-1 Glycoprotein Gp41 in Sera of HIV-1-Seropositive Patients Treated With T20. J Acquir. Immune. Defic. Syndr. 38, 254–262.

90. Fu et al. 2018. Structure of the membrane proximal external region of HIV-1 envelope glycoprotein. Proc Natl Acad Sci U S A. pii: 201807259. doi: 10.1073/pnas.1807259115.

91. Ward et al. 1988. Transmission of Human Immunodeficiency Virus (HIV) by Blood Transfusions Screened as Negative for HIV Antibody. N Engl J Med 318:473-478

DOI: 10.1056/NEJM198802253180803

# Chapter IV: General Discussion

Over the past decade, a number of cellular host factors regulating HIV-1 infection have been identified and studied, highlighting a complex interplay between HIV-1 and host cells. Many host proteins, such as transcriptional regulators, nucleoporins and other cellular machinery, are involved in distinct stages of HIV-1 lifecycle (7). However, several host proteins, known as restriction factors, defend against viral infection and can reduce HIV-1 infectivity. Examples of these restriction fators include Apolipoprotein B Editing Catalytic (APOBEC) proteins, which cause viral genome hypermutations through cytidine deamination, tetherin, which traps viral particles at the cell surface, and Sterile Alpha Motif and Histidine-aspartate Domain 1 (SAMHD1), which restricts HIV-1 infection by limiting the pool of deoxyribonucleoside triphosphates, thereby interfering with HIV-1 reverse transcription (8, 9, 10, 11, 12, 13, 14). Trim5a and Mx2/MXB can destabilize viral cores and target it to degradation (15, 16, 17, 18). Unfortunately, HIV-1 proteins, such as Vif and Vpu, antagonize these host defenses (19).

The results reported in Chapters II and III provide new fundamental insights into the role of novel host factors that regulate the HIV-1 Env function. We focused on Env-interacting host factors, the FIP1C/Rab11 complex and the recently identified restriction factor SERINC5 that facilitate Env trafficking/virus incorporation and inhibit HIV-1 fusion, respectively (4,5). We and others sought to understand the effects of SERINC5 on the conformation and function of Env (5, 25), as well as interactions with the viral protein Nef (23, 24). Athough thus far direct interactions between Env and FIP1C/Rab11 complex or with SERINC5 have not been demonstrated, several lines of evidence support

binding of these host factorts to Env. Future studies will reveal whether this binding is direct or mediated by additional, yet unidentified cellular proteins. Irrespective of the outcome, future studies will likely reveal new targets for intervention.

Targeting proviral host factors is a promising antiviral strategy, since, unlike the virus, these proteins do not readily mutate and thus drug resistance is less of a concern. There are currently no antiretroviral drugs targeting Env incorporation into virions. Therefore, uncovering the molecular mechanism of Env trafficking via FIP1C/Rab11 can lead to development of a novel class of HIV-1 inhibitors. If future studies demonstrate direct binding of Rab11-FIP1C to Env, disrupting this interaction could help to curbe HIV-1 infection. We also anticipate that inhibitors disrupting Nef-SERINC5 interactions will potentiate the antiviral activity of this restriction factor and inhibit HIV-1 replication.

**Conclusions and future directions**

SERINC5

**Conclusions** – Based on the literature and our own data, there appears to be a general trend for SERINC5 sensitivity. The more open Env of lab-adapted HIV-1 strains tend to be sensitive to SERINC5, whereas primary isolates and T/F viruses that maintain the closed Env conformation to avoid antibody neutralization are more resistant to this restriction factor. Our mutagenesis and conformational inhibitor studies are in line with the original hypothesis that SERINC5 targets a yet unidentified intermediate conformation of Env by promoting its conformational changes and, ultimately, functional inactivation.

**Future directions** – develop a technique to measure Env-SERINC5 interactions and re-assess the effects of mutations and conformational blockers on interactions between these proteins. This approach will complement our functional data and enable rationalization of the obtained results.

FIP1C

**Conclusions** – We conclude that dominant negative effect of $FIP1C_{549-650}$ revealed an important indispensable endocytic pathway during Env transport to PM. The dominant negative effect was HIV-1 specific and was dependent on the major endocytosis motif and tyrosine motif in Env CT.

**Future directions** – In the future, it would be interesting to study Rab14 and its interacting motor proteins responsible for Env transport to the assembly sites. Also, improvement in the Env tagging methods should enable real time imaging of Env trafficking with FIPs.

*Future work on FIPs*

1) We may generate a stable, inducible T cell line expressing $FIP1C_{549-650}$ to evaluate the dominant-negative effect on multi-cycle replication of HIV-1. Generation of stable human T cell lines under selection by tetracycline has the advantage of avoiding adverse effects on cellular growth/proliferation defects and unwanted cell differentiation (1). Thus far, our work was performed in TZM-bl cells (not counting the preliminary work on human macrophages) and therefore requires validation using other, more relevant cell types. CD4+ T cells are typical targets for HIV-1, although they present challenges due to

the smaller size of the cytoplasm compared to cell lines such as Jurkat or Hela or human macrophages induced from monocytes. This makes visualization of the ERC difficult. Confirmation of the dominant negative effect of $FIP1C_{549-650}$ in T cells will be valuable for understanding the mechanism of host cell-dependent regulation of HIV-1 Env trafficking. A transient overexpression system using a dominant negative fragment of FIP1C would be further optimized with a stable expression system in T cell lines and biochemical assays, which will be used to measure the dominant negative effect in T cells.

2) We can define a minimal inhibitory domain responsible for Env trapping in ERC (RBD mapping). Rab14 binding motif mutations have been used to measure the dominant negative effect (Suppl. Fig. 1) and we confirmed that the Rab14 binding site is partially responsible for the dominant negative effect. This can be explained by (1) the possible presence of an additional Rab14 binding site (i.e., I621E) (2), (2) an additional unknown host adaptor protein assisting Env trafficking from the ERC without the help of Rab14, or (3) residual expression of WT-FIP1C might have assisted the outward sorting of Env from the ERC to the PM. As shown in a previous published work from the Spearman lab (6), dominant-negative (S25N) forms of Rab14 disrupts the WT-FIP1C trafficking with HIV-1 Env to the PM while constitutively-active (Q70L) forms of Rab14 enhanced Env incorporation onto HIV-1 virus particles. We expect a dominant negative form of Rab14 will show a somewhat diminished dominant negative effect (less Env trapping ERC).

3) We will determine if there is a direct interaction between Env CT and FIP1C or if any indirect interaction exists between Env and RBD-FIP1C, although co-IP of HIV-1 Env CT and GFP-FIP1C$_{560-649}$ was not successful (data not shown). Co-IP with a smaller tag such as HA could improve our capability to detect such interaction. As the FIP family members were originally found via a yeast-two hybrid system, we may consider using a similar system or alternatively utilize bi-molecular fluorescence complementation (BiFC) imaging methods or Proximity ligation assay (PLA) to directly visualize the interaction between Env and FIP1C.

4) We can also synchronize the ERC formation before photoactivation and then use a pulse-chase approach to track Env and GFP-FIP1C$_{560-649}$. Since we used NL4-3 provirus, which replicates in HeLa cells, it would be useful to use pseudotyped viruses with the same pNL4-3 background and perform transfection with GFP-FIP1C$_{560-649}$. Once Env, Rab14 and GFP-FIP1C$_{560-649}$ are all resident in the ERC, we can perform photoactivation on ERC and then perform a pulse-chase in real time (3). Our model suggests Rab14, Env and WT FIP1C forms a heterotrimer before outward sorting in the ERC, but through pulse-chase we may also observe how Gag meets the heterotrimeric complex in a spatiotemporal manner.

5) We believe vesicle fractionation and isolation of individual compartments coupled with proteomics and Mass-Spectrometry will reveal important components of the dominant negative effect. Not only can we then confirm the presence of Rab14 and HIV-

1 Env inside the ERC, but also quantify the viral proteins and find other possible adaptor proteins during this trafficking. When stable T cell lines are generated, comparing the ERC components among T cells, H9, HeLa, and human macrophages will allow us to explore more components of the dominant negative effect.

6) The dominant negative effect was shown in the presence of WT FIP1C, but there remains a possibility that WT FIP1C might compete with $FIP1C_{560-649}$ during the Rab14 binding motif experiment. To address this question, we can generate RBD-FIP1C in WT-FIP1C KD T cells and also RBD-lacking FIP1C and compare if the dominant negative effect was solely specific to the Rab binding domain in the C-terminal fragment of FIP1C.

*SERINC5: Limitations of the current approach*

1) Absence of Nef.

Our previous and current work was performed in the absence of Nef. In the future, using a non-antagonizing version of Nef including mutations or deletions would be another way to assess SERINC5 restriction (4). Our results showed a weaker phenotype of SERINC5 inhibition compared to previous reports. Also, Nef is known to have multiple functions that are essential for HIV infection (21, 22). Studies of SERINC5 activity in cells expressing a non-antagonizing Nef mutants is an interesting direction to rule out undesired effects of Nef deletion on other steps of HIV-1 lifecycle.

2) Overexpression of SERINC5.

Since commercial antibodies to SERINC5 antibodies that do not cross-react with other SERINC family members are not available, current studies ectopically overexpress SERINC5 under common viral promoters, such as CMV or SV40. Even though the optimal ratio for transfection of packaging vector versus SERINC5-HA plasmids have been reported by several lab, overexpression may disturb the normal functional pathways of SERINC5.

3) Lack of evidence for direct interaction between SERINC5 and Env.

Our laboratory and others have failed to co-IP SERINC5 and Env (5) However, at the 2018 Cold Spring Harbor Laboratory Retrovirus meeting, SERINC5 interaction with HIV-1 Env has been reported by two groups using Co-IP and BiFC approaches (Diaz-Griffero; Zeng (unpublished)). Since SERINC5 should be incorporated into virions, it is likely that the interaction happens in the proximity of the viral membrane. If the SERINC5 binding motif is located in the hydrophobic gp41 domain which is exposed transiently during fusion, as is the MPER (5) favoring alternative conformations of Env could be another strategy to aid SERINC5-Env binding. Gag might also play a role in this interaction.

Reference

1. MG Martinez, DSchmitz, A Hergovich. 2013. Generation of Stable Human Cell Lines with Tetracycline-inducible (Tet-on) shRNA or cDNA Expression. J Vis Exp. (73): 50171.doi: 10.3791/50171

2. Lall P, Lindsay AJ, Hanscom S, Kecman T, Taglauer ES, McVeigh UM, Franklin E, McCaffrey MW, Khan AR. 2015. Structure-function analyses of the interactions between Rab11 and Rab14 small GTPases with their shared effector Rab coupling protein (RCP). J Biol Chem 290: 18817–18832. https://doi.org/10.1074/jbc.M114.612366.

3. Roy S, Yang G, Tang Y, Scott DA. 2011. A simple photoactivation and image analysis module for visualizing and analyzing axonal transport with high temporal resolution. Nat Protoc. 7(1):62-8. doi: 10.1038/nprot.2011.428.

4. Usami Y, Wu Y, Göttlinger HG. 2015. SERINC3 and SERINC5 restrict HIV-1 infectivity and are counteracted by Nef. Nature. 526(7572):218-23. doi: 10.1038/nature15400.

5. Sood C, Marin M, Chande A, Pizzato M, Melikyan GB. 2017. SERINC5 protein inhibits HIV-1 fusion pore formation by promoting functional inactivation of envelope glycoproteins. J Biol Chem. 292(14):6014-6026. doi: 10.1074/jbc.M117.777714.

6. Qi M, Williams JA, Chu H, Chen X, Wang JJ, Ding L, Akhirome E, Wen X, Lapierre LA, Goldenring JR, Spearman P. 2013. Rab11-FIP1C and Rab14 direct plasma membrane sorting and particle incorporation of the HIV-1 envelope glycoprotein complex. PLoS Pathog 9:e1003278. https://doi.org/10.1371/journal.ppat.1003278.

7. Ghimire D, Rai M, Gaur R. 2018. Novel host restriction factors implicated in HIV-1 replication. J Gen Virol. 99(4):435-446. doi: 10.1099/jgv.0.001026

8. Smith HC, Bennett RP, Kizilyer A, McDougall WM, Prohaska KM. 2012. Functions and regulation of the APOBEC family of proteins. Semin Cell Dev Biol. 23(3):258-68. doi: 10.1016/j.semcdb.2011.10.004.

9. Goila-Gaur R, Strebel K. 2008. HIV-1 Vif, APOBEC, and intrinsic immunity. Retrovirology 5:51.

10. Malim MH. 2009. APOBEC proteins and intrinsic resistance to HIV-1 infection. Philos Trans R Soc Lond B Biol Sci 364:675–687.

11. Smith JL, Bu W, Burdick RC, Pathak VK. 2009. Multiple ways of targeting APOBEC3-virion infectivity factor interactions for anti-HIV-1 drug development. Trends Pharmacol Sci 30:638–646.

12. Smith HC, Bennett RP, Kizilyer A, McDougall WM, Prohaska KM. 2012.

Functions and regulation of the APOBEC family of proteins. Semin Cell Dev Biol 23:258–268.

13. Sheehy AM, Gaddis NC, Choi JD, Malim MH. 2012. Isolation of a human gene that inhibits HIV-1 infection and is suppressed by the viral Vif protein. Nature 418:646–650.

14. Ahn J. 2016. Functional organization of human SAMHD1 and mechanisms of HIV-1 restriction. Biol Chem 397:373–379

15. Kuang YQ, Liu HL, Zheng YT. 2015. The innate immune roles of host factors TRIM5a and Cyclophilin A on HIV-1 replication. Med Microbiol Immunol 204:557–565

16. Goujon C, Moncorgé O, Bauby H, Doyle T, Ward CC, Schaller T, Hué S, Barclay WS, Schulz R, Malim MH. 2013. Human MX2 is an interferon-induced post-entry inhibitor of HIV-1 infection. Nature 502:559–562. doi:10.1038/nature12542.CrossRefPubMedGoogle Scholar

17.Kane M, Yadav SS, Bitzegeio J, Kutluay SB, Zang T, Wilson SJ, Schoggins JW, Rice CM, Yamashita M, Hatziioannou T, Bieniasz PD. 2013. MX2 is an interferon-induced inhibitor of HIV-1 infection. Nature 502:563–566. doi:10.1038/nature12653.CrossRefPubMedGoogle Scholar

18.Liu Z, Pan Q, Ding S, Qian J, Xu F, Zhou J, Cen S, Guo F, Liang C. 2013. The interferon-inducible MxB protein inhibits HIV-1 infection. Cell Host Microbe 14:398–410. doi:10.1016/j.chom.2013.08.015.

19. Jia X, Zhao Q, Xiong Y. 2015. HIV suppression by host restriction factors and viral immune evasion. Curr Opin Struct Biol. 31:106-14. doi: 10.1016/j.sbi.2015.04.004.

20. Fackler. 2015. Spotlight on HIV-1 Nef: SERINC3 and SERINC5 Identified as Restriction Factors Antagonized by the Pathogenesis Factor. Viruses. 7(12):6730-8. doi: 10.3390/v7122970.

21. Collins KL, Chen BK, Kalams SA, Walker BD, Baltimore D. 1998. HIV-1 Nef protein protects infected primary cells against killing by cytotoxic T lymphocytes. Nature. 22;391(6665):397-401.

22. Shah AH, Sowrirajan B, Davis ZB, Ward JP, Campbell EM, Planelles V, Barker E. 2010. Degranulation of natural killer cells following interaction with HIV-1-infected cells is hindered by downmodulation of NTB-A by Vpu. Cell Host Microbe. 8(5):397-409. doi: 10.1016/j.chom.2010.10.008.

23. Schulte B, Selyutina A, Opp S, Herschhorn A, Sodroski JG, Pizzato M, Diaz-Griffero F. 2018. Localization to detergent-resistant membranes and HIV-1 core entry inhibition

correlate with HIV-1 restriction by SERINC5. Virology. 515:52-65. doi: 10.1016/j.virol.2017.12.005.

24. Dai W, Usami Y, Wu Y, Göttlinger H. 2018. A Long Cytoplasmic Loop Governs the Sensitivity of the Anti-viral Host Protein SERINC5 to HIV-1 Nef. Cell Rep. 22(4):869-875. doi: 10.1016/j.celrep.2017.12.082.

25. Beitari S, Ding S, Pan Q, Finzi A, Liang C. 2017. Effect of HIV-1 Env on SERINC5 Antagonism. J Virol. 91(4). pii: e02214-16. doi: 10.1128/JVI.02214-16.

Appendix figure

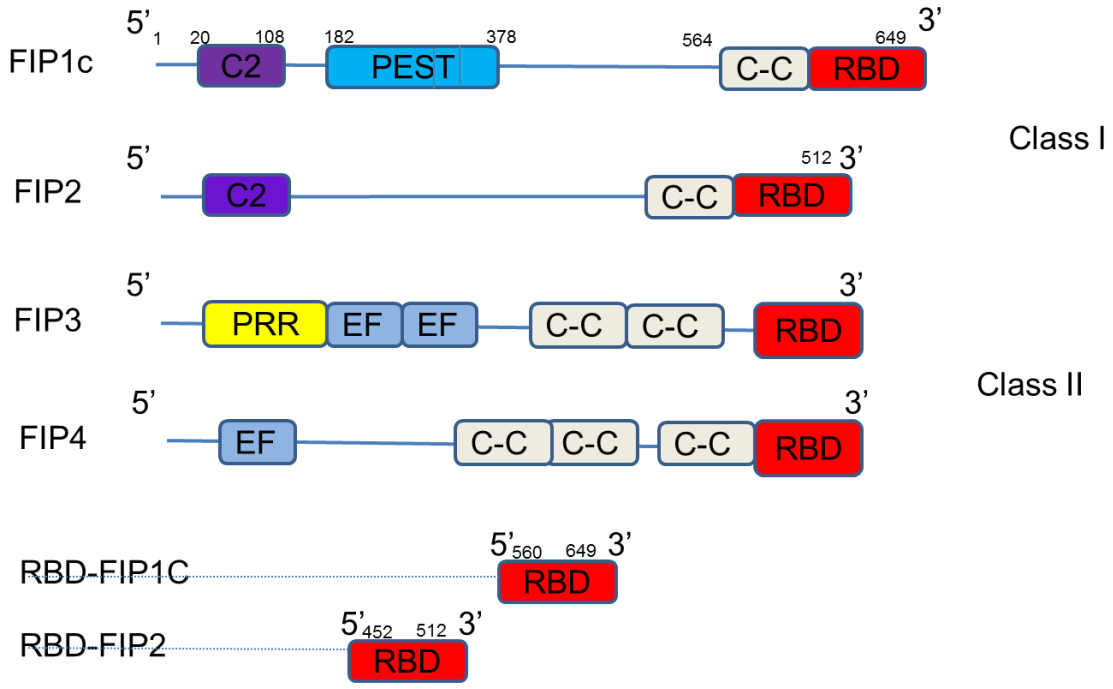


**Fig 1. Rab11-Family Interacting Proteins (FIPs).**

This diagram shows that FIP1C$_{560\text{-}649}$ contains onlya  short C-terminus fragment which is defined as FIP1C WT. PRR, Proline rixh region; C-C, Coiled Coil; EF, E-F hand; RBD, Rab binding domain; PEST, PEST sequence.

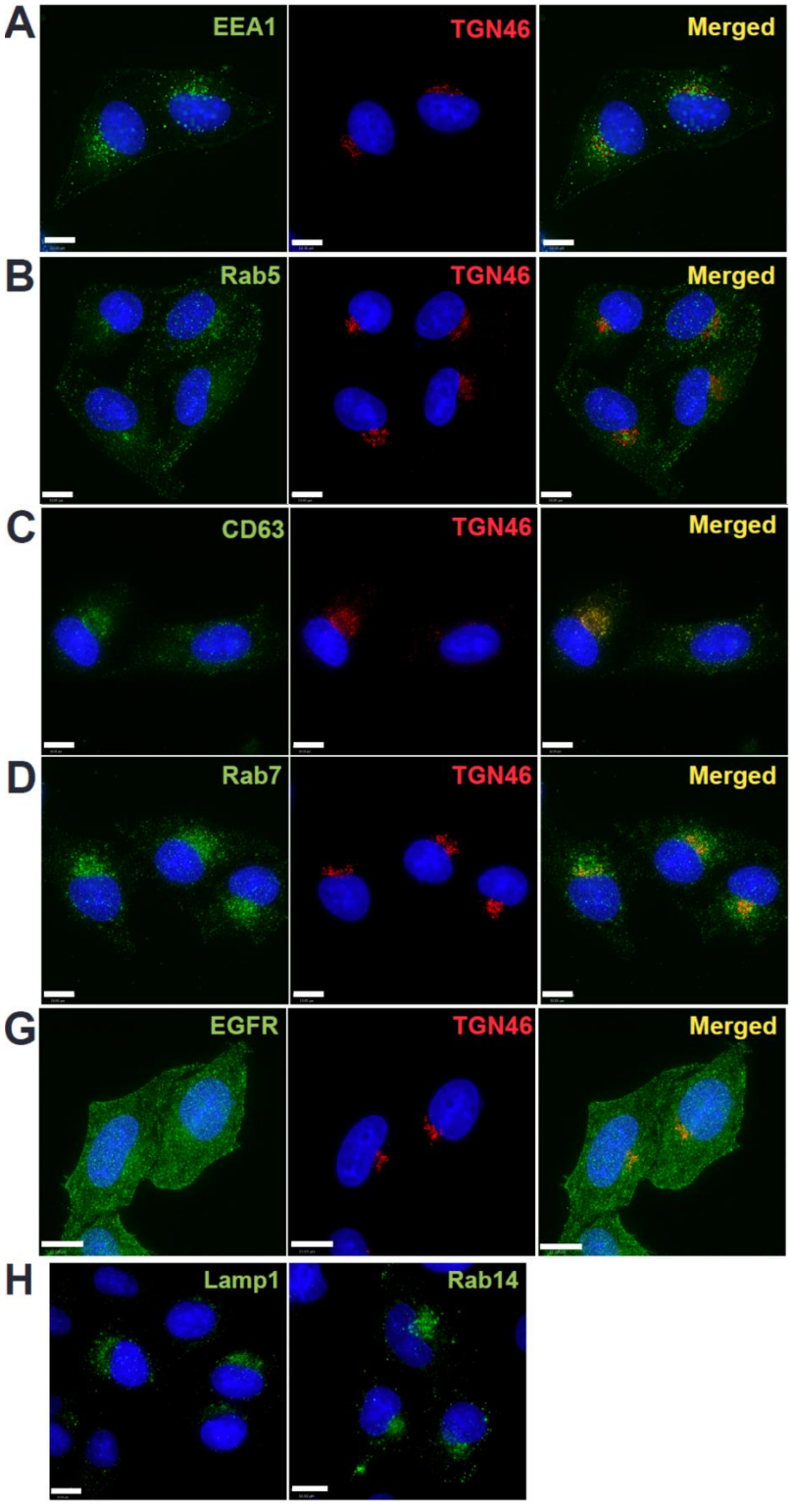
A
EEA1
TGN46
Merged
B
Rab5
TGN46
Merged
C
CD63
TGN46
Merged
D
Rab7
TGN46
Merged
G
EGFR
TGN46
Merged
H
Lamp1
Rab14

**Fig. 2. Endogenous expression of endocytic pathway markers**

(A-F) In the absence of virus production, TZM-bl cells were stained with antibodies targeting the endocytic pathway (Green). The Trans-Golgi network was stained with mcherry secondary antibody.

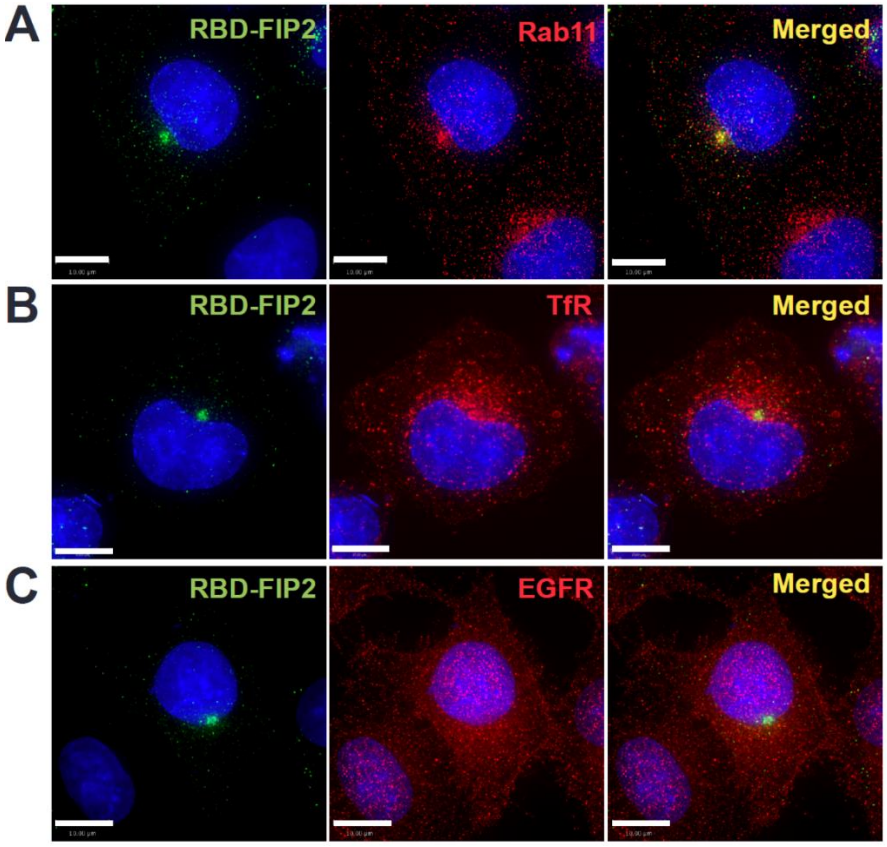


**Fig. 3 RBD-FIP2 and endocytotic pathway**

(A-C) After transfection with GFP-RBD-FIP2, TZM-bl cells were stained with Rab11, Transferrin Receptor and EGF receptor-targeting antibodies.

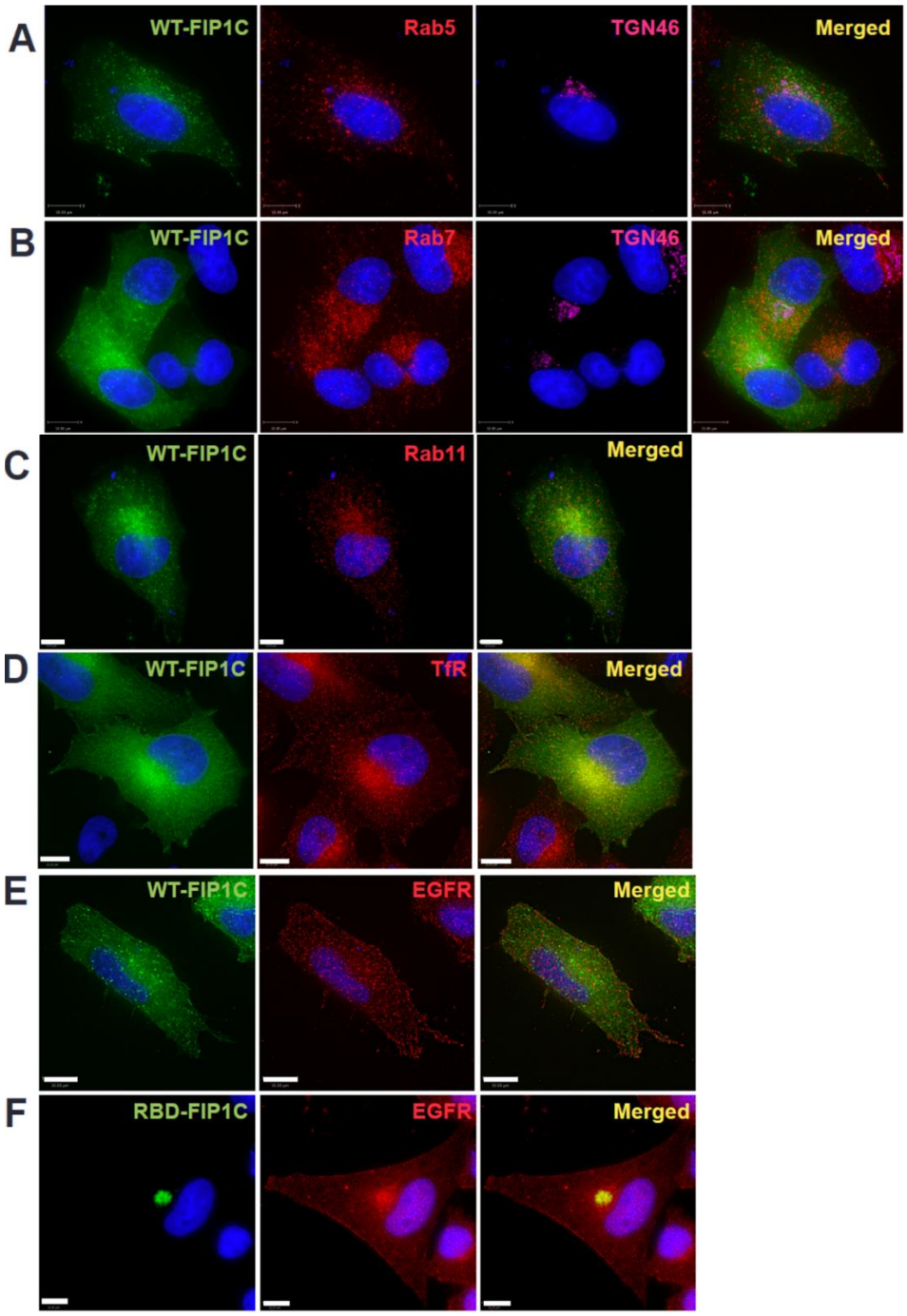


**Fig. 4 WT-FIP1C and endocytotic pathway**

(A-E) After transfection with GFP-WT FIP1C, TZM-bl cells were stained with Rab5, Rab7, Rab11, Transferrin Receptor and EGF receptor-targeting antibodies. (F) GFP-RBD-FIP1C was overexpressed before staining with EGF receptor-targeting antibody.

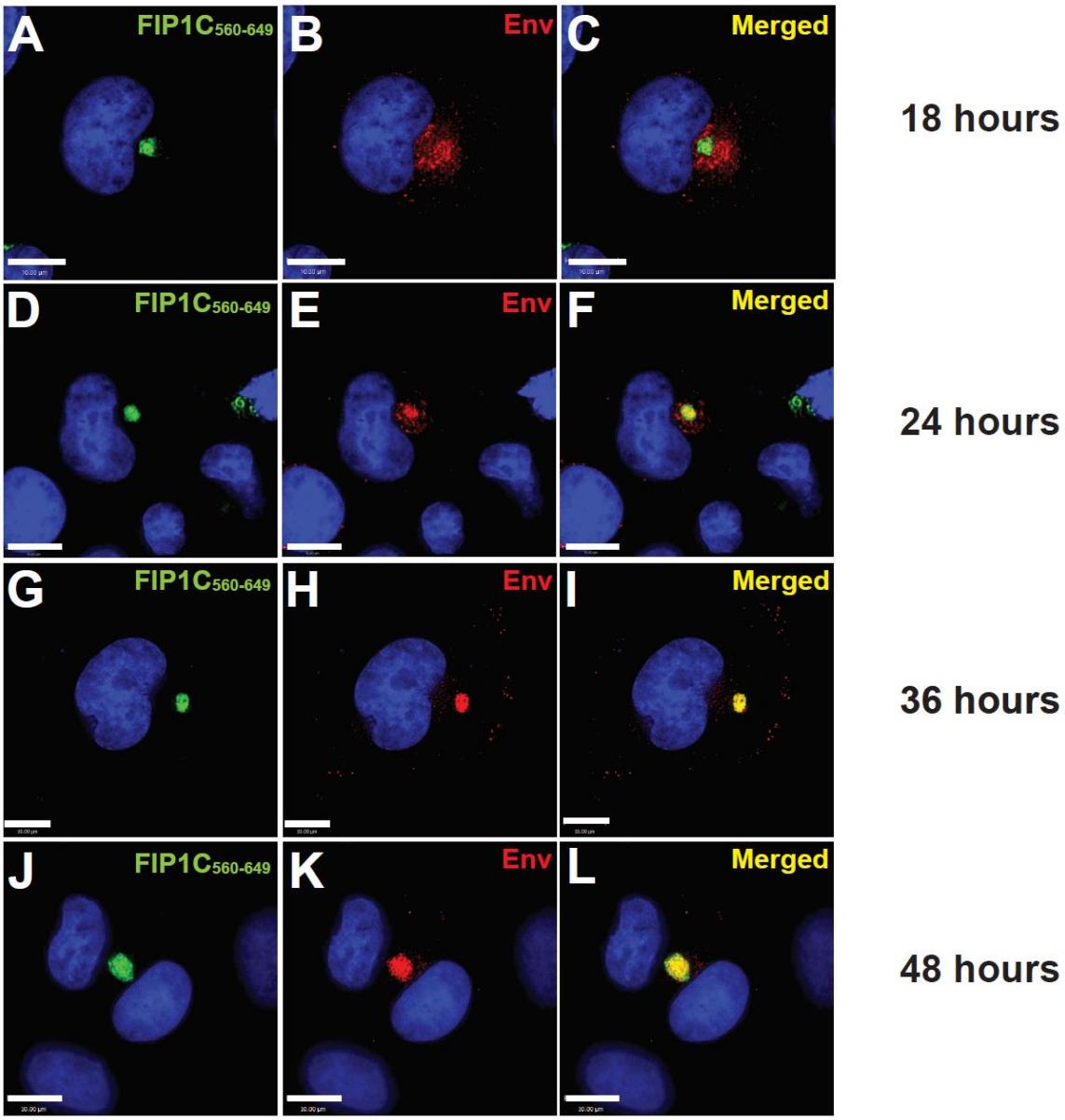


**Fig. 5 Early expression of FIP1C$_{560-649}$ in TZM bl**

Protein expression of FIP1C$_{560-649}$ was chased until 48 hours. At each time point, TZM-bl cells were fixed and starined with 2G12 bnAb.

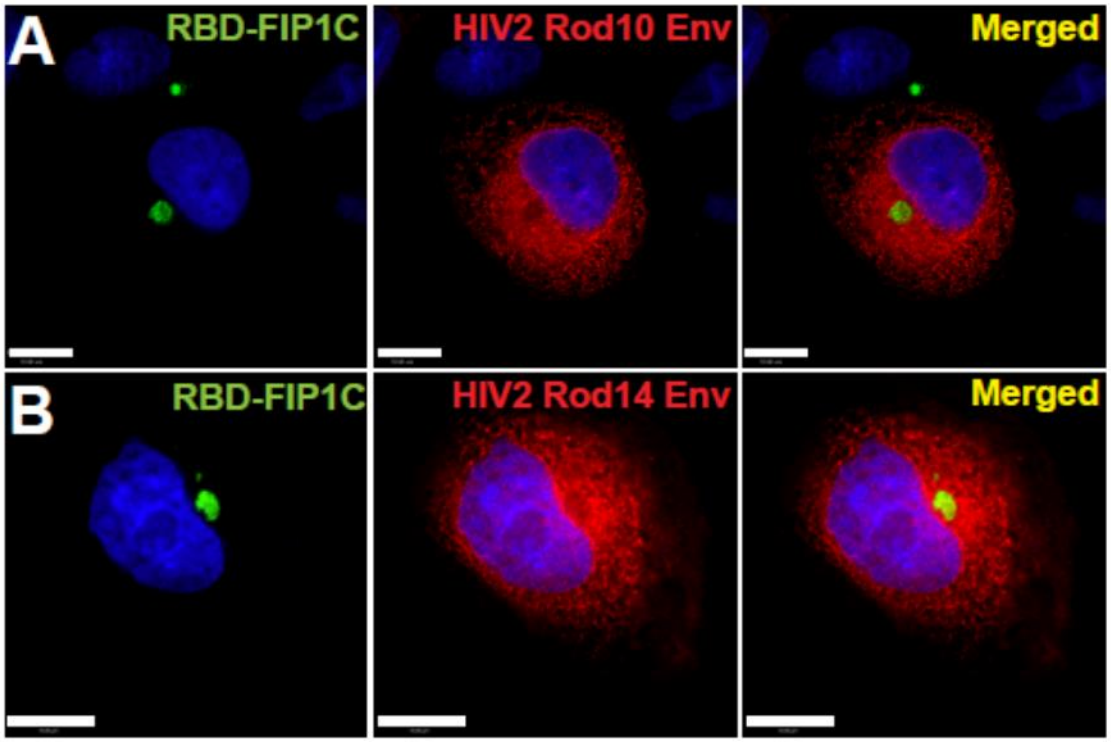


**Fig. 6 RBD-FIP1C and HIV2 Envs**

After transfection with GFP-RBD-FIP1C and HIV2 proviruses, TZM-bl cells were stained with HIV2 Env-targeting antibodies.